AFCRL-72-0082
22 DECEMBER 1972
PHYSICAL SCIENCES RESEARCH PAPERS, NO. 477

AIR FORCE CAMBRIDGE RESEARCH LABORATORIES
L. G. HANSCOM FIELD, BEDFORD, MASSACHUSETTS

The Temperature Coefficients of Acoustic Surface Wave Velocity and Delay on Lithium Niobate, Lithium Tantalate, Quartz, and Tellurium Dioxide

ANDREW J. SLOBODNIK, Jr.

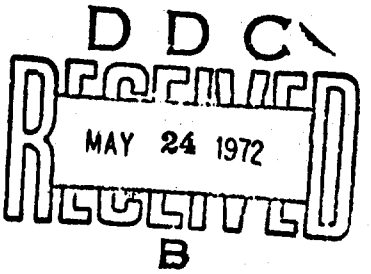

AIR FORCE SYSTEMS COMMAND
United States Air Force

Qualified requestors may obtain additional copies from the Defense Documentation Center. All others should apply to the National Technical Information Service.

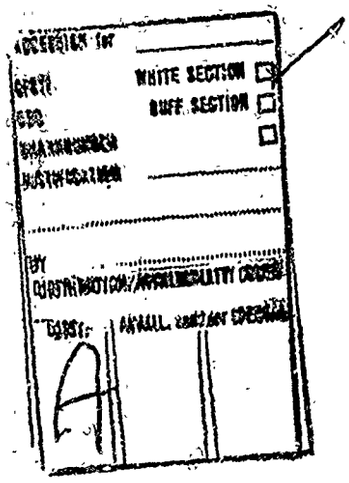

Unclassified

Security Classification

DOCUMENT CONTROL DATA - R&D

(Security classification of title, body of abstract and indexing annotation must be entered when the overall report is classified)

1. ORIGINATING ACTIVITY (Corporate author) Air Force Cambridge Research Laboratories (LZM) L. G. Hanscom Field Bedford, Massachusetts 01730	2a. REPORT SECURITY CLASSIFICATION Unclassified 2b. GROUP

3. REPORT TITLE

THE TEMPERATURE COEFFICIENTS OF ACOUSTIC SURFACE WAVE VELOCITY AND DELAY ON LITHIUM NIOBATE, LITHIUM TANTALATE, QUARTZ, AND TELLURIUM DIOXIDE

4. DESCRIPTIVE NOTES (Type of report and inclusive dates)

Scientific. Interim.

5. AUTHOR(S) (First name, middle initial, last name)

Andrew J. Slobodnik, Jr.

6. REPORT DATE	7a. TOTAL NO. OF PAGES	7b. NO. OF REFS
22 December 1971	128	29

8a. CONTRACT OR GRANT NO.	9a. ORIGINATOR'S REPORT NUMBER(S) AFCRL-72-0082
b. PROJECT, TASK, WORK UNIT NOS. 5635-03-01 c. DOD ELEMENT 61102F d. DOD SUBELEMENT 681305	9b. OTHER REPORT NO(S) (Any other numbers that may be assigned this report) PSRP No. 477

10. DISTRIBUTION STATEMENT

Approved for public release; distribution unlimited.

11. SUPPLEMENTARY NOTES	12. SPONSORING MILITARY ACTIVITY
TECH, OTHER	Air Force Cambridge Research Laboratories (LZM) L. G. Hanscom Field Bedford, Massachusetts 01730

13. ABSTRACT

A systematic search for zero temperature coefficient of acoustic surface wave delay has been made on the materials, TeO_2, quartz, $LiTaO_3$ and $LiNbO_3$. Such temperature compensated orientations are needed for application to wide-band multifunction modems and other signal processing devices.

Two temperature compensated cuts of TeO_2 have been discovered. These two orientations possess simultaneously zero temperature coefficients of delay, zero power flow angles and ultra-low surface wave velocities (1387 and 1424 m/sec). This last property allows long time delays in short spaces with consequent reductions in size and weight. The piezoelectric coupling parameters ($\Delta v/v$) for these orientations are 2×10^{-6} and 8×10^{-5}.

The lowest temperature coefficient of delay on $LiTaO_3$ was found to be 23 ppm/°C for an orientation having 1.55° of beam steering. The sacrifice of several parts per million in temperature sensitivity (to 30 and 33 ppm/°C) yields two pure mode orientations having velocities of 3300 m/sec and moderate coupling ($\Delta v/v$ = 0.0037 and 0.0045). An orientation of $LiTaO_3$ has been discovered having substantially higher coupling ($\Delta v/v$ = 0.0084) than any previously known.

The 41.5° rotated cut, X-propagating orientation of $LiNbO_3$ has a temperature coefficient of delay of 72 ppm/°C which is the best yet found for this material.

DD FORM 1 NOV 65 1473

Unclassified

Security Classification

Unclassified

Security Classification

14. KEY WORDS	LINK A		LINK B		LINK C	
	ROLE	WT	ROLE	WT	ROLE	WT
Accustic surface waves						
Temperature coefficient of delay						
Temperature coefficient of velocity						
Acoustic surface wave velocities						
Coupling to interdigital transducers						
Surface wave pure mode axes						
Tellurium dioxide						
Lithium tantalate						
Microwave acoustic material constants						
Acoustic signal processing						
Quartz						
Lithium niobate						
Surface wave numerical data						
Wave propagation						
Piezoelectric materials						
Acoustic delay lines						
Zero temperature coefficient cuts of TeO_2						
Surface wave power flow angle						

Unclassified

Security Classification

AFCRL-72-0082
22 DECEMBER 1971
PHYSICAL SCIENCES RESEARCH PAPERS, NO. 477

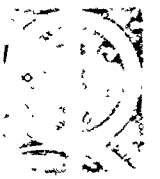

MICROWAVE PHYSICS LABORATORY PROJECT 5635
AIR FORCE CAMBRIDGE RESEARCH LABORATORIES
L. G. HANSCOM FIELD, BEDFORD, MASSACHUSETTS

The Temperature Coefficients of Acoustic Surface Wave Velocity and Delay on Lithium Niobate, Lithium Tantalate, Quartz, and Tellurium Dioxide

ANDREW J. SLOBODNIK, Jr.

AIR FORCE SYSTEMS COMMAND
United States Air Force

Abstract

A systematic search for zero temperature coefficient of acoustic surface wave delay has been made on the materials TeO_2, quartz, $LiTaO_3$ and $LiNbO_3$. Such temperature compensated orientations are needed for application to wideband multi-function modems and other signal processing devices.

Two temperature compensated cuts of TeO_2 have been discovered. These two orientations possess simultaneously zero temperature coefficients of delay, zero power flow angles and ultra-low surface wave velocities (1387 and 1424 m/sec). This last property allows long time delays in short spaces with consequent reductions in size and weight. The piezoelectric-coupling parameters ($\Delta v/v$) for these orientations are 2×10^{-6} and 8×10^{-5}.

The lowest temperature coefficient of delay on $LiTaO_3$ was found to be 23 ppm/°C for an orientation having 1.55° of beam steering. The sacrifice of several parts per million in temperature sensitivity (to 30 and 33 ppm/°C) yields two pure mode orientations having velocities of 3300 m/sec and moderate coupling ($\Delta v/v$ = 0.0037 and 0.0045). An orientation of $LiTaO_3$ has been discovered having substantially higher coupling ($\Delta v/v$ = 0.0084) than any previously known.

The 41.5° rotated cut, X-propagating orientation of $LiNbO_3$ has a temperature coefficient of delay of 72 ppm/°C which is the best yet found for this material.

Preface

This work was undertaken in response to the Rome Air Development Center (RADC) Research Need 71-21 as documented on AF Form 111 and entitled "Research on Surface Wave Phenomena for Application to Wideband Multi-Function Modems." The following statements are quoted from this document. "New materials or cut orientations are needed which can support acoustic surface waves and which possess zero or very small temperature coefficients with low insertion loss." "Currently, the most popular materials used to provide signal processing functions with acoustic surface waves are the piezoelectrics. Of those used, only the ST cut of quartz provides a zero temperature coefficient over any appreciable range."

Contents

Illustrations

Illustrations

Tables

The Temperature Coefficients of Acoustic Surface Wave Velocity and Delay on Lithium Niobate, Lithium Tantalate, Quartz, and Tellurium Dioxide

1. INTRODUCTION

Surface wave acoustic devices are currently coming into widespread systems use for the performance of a variety of delay and signal processing functions (Bush et al, 1970; Bush, 1971). However, for many applications it is highly desirable to use a temperature compensated cut to support the surface waves, that is, a crystalline orientation having zero temperature coefficient of delay. In fact, Carr et al (1971) have shown that a limitation on the application of surface wave encoders and decoders to multiple-access, secure communications systems is the degradation of the peak-to-sidelobe ratio of the autocorrelation function due to temperature differences.

In spite of several recent theoretical and experimental searches (Schulz et al, 1970; Holland and Schulz, 1970; Welsh, 1971; Lewis et al, 1971, and Schulz and Holland, 1971) the only temperature compensated cuts presently known are on α quartz. The most widely used is the ST-cut, X-propagating orientation discovered by Schulz et al (1970). Unfortunately, crystalline quartz possesses a very low piezoelectric coupling constant which leads to undesirably high insertion losses for any devices constructed using this material.

Two materials which have relatively high piezoelectric coupling are lithium niobate and lithium tantalate. An orientation having zero temperature coefficient

(Received for publication 17 December 1971)

Here T is temperature and v_s is the surface wave velocity. A desired temperature compensated cut occurs at room temperature whenever Eq. (1) equals zero for $T_1 = 25^oC$.

For the purposes of numerical calculation, the following approximation to Eq. (1) was used to compute the temperature coefficient of velocity (for TeO_2, 20^oC was used as the center reference temperature):

$$TCV \approx \frac{1}{v_s(25^oC)} \left[\frac{v_s(35^oC) - v_s(15^oC)}{20^oC} \right]. \qquad (2)$$

The actual procedure consisted of three steps:

I Computation of material constants at 15^oC, 25^oC and 35^oC (10^oC, 20^oC and 30^oC for TeO_2)

II Computation of surface wave velocities at each of these temperatures using the results of step I

III Use of Eq. (2) to compute TCV.

As the surface wave velocity is highly anisotropic, each of these three steps had to be repeated at one degree intervals for all orientations investigated.

Step I was accomplished using the temperature coefficients of the material constants themselves, as tabulated in Appendix A, in conjunction with Eq. (3) which is merely a truncated Taylor Series expansion.

$$X(T) \approx X(T_o) \left[1 + \frac{1}{X(T_o)} \frac{\partial X}{\partial T} (T-T_o) + \frac{1}{2X(T_o)} \frac{\partial^2 X}{\partial T^2} (T-T_o)^2 \right] \qquad (3)$$

Here X is the desired material constant, T_o is room temperature and $1/X(T_o)\, \partial X/\partial T$ and $1/2X(T_o)\, \partial^2 X/\partial T^2$ are the first and second order normalized temperature coefficients respectively. Where second order coefficients of the material constants were not readily available, Eq. (3) was truncated after the first order term. Also, where direct measurements of the temperature coefficients of the density were not available, these coefficients were calculated from the coefficients of thermal expansion according to Eq. (4) which is derived in Appendix B.

$$\frac{1}{\rho(T_o)} \frac{\partial \rho}{\partial T} = -\left[\alpha_{11} + \alpha_{22} + \alpha_{33} \right]. \qquad (4)$$

Here ρ is the density and α_{ii} are the coefficients of thermal expansion.

The results of step I, that is complete material constant matrices for lithium niobate, lithium tantalate, quartz and tellurium dioxide at 15^oC, 25^oC and 35^oC (10^oC, 20^oC and 30^oC for TeO_2), are tabulated in Appendix C.

Step II consisted of computing the surface wave velocities at 15°C, 25°C and 35°C using the results of step I. The calculations were made using a computer program based on the work of Campbell and Jones (1968, 1970a and 1970b).

The results of step II were then directly substituted into Eq. (2) thus determining the temperature coefficient of velocity.

For most delay line, filter and other signal processing applications the actual parameter of interest is not the temperature coefficient of velocity but is in fact the change in delay time with temperature (Holland and Schulz, 1970). The first order temperature coefficient of delay is given by Eq. (5).

$$TCD = \frac{1}{\tau}\frac{\partial \tau}{\partial T}\bigg|_{T_1} . \tag{5}$$

Here $\tau = \ell/v_s$ is the delay time and ℓ is the distance between two material points.

The temperature coefficient of delay is related to the temperature coefficient of velocity through the coefficient of thermal expansion, α.

$$\frac{1}{\tau}\frac{\partial \tau}{\partial T} = \left(\frac{\ell}{v_s}\right)^{-1} \frac{\partial}{\partial T}\left(\frac{\ell}{v_s}\right) = \frac{1}{\ell}\frac{\partial \ell}{\partial T} - \frac{1}{v_s}\frac{\partial v_s}{\partial T} \tag{6a}$$

$$\frac{1}{\tau}\frac{\partial \tau}{\partial T} = \alpha - \frac{1}{v_s}\frac{\partial v_s}{\partial T} \tag{6b}$$

Note that the appropriate value of α in this equation depends very much on the orientation being considered since the matrix of the coefficient of thermal expansion is anisotropic. The proper value of α is obtained by rotating the basic matrix through the appropriate Euler angles (Goldstein, 1970) and combining in the standard manner similar to the methods used in rotating the elastic, piezoelectric and dielectric constants for velocity calculations (Campbell and Jones, 1968).

For the purposes of this report, Eq. (6) was used directly for calculating TCD by using the previously determined approximate value of TCV along with the appropriate value of α.

3. DATA

The purpose of this section is to present a tabulation (beginning on page 9) of the temperature coefficients of velocity and delay for a wide variety of cuts and orientations of $LiNbO_3$, $LiTaO_3$, quartz and tellurium dioxide. In addition, the surface wave velocity, the coupling parameter, $\Delta v/v$ (Campbell and Jones, 1968 and 1970b), and the electromechanical power flow angle, ϕ (the deviation of the time

average power flow from the phase velocity vector) are presented on facing pages. This information allows the device designer to choose a given material orientation with full knowledge of all applicable parameters including coupling of electromagnetic to acoustic energy, pure mode axes (directions for which $\phi = 0$) and the effect of beam steering (Slobodnik et al, 1970 and Slobodnik and Conway, 1970b). Use of electromechanical power flow rather than the incomplete mechanical power provides greater accuracy than previously available (Slobodnik and Conway, 1970a).

The orientations tabulated are quantitatively defined using the Euler angles lamda, mu and theta as explained in Figure 1. The standard cuts and orientations are shown in Figure 2a to o along with their corresponding Euler angles. Many non-standard orientations have also been investigated in the attempt to discover zero or minimum values of the temperature coefficient of delay. These orientations are identified only by their Euler angles. The use of "rotated constants" allows further flexibility in the investigation of off-axis orientations (although round-off errors are somewhat greater in computation of temperature coefficients). In these cases the propagation axes 1, 2 and 3 do not initially line up with the crystalline axes X, Y and Z but rather with those crystalline orientations resulting from a preliminary Euler angle rotation through the "rotated constant" angles. For further details of this notation the reader is referred to Appendix D.

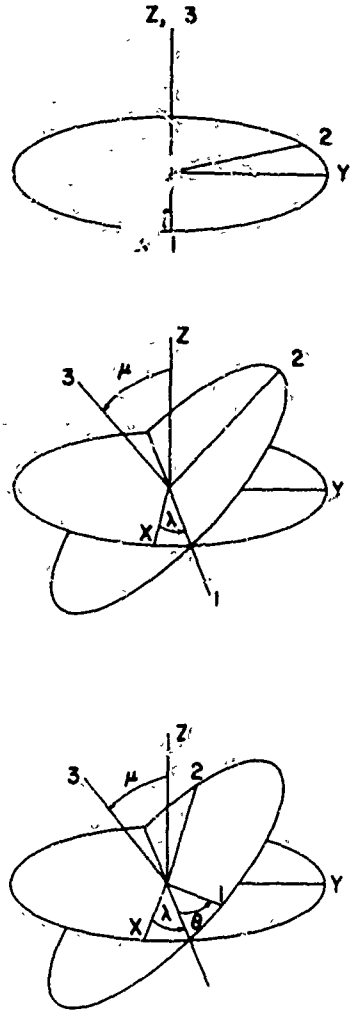

Figure 1. Coordinate System Used to Define Acoustic Surface Wave Propagation. The phase velocity vector lies along the 1 axis while the plate normal lies along the negative 3 axis. The crystalline axes are given by X, Y, and Z while the Euler angles are λ, μ, and θ (after H. Goldstein in Classical Mechanics).

Finally it can be noted that, wherever possible, the data tabulated in this section was compared with previous theoretical and experimental results (Schulz et al, 1970; Holland and Schulz, 1970; Welsh, 1971; Lewis et al, 1971; and Schulz and Holland, 1971). In all cases reasonable agreement was obtained.

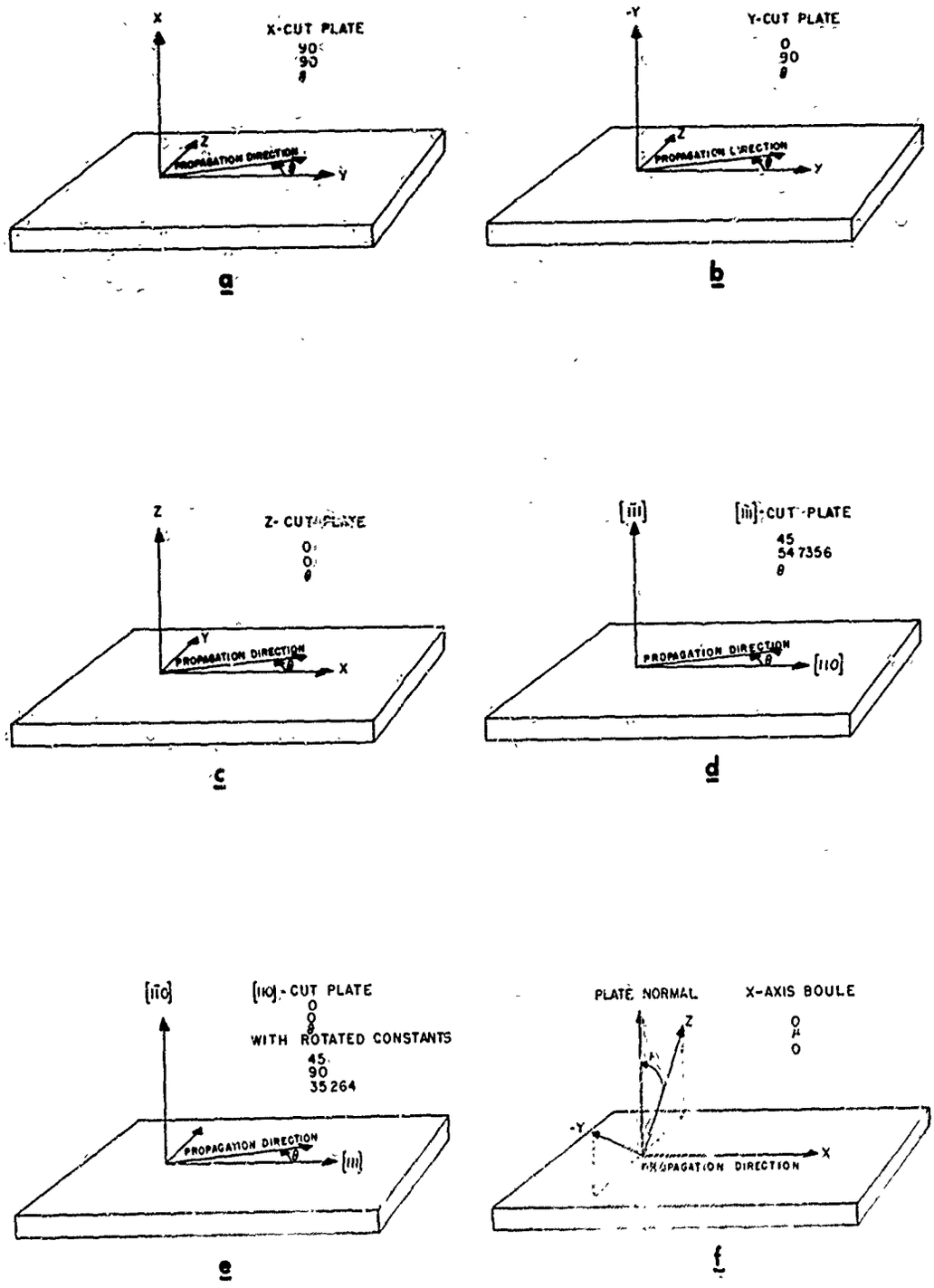

Figure 2. Fifteen Standard Crystalline Orientations Along with Corresponding Euler Angle Notation

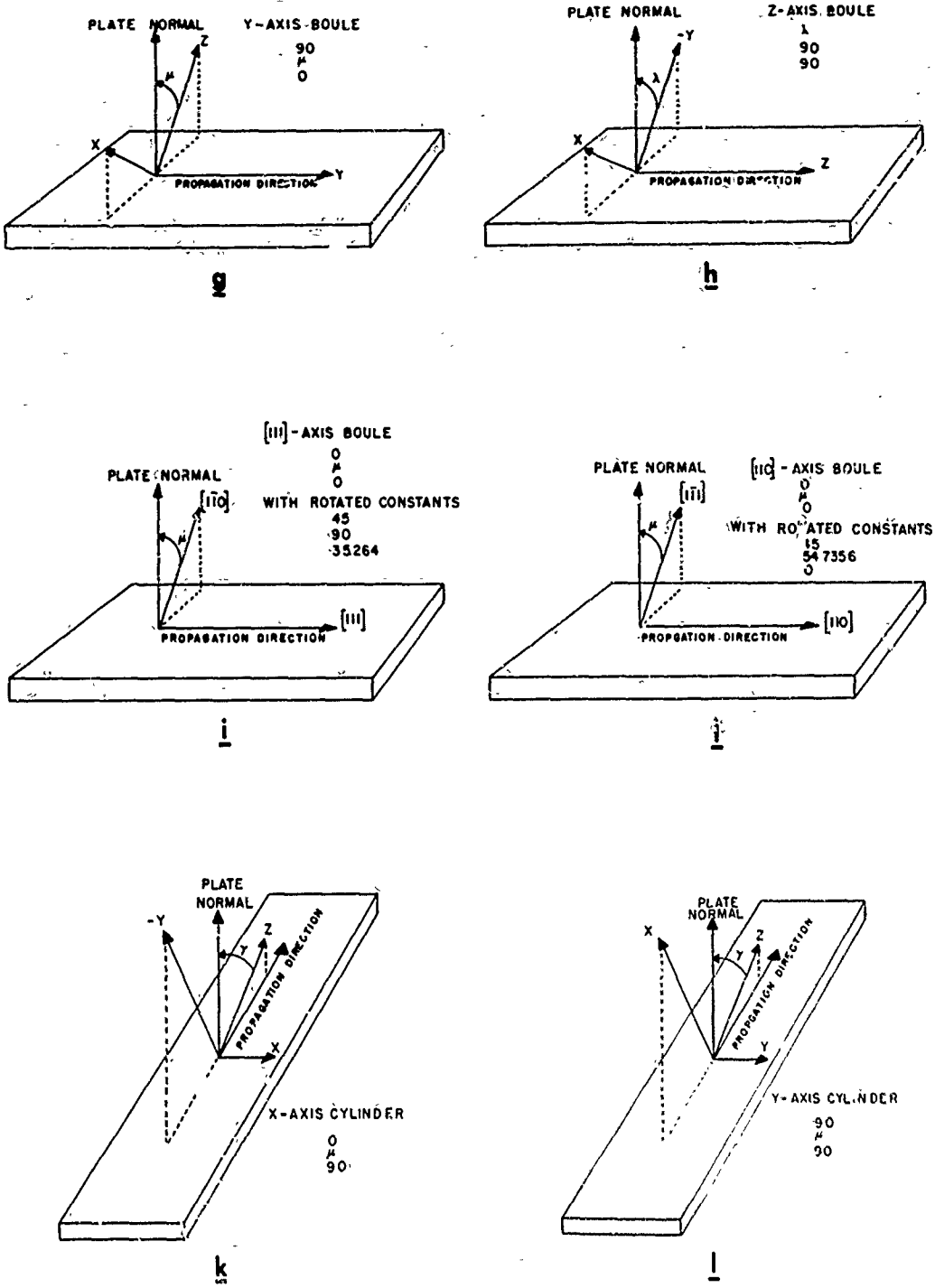

Figure 2 (Contd). Fifteen Standard Crystalline Orientations Along With Corresponding Euler Angle Notation

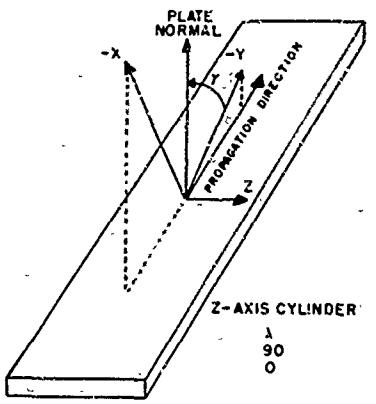

m

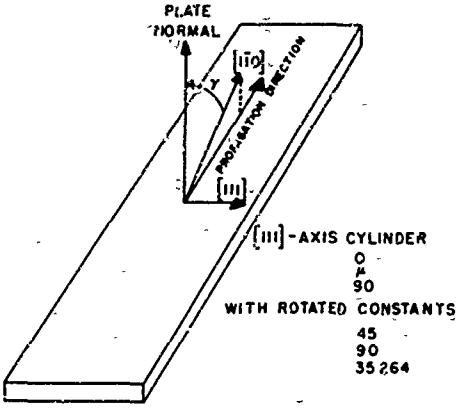

n

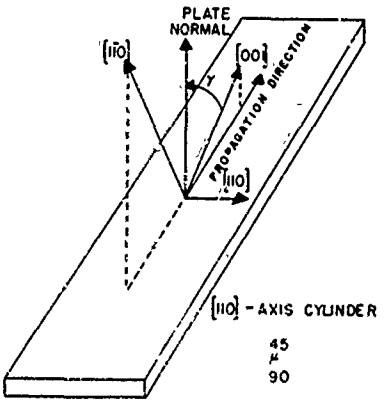

o

Figure 2 (Contd). Fifteen Standard Crystalline Orientations Along With Corresponding Euler Angle Notation

EIGHTY-FOUR DATA CURVES FOLLOW

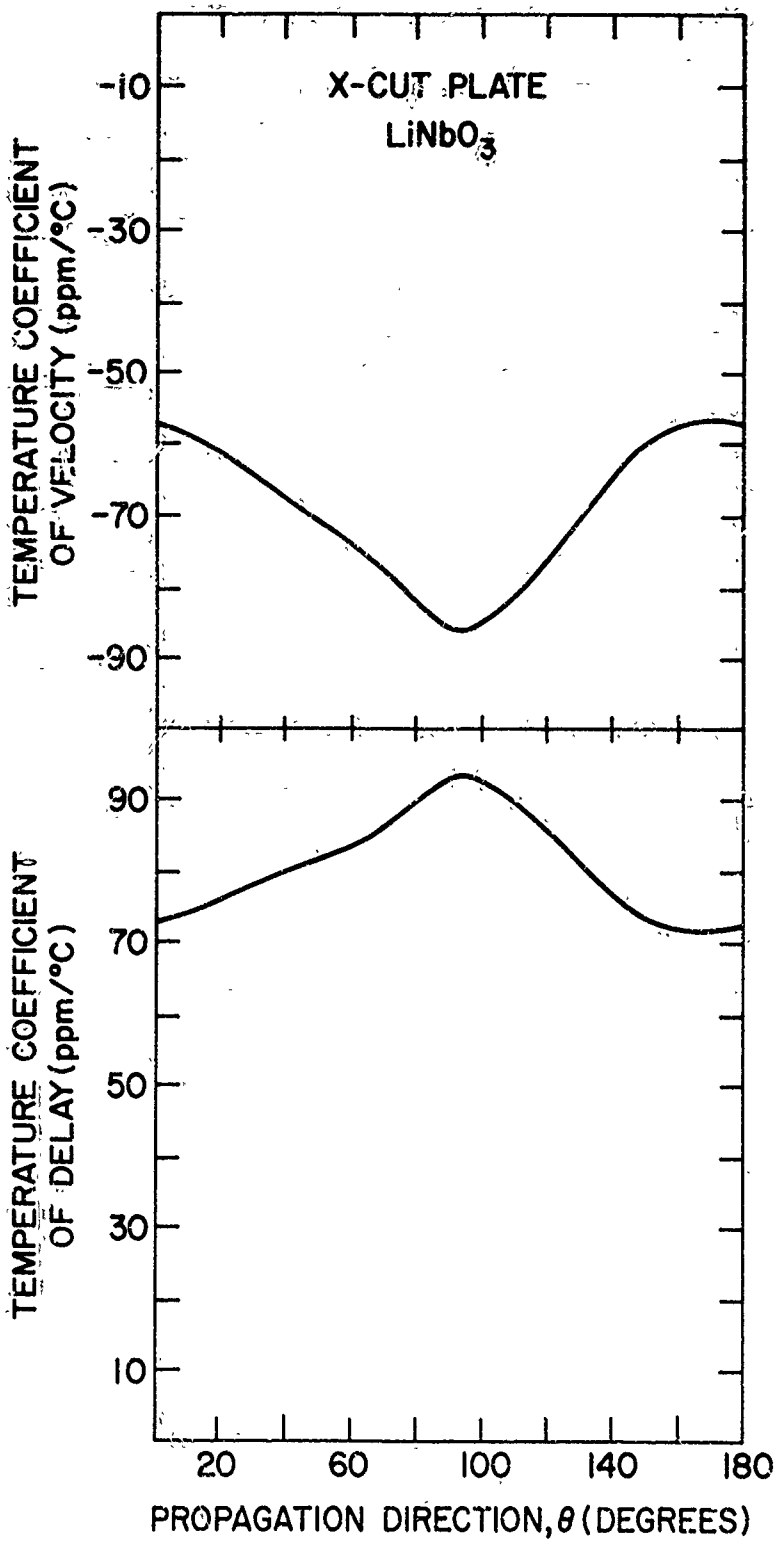
X-CUT PLATE
LiNbO3
TEMPERATURE COEFFICIENT OF VELOCITY (ppm/°C)
-10
-30
-50
-70
-90
TEMPERATURE COEFFICIENT OF DELAY (ppm/°C)
90
70
50
30
10
20
60
100
140
180
PROPAGATION DIRECTION, θ (DEGREES)

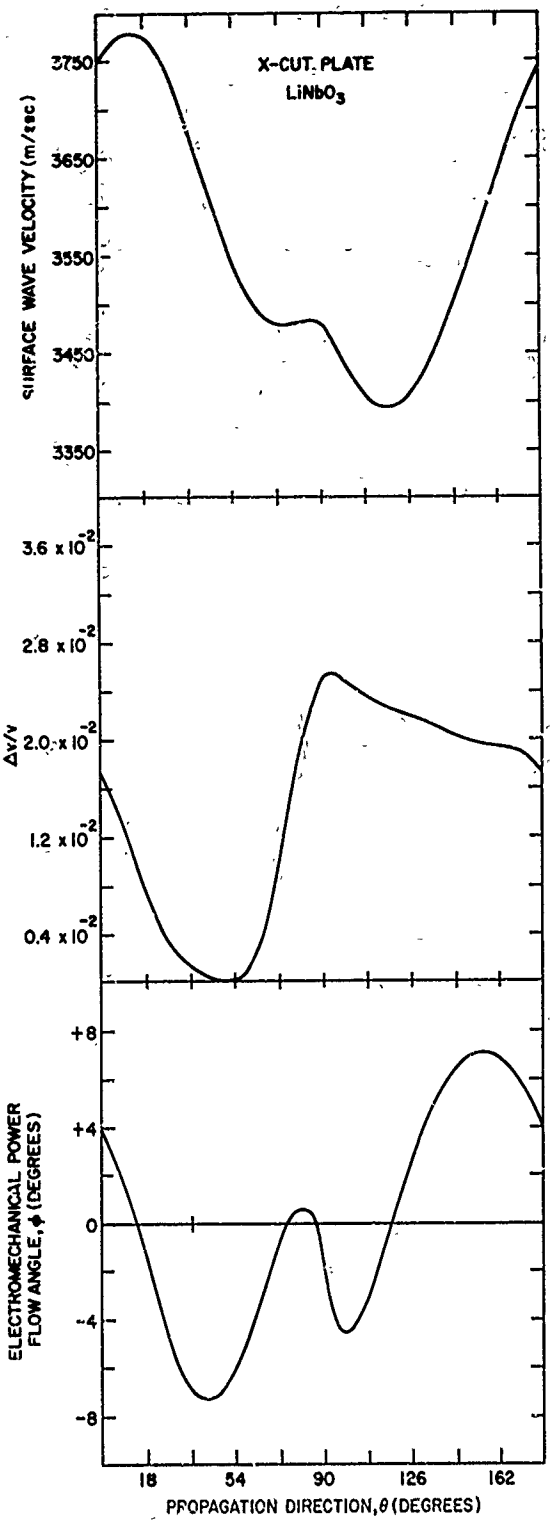
X-CUT PLATE
LiNbO3
SURFACE WAVE VELOCITY (m/sec)
3750
3650
3550
3450
3350
Δv/v
3.6 x 10-2
2.8 x 10-2
2.0 x 10-2
1.2 x 10-2
0.4 x 10-2
ELECTROMECHANICAL POWER FLOW ANGLE, ϕ (DEGREES)
+8
+4
0
-4
-8
18
54
90
126
162
PROPAGATION DIRECTION, θ (DEGREES)

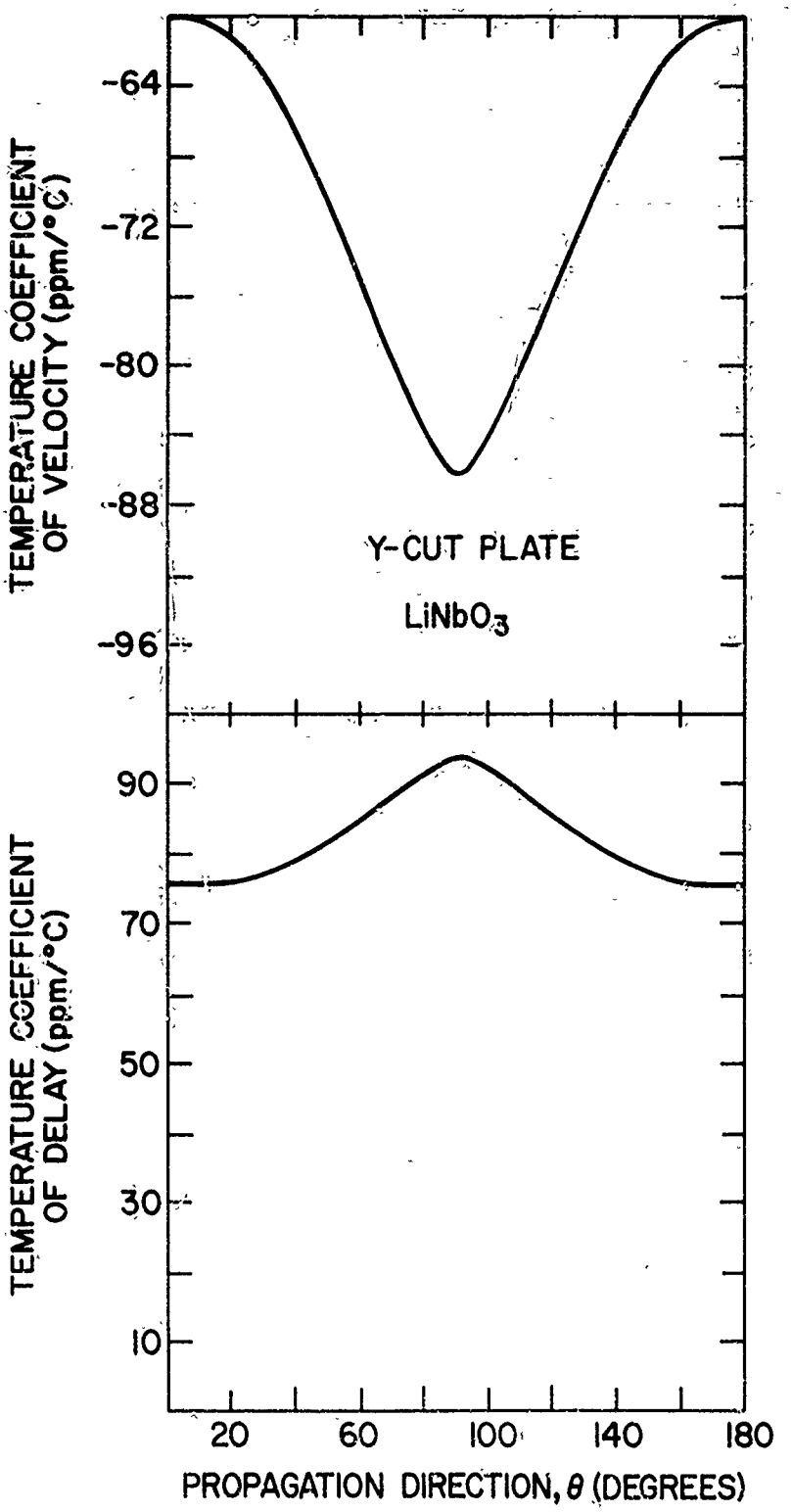
TEMPERATURE COEFFICIENT OF VELOCITY (ppm/°C)
-64
-72
-80
-88
-96
Y-CUT PLATE
LiNbO3
TEMPERATURE COEFFICIENT OF DELAY (ppm/°C)
90
70
50
30
10
20
60
100
140
180
PROPAGATION DIRECTION, θ (DEGREES)

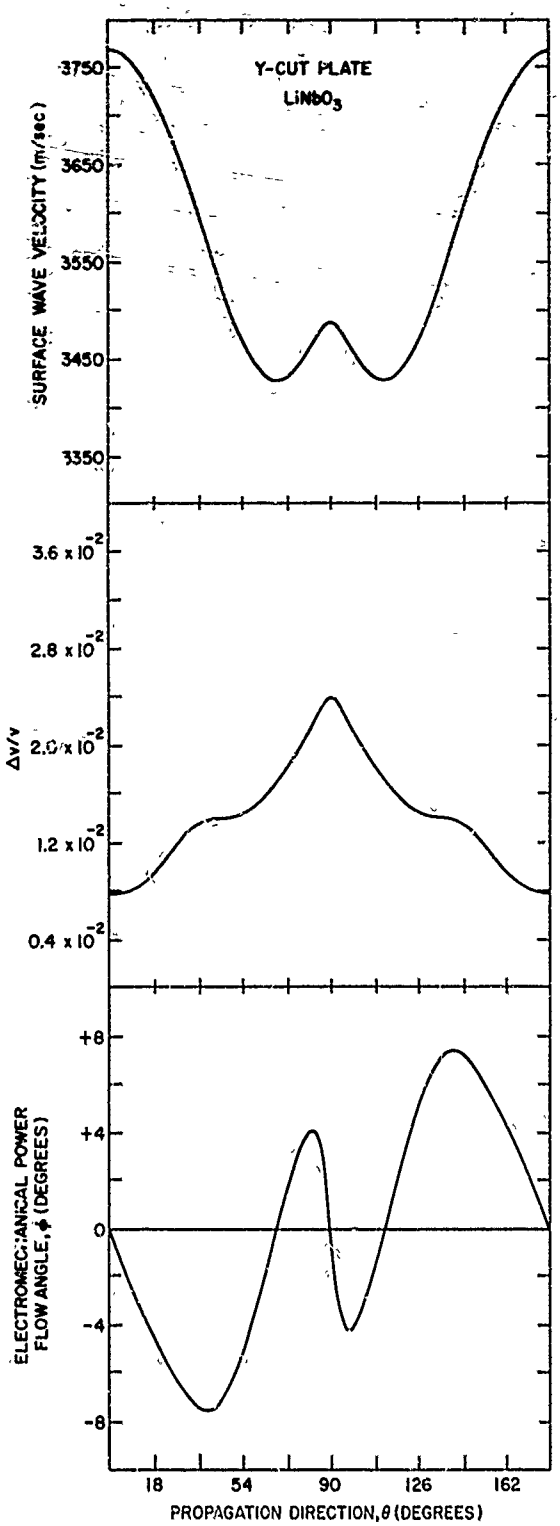
Y-CUT PLATE
LiNbO3
SURFACE WAVE VELOCITY (m/sec)
3750
3650
3550
3450
3350
Δv/v
3.6 x 10^-2
2.8 x 10^-2
2.0 x 10^-2
1.2 x 10^-2
0.4 x 10^-2
ELECTROMECHANICAL POWER FLOW ANGLE, ϕ (DEGREES)
+8
+4
0
-4
-8
18
54
90
126
162
PROPAGATION DIRECTION, θ (DEGREES)

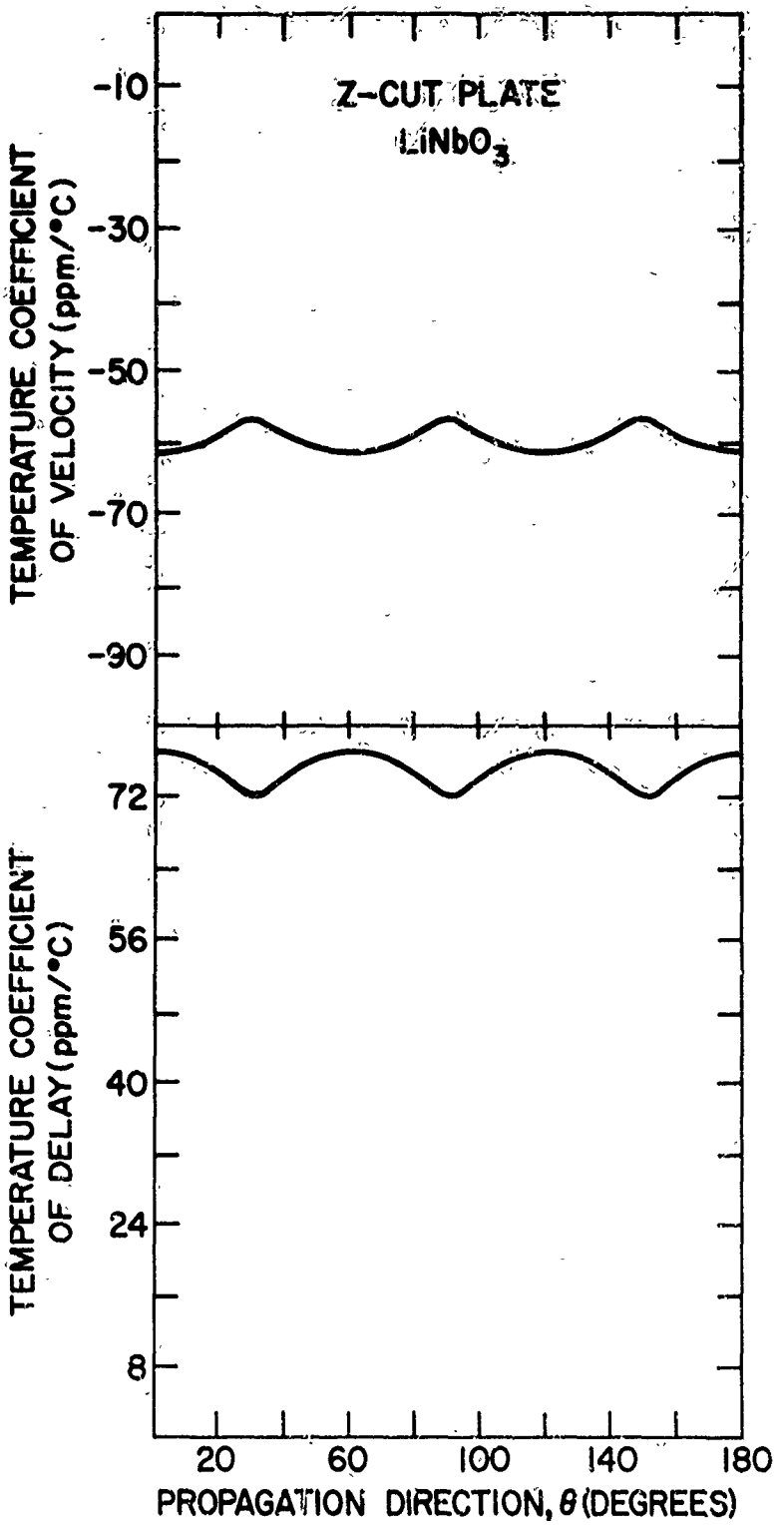
Z-CUT PLATE
LiNbO3
TEMPERATURE COEFFICIENT OF VELOCITY (ppm/°C)
-10
-30
-50
-70
-90
TEMPERATURE COEFFICIENT OF DELAY (ppm/°C)
72
56
40
24
8
20
60
100
140
180
PROPAGATION DIRECTION, θ (DEGREES)

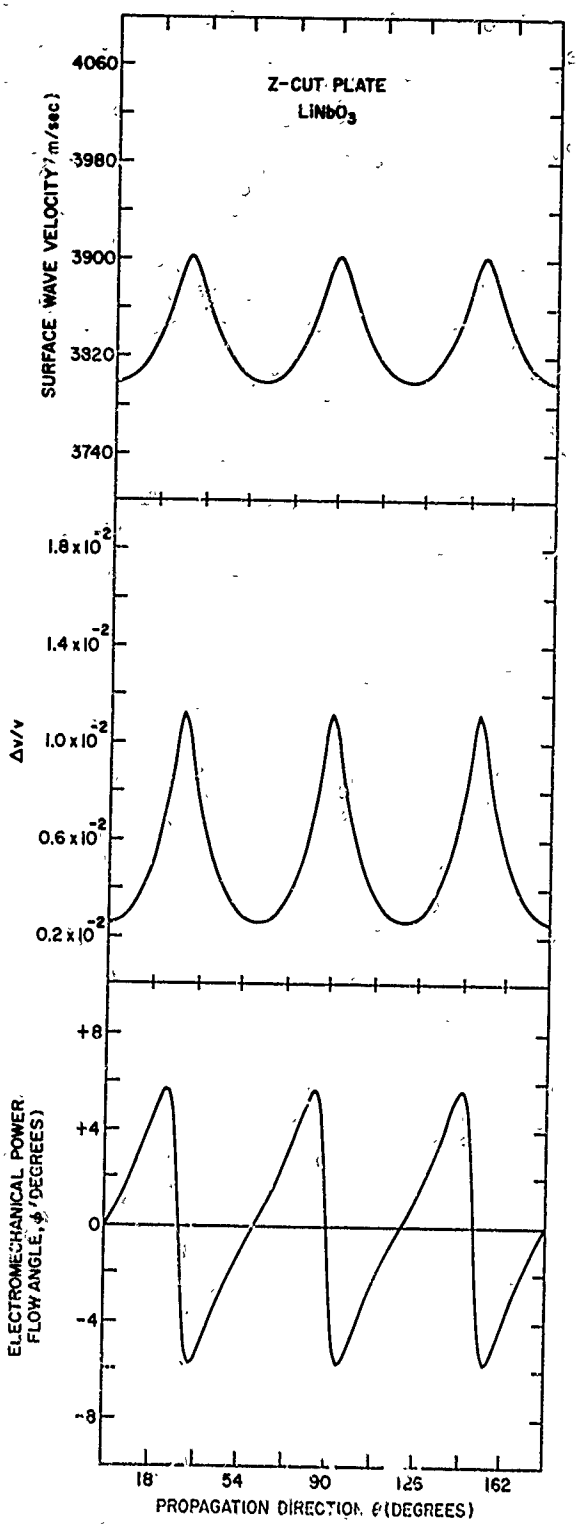
Z-CUT PLATE
LiNbO3
SURFACE WAVE VELOCITY (m/sec)
4060
3980
3900
3820
3740
Δv/v
1.8 x 10-2
1.4 x 10-2
1.0 x 10-2
0.6 x 10-2
0.2 x 10-2
ELECTROMECHANICAL POWER FLOW ANGLE, ψ (DEGREES)
+8
+4
0
-4
-8
18
54
90
125
162
PROPAGATION DIRECTION θ (DEGREES)

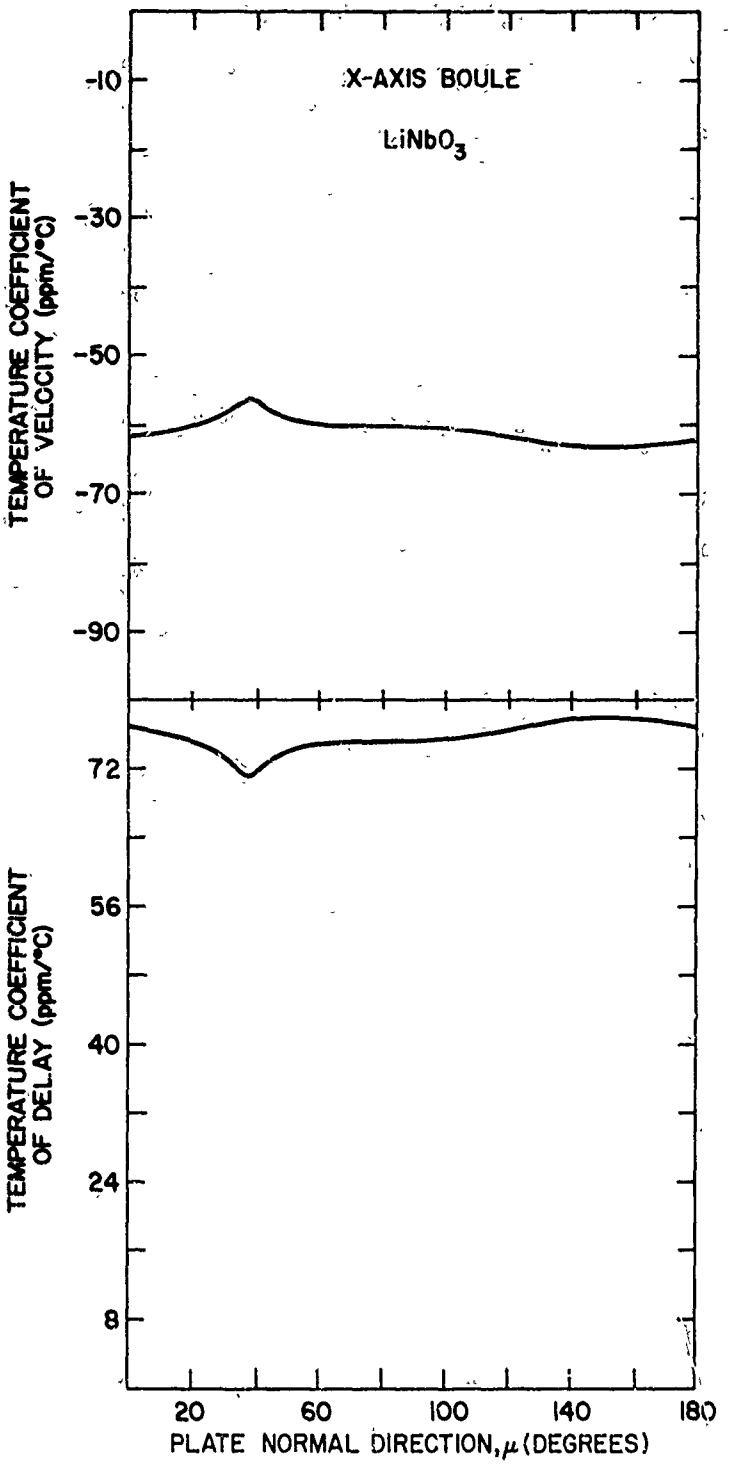
X-AXIS BOULE
LiNbO3
TEMPERATURE COEFFICIENT OF VELOCITY (ppm/°C)
-10
-30
-50
-70
-90
TEMPERATURE COEFFICIENT OF DELAY (ppm/°C)
72
56
40
24
8
20
60
100
140
180
PLATE NORMAL DIRECTION, μ (DEGREES)

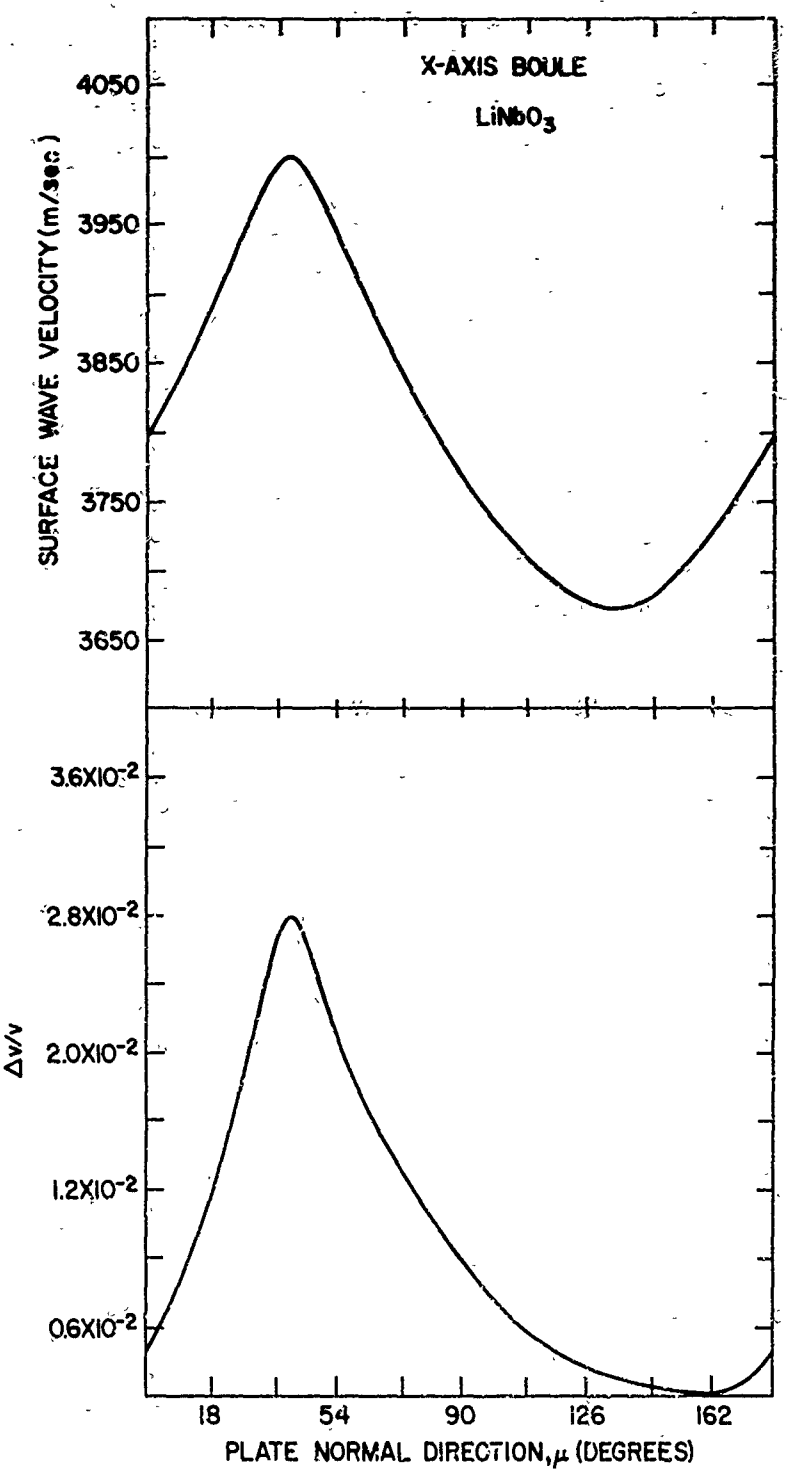

NOTE: TIME AVERAGE POWER FLOW ANGLE IDENTICALLY ZERO.

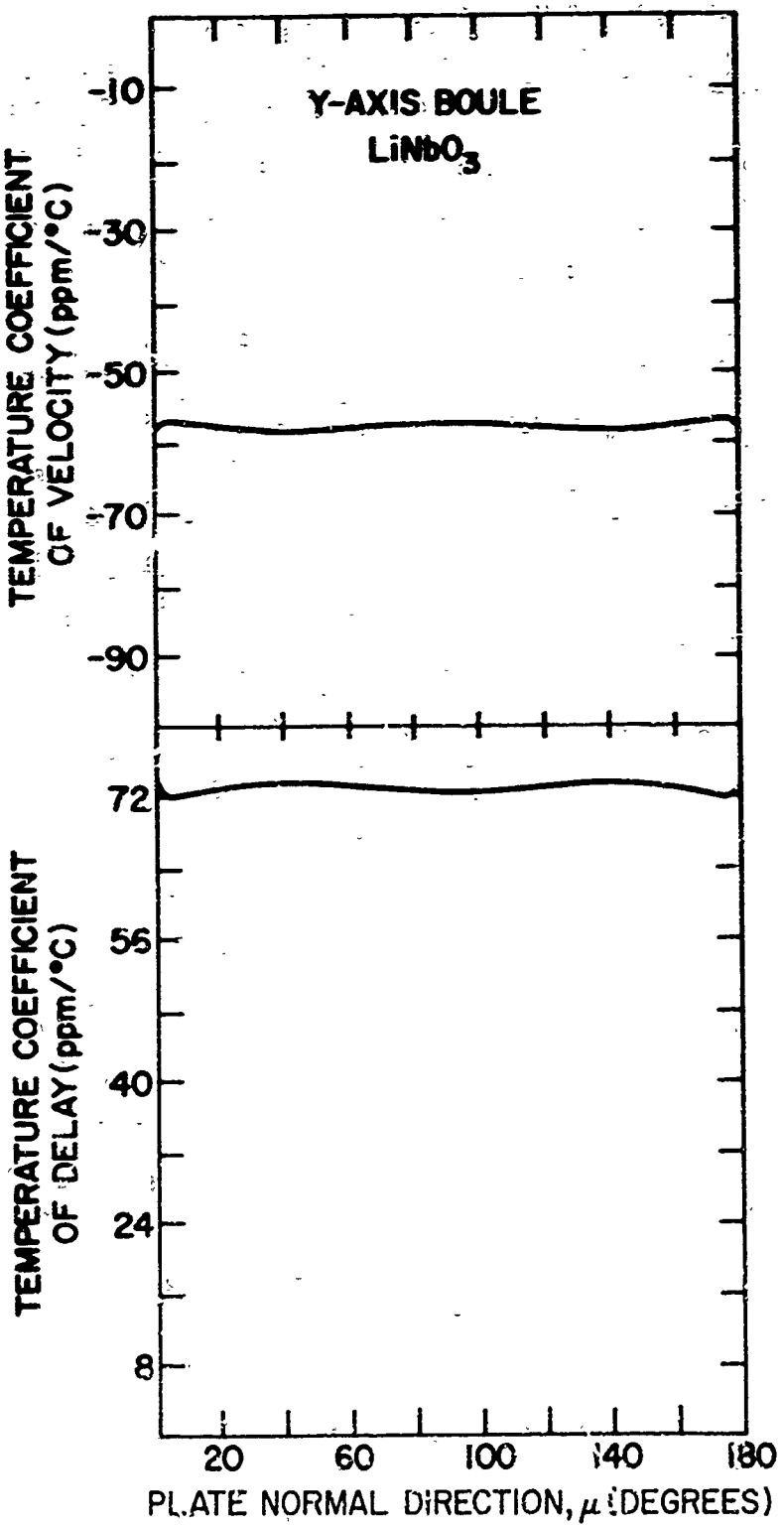
Y-AXIS BOULE
LiNbO3
TEMPERATURE COEFFICIENT OF VELOCITY (ppm/°C)
-10
-30
-50
-70
-90
TEMPERATURE COEFFICIENT OF DELAY (ppm/°C)
72
56
40
24
8
20
60
100
140
180
PLATE NORMAL DIRECTION, μ (DEGREES)

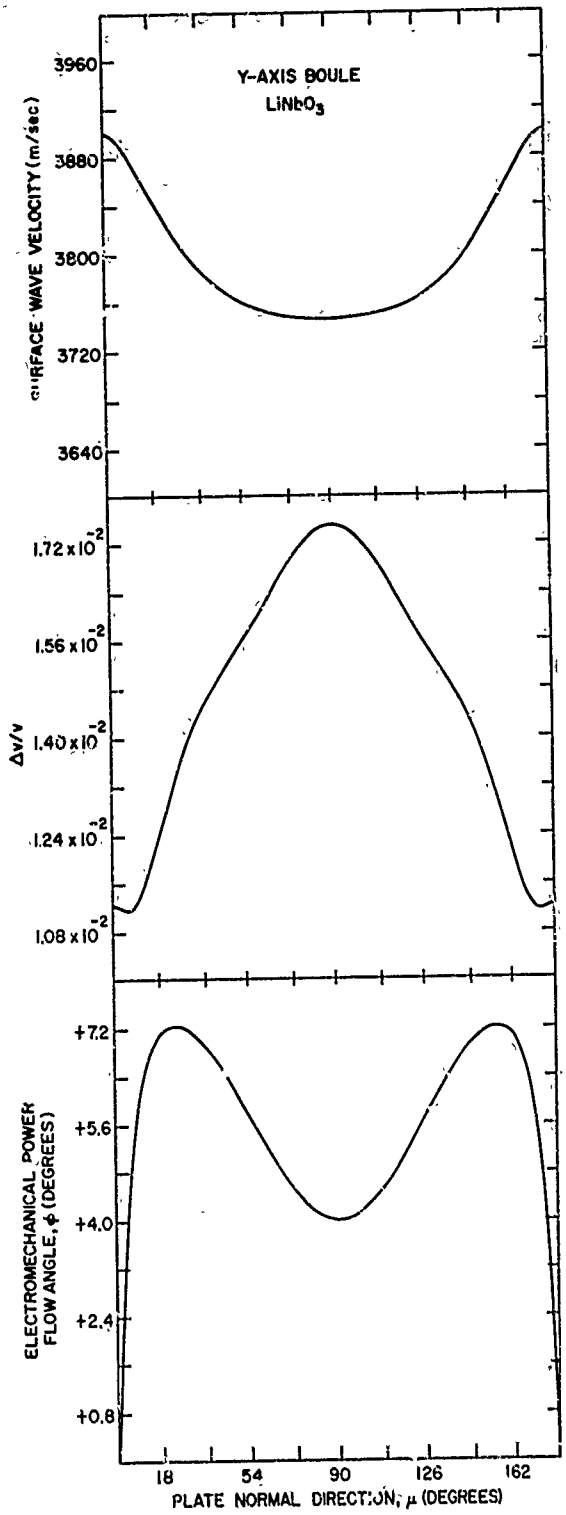
Y-AXIS BOULE
LiNbO3
SURFACE WAVE VELOCITY (m/sec)
3960
3880
3800
3720
3640
Δv/v
1.72 x 10-2
1.56 x 10-2
1.40 x 10-2
1.24 x 10-2
1.08 x 10-2
ELECTROMECHANICAL POWER FLOW ANGLE, φ (DEGREES)
+7.2
+5.6
+4.0
+2.4
+0.8
18
54
90
126
162
PLATE NORMAL DIRECTION, μ (DEGREES)

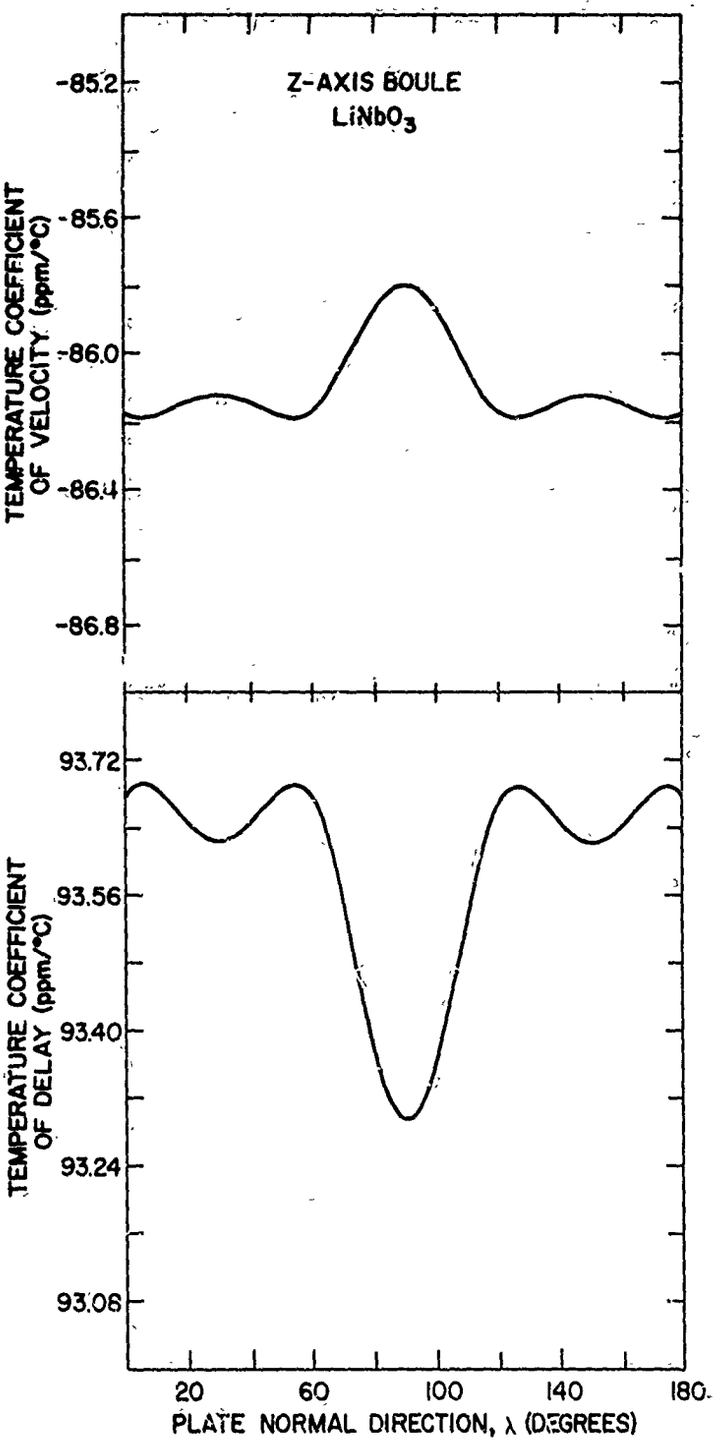
Z-AXIS BOULE
LiNbO3
TEMPERATURE COEFFICIENT OF VELOCITY (ppm/°C)
-85.2
-85.6
-86.0
-86.4
-86.8
TEMPERATURE COEFFICIENT OF DELAY (ppm/°C)
93.72
93.56
93.40
93.24
93.08
20
60
100
140
180
PLATE NORMAL DIRECTION, λ (DEGREES)

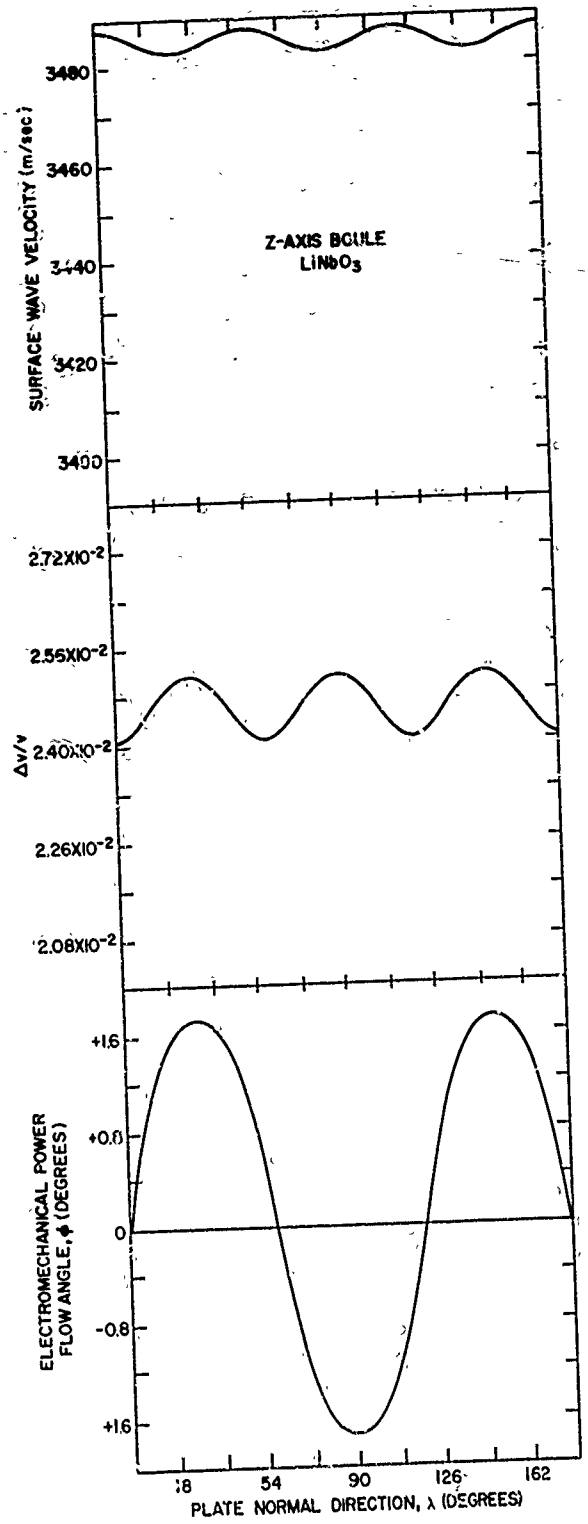
Z-AXIS BOULE
LiNbO3
SURFACE WAVE VELOCITY (m/sec)
3480
3460
3440
3420
3400
Δv/v
2.72X10-2
2.55X10-2
2.40X10-2
2.26X10-2
2.08X10-2
ELECTROMECHANICAL POWER FLOW ANGLE, φ (DEGREES)
+1.6
+0.8
0
-0.8
+1.6
18
54
90
126
162
PLATE NORMAL DIRECTION, λ (DEGREES)

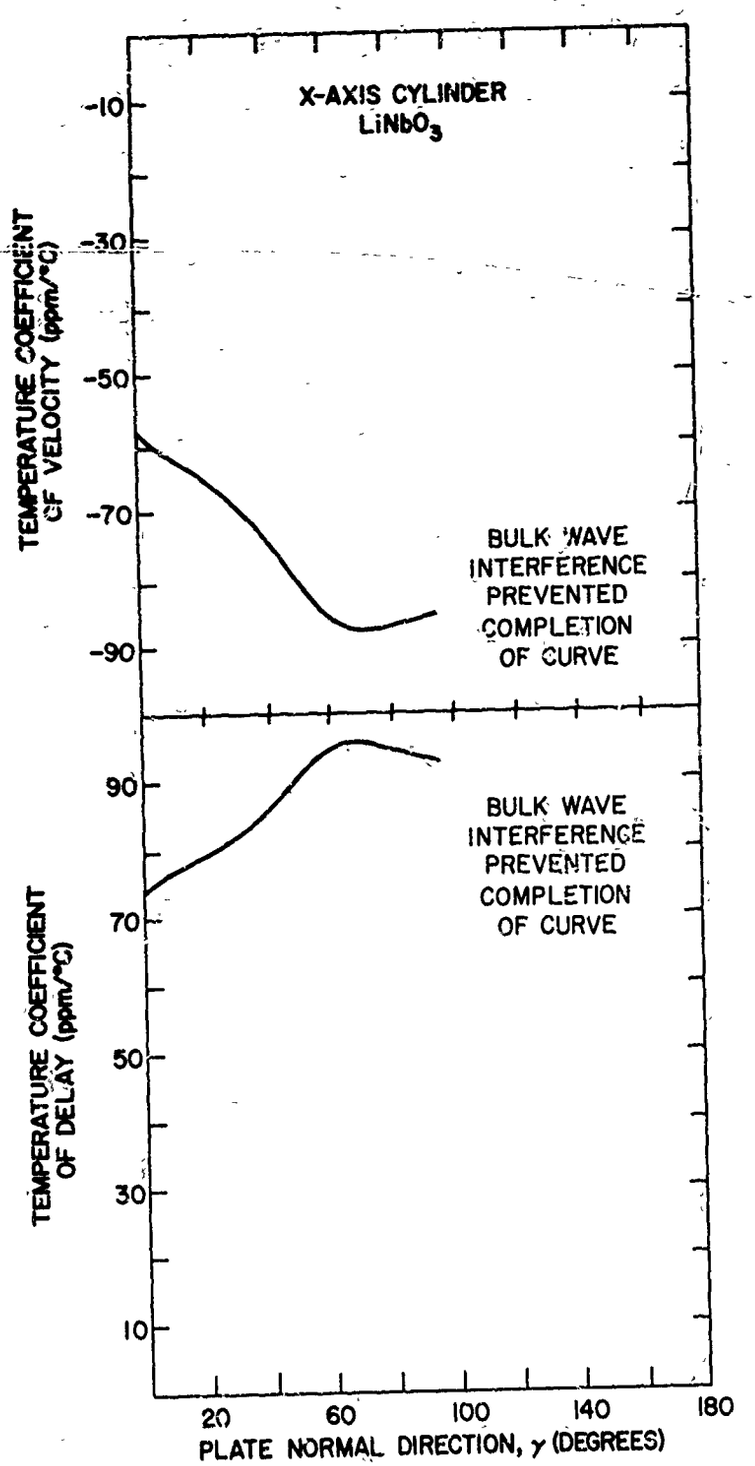
X-AXIS CYLINDER
LiNbO3
-10
-30
-50
-70
-90
TEMPERATURE COEFFICIENT OF VELOCITY (ppm/°C)
BULK WAVE INTERFERENCE PREVENTED COMPLETION OF CURVE
90
70
50
30
10
TEMPERATURE COEFFICIENT OF DELAY (ppm/°C)
BULK WAVE INTERFERENCE PREVENTED COMPLETION OF CURVE
20
60
100
140
180
PLATE NORMAL DIRECTION, γ (DEGREES)

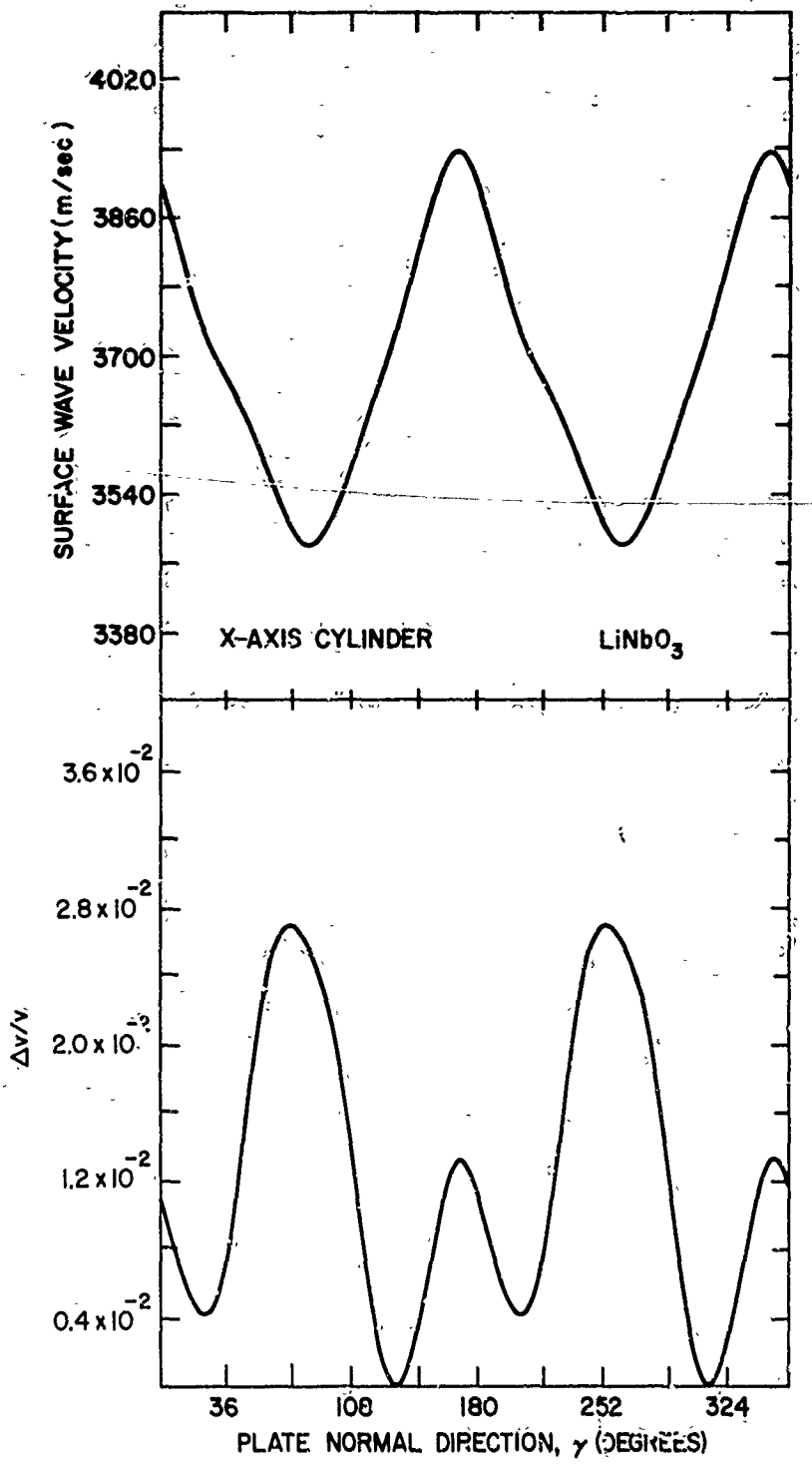

NOTE: TIME AVERAGE POWER FLOW ANGLE IDENTICALLY ZERO.

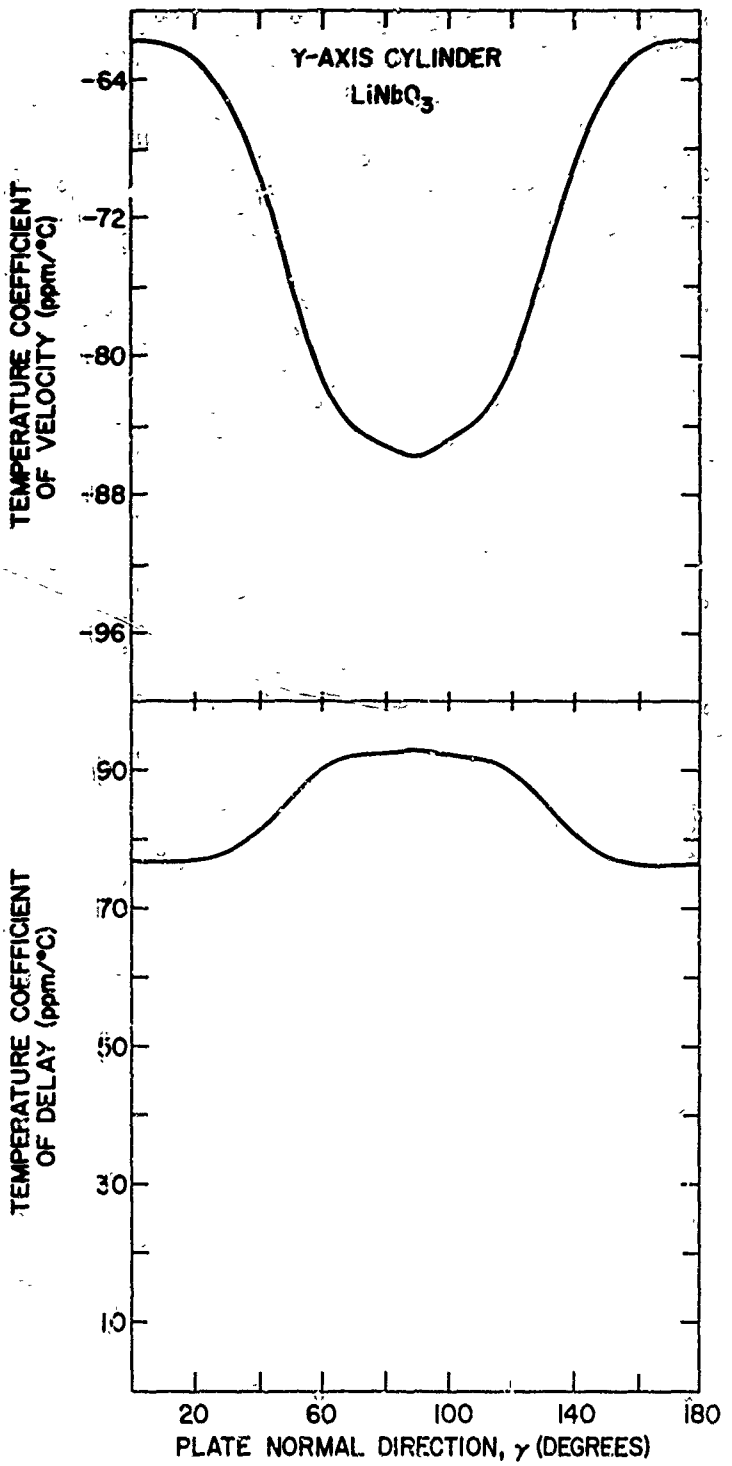
Y-AXIS CYLINDER
LiNbO3
TEMPERATURE COEFFICIENT OF VELOCITY (ppm/°C)
-64
-72
-80
-88
-96
TEMPERATURE COEFFICIENT OF DELAY (ppm/°C)
90
70
50
30
10
20
60
100
140
180
PLATE NORMAL DIRECTION, γ (DEGREES)

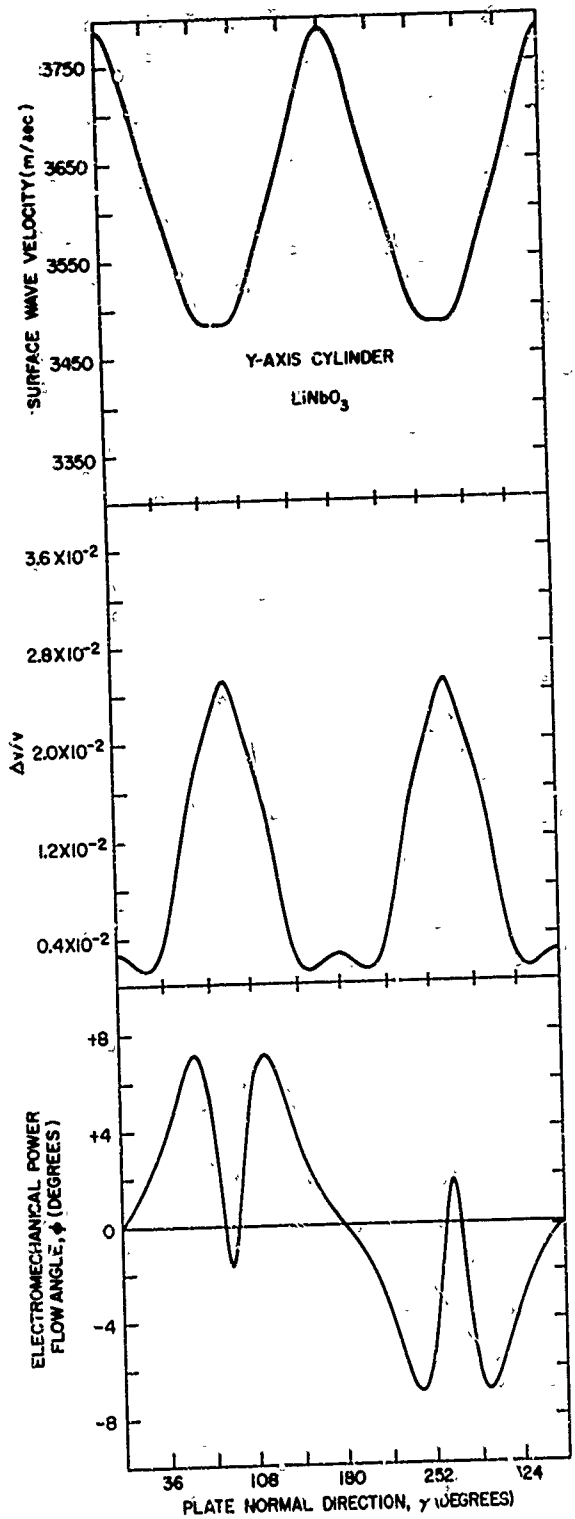
SURFACE WAVE VELOCITY (m/sec)
3750
3650
3550
3450
3350
Y-AXIS CYLINDER
LiNbO3
Δv/v
3.6X10-2
2.8X10-2
2.0X10-2
1.2X10-2
0.4X10-2
ELECTROMECHANICAL POWER FLOW ANGLE, ϕ (DEGREES)
+8
+4
0
-4
-8
36
108
180
252
124
PLATE NORMAL DIRECTION, γ (DEGREES)

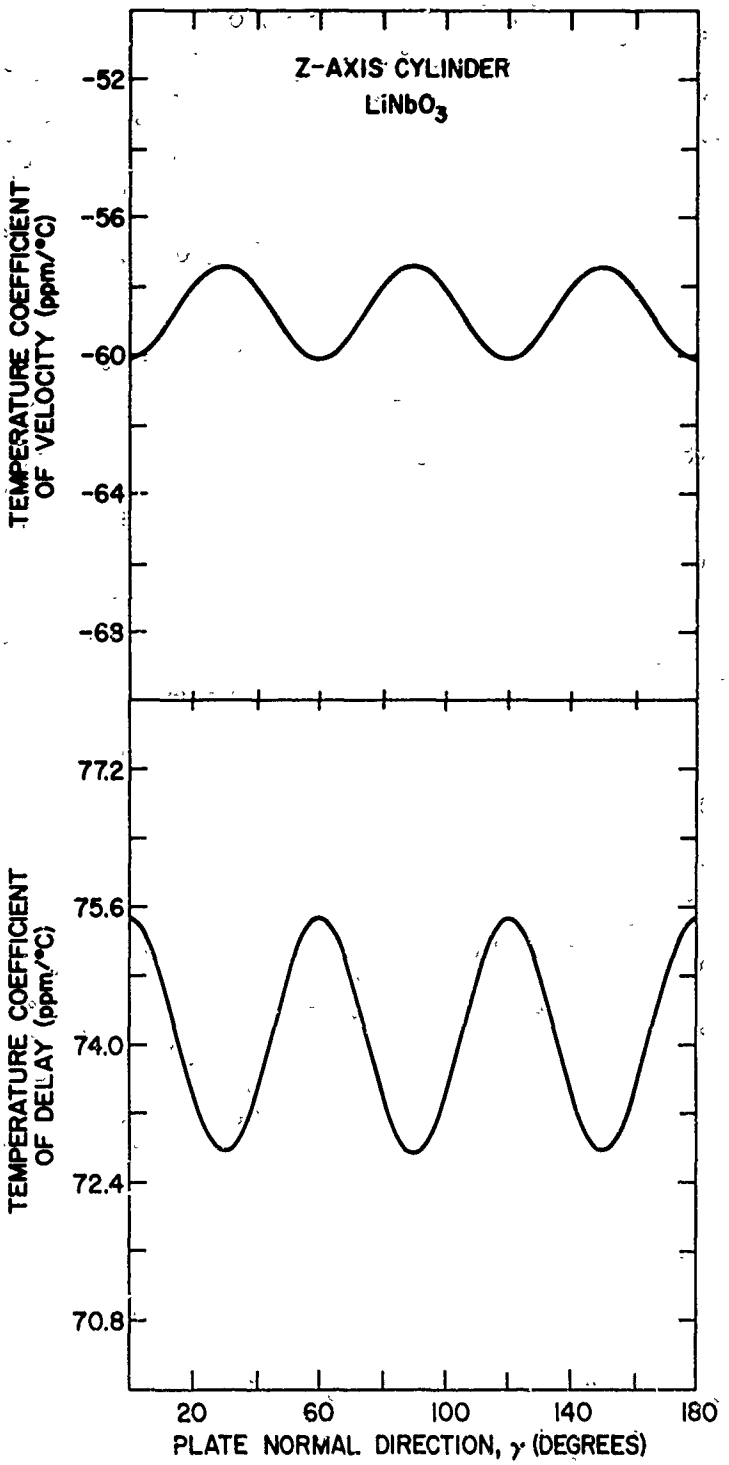
Z-AXIS CYLINDER
LiNbO3
TEMPERATURE COEFFICIENT OF VELOCITY (ppm/°C)
-52
-56
-60
-64
-68
TEMPERATURE COEFFICIENT OF DELAY (ppm/°C)
77.2
75.6
74.0
72.4
70.8
20
60
100
140
180
PLATE NORMAL DIRECTION, γ (DEGREES)

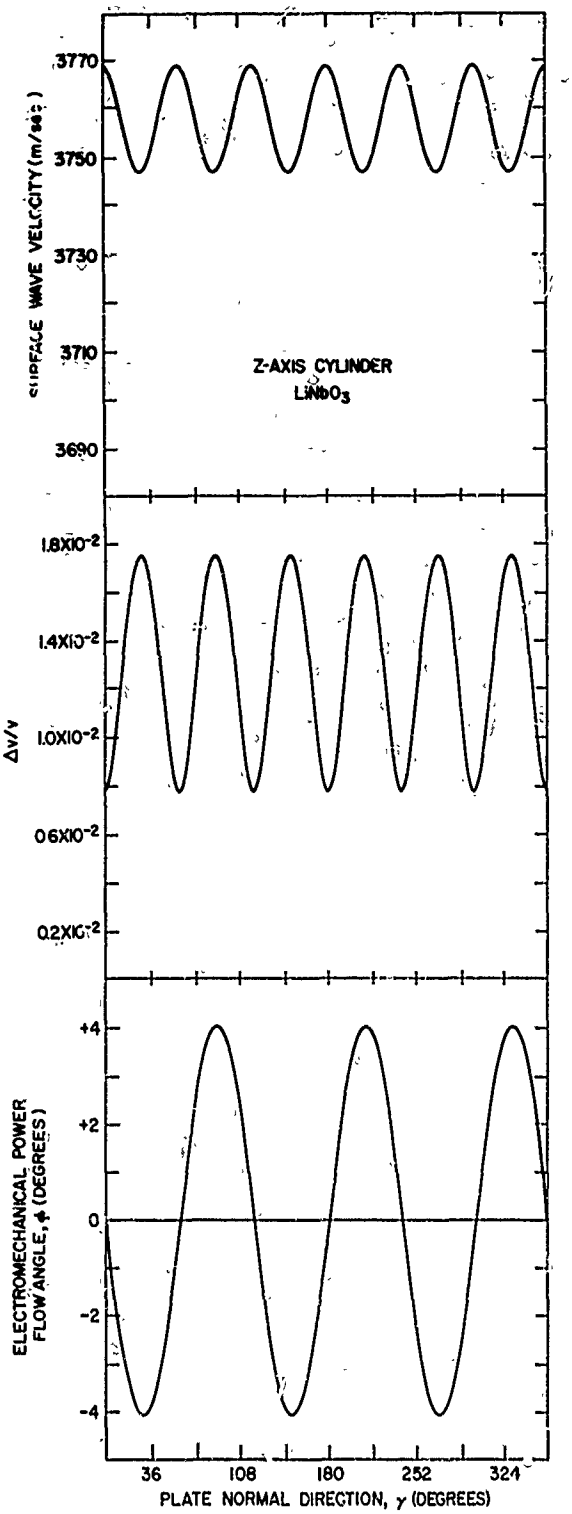
3770
3750
3730
3710
3690
Z-AXIS CYLINDER
LiNbO3
1.8X10-2
1.4X10-2
1.0X10-2
0.6X10-2
0.2X10-2
Δv/v
+4
+2
0
-2
-4
ELECTROMECHANICAL POWER FLOW ANGLE, ϕ (DEGREES)
36
108
180
252
324
PLATE NORMAL DIRECTION, γ (DEGREES)

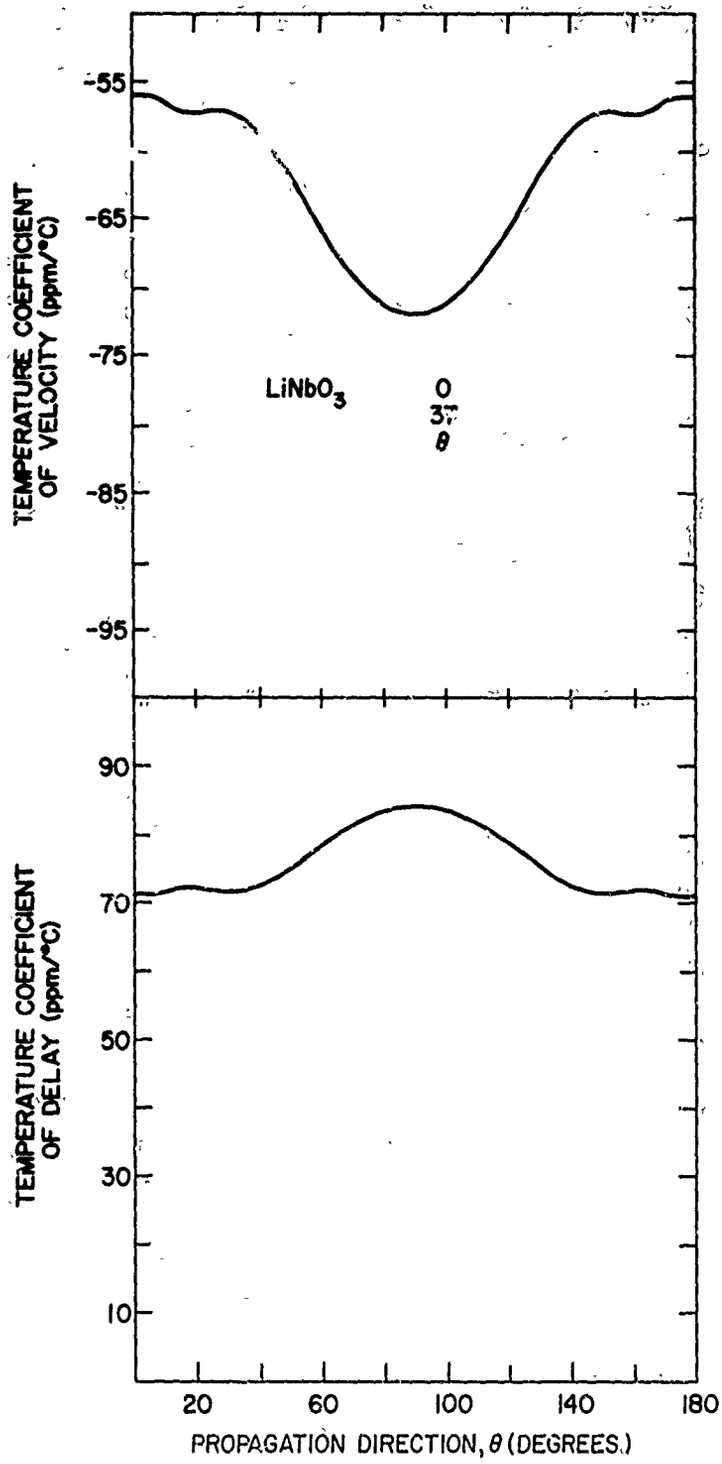
-55
-65
-75
-85
-95
TEMPERATURE COEFFICIENT OF VELOCITY (ppm/°C)
LiNbO3
0
θ
90
70
50
30
10
TEMPERATURE COEFFICIENT OF DELAY (ppm/°C)
20
60
100
140
180
PROPAGATION DIRECTION, θ (DEGREES.)

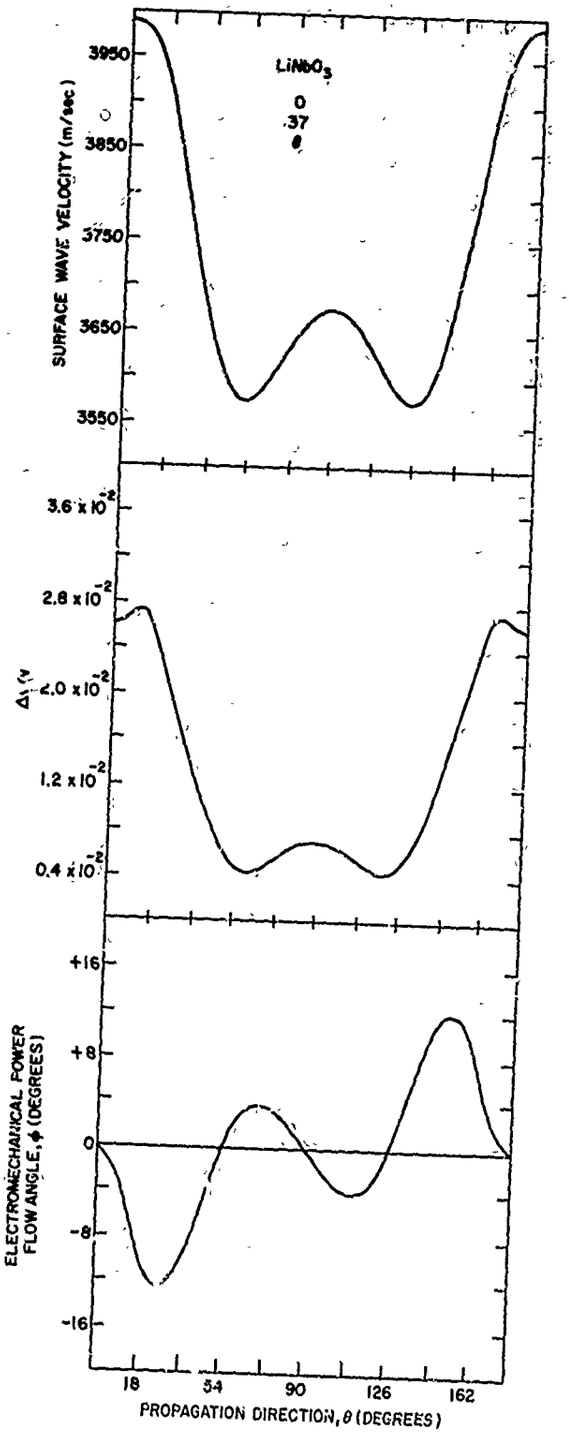
LiNbO3
0
37
θ
SURFACE WAVE VELOCITY (m/sec)
3950
3850
3750
3650
3550
3.6 x 10^-2
2.8 x 10^-2
2.0 x 10^-2
1.2 x 10^-2
0.4 x 10^-2
Δv/v
+16
+8
0
-8
-16
ELECTROMECHANICAL POWER FLOW ANGLE, φ (DEGREES)
18
54
90
126
162
PROPAGATION DIRECTION, θ (DEGREES)

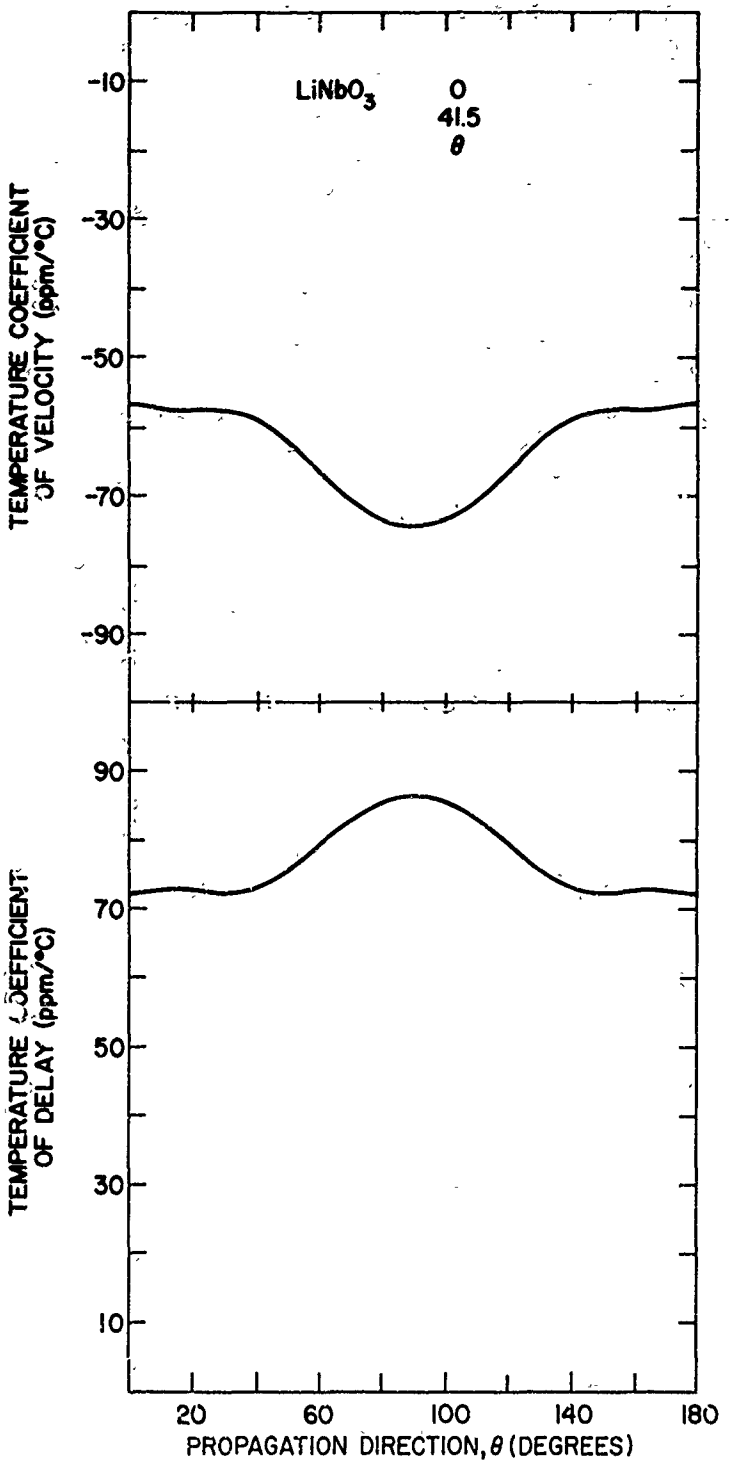
LiNbO3
0
41.5
θ
-10
-30
-50
-70
-90
TEMPERATURE COEFFICIENT OF VELOCITY (ppm/°C)
90
70
50
30
10
TEMPERATURE COEFFICIENT OF DELAY (ppm/°C)
20
60
100
140
180
PROPAGATION DIRECTION, θ (DEGREES)

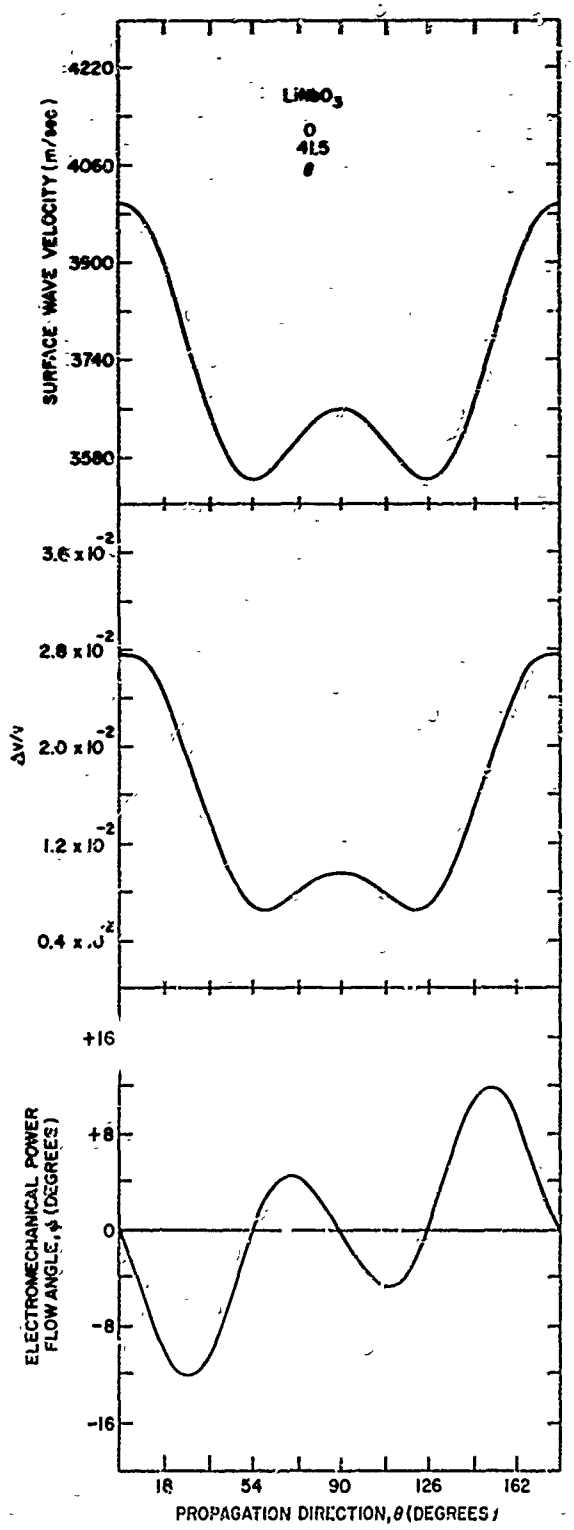
LiNbO3
0
41.5
θ
SURFACE WAVE VELOCITY (m/sec)
4220
4060
3900
3740
3580
Δv/v
3.6 x 10-2
2.8 x 10-2
2.0 x 10-2
1.2 x 10-2
0.4 x 10-2
+16
+8
0
-8
-16
ELECTROMECHANICAL POWER FLOW ANGLE, ψ (DEGREES)
18
54
90
126
162
PROPAGATION DIRECTION, θ (DEGREES)

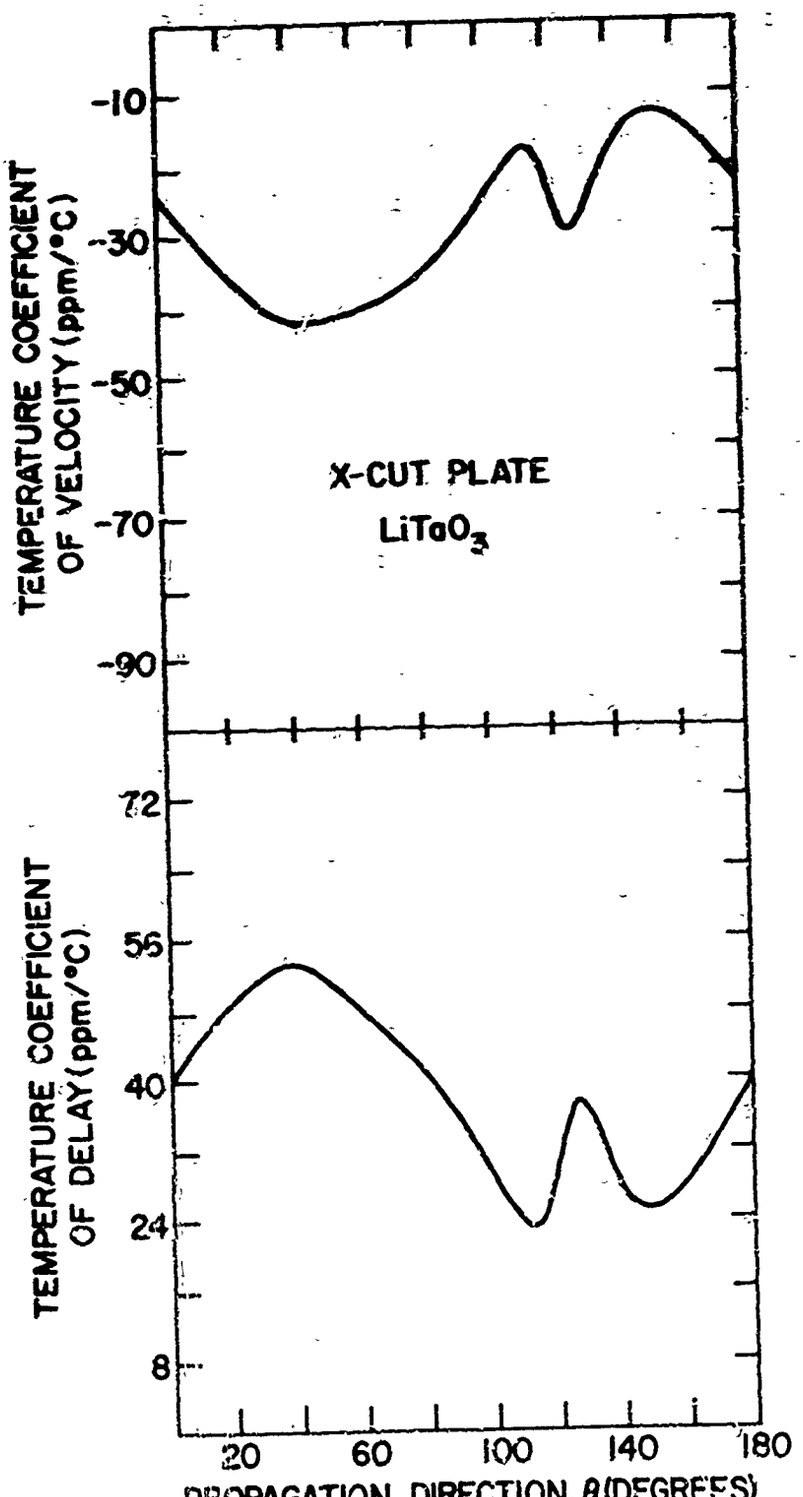
-10
-30
-50
-70
-90
TEMPERATURE COEFFICIENT OF VELOCITY (ppm/°C)
X-CUT PLATE
LiTaO3
72
56
40
24
8
TEMPERATURE COEFFICIENT OF DELAY (ppm/°C)
20
60
100
140
180
PROPAGATION DIRECTION, θ (DEGREES)

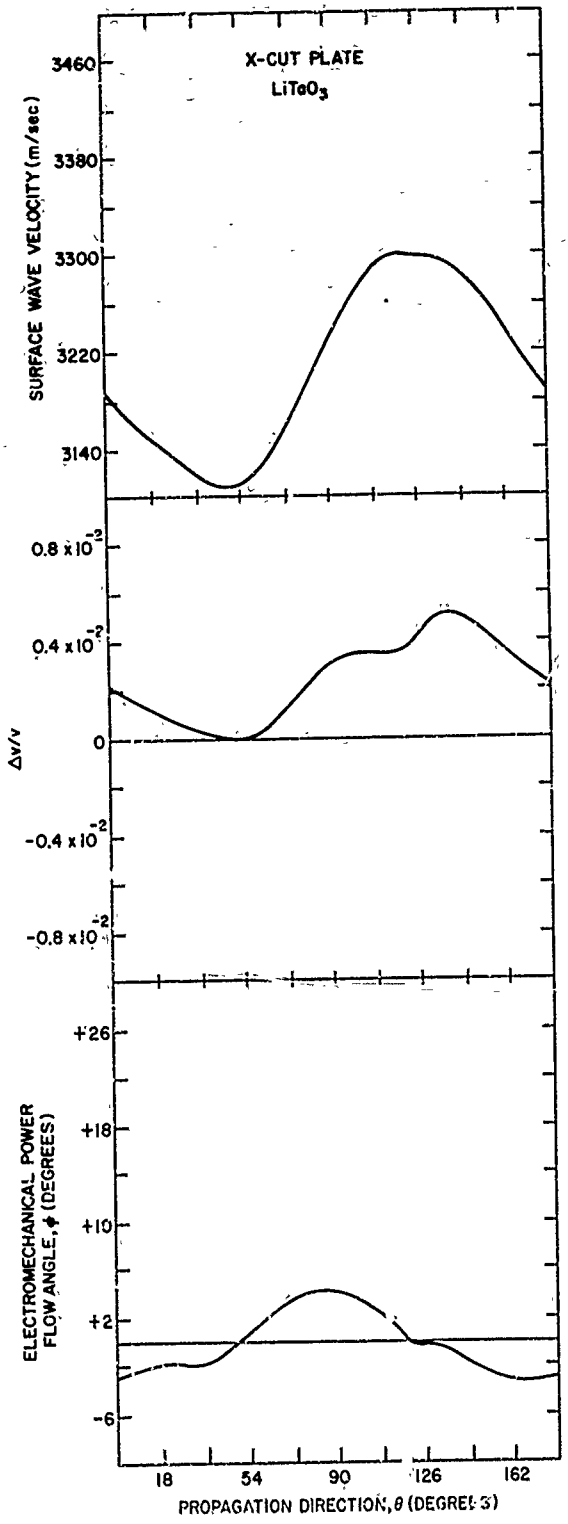
X-CUT PLATE
LiTaO3
SURFACE WAVE VELOCITY (m/sec)
3460
3380
3300
3220
3140
0.8 x10-3
0.4 x10-2
0
-0.4 x10-2
-0.8 x10-2
Δv/v
+26
+18
+10
+2
-6
ELECTROMECHANICAL POWER FLOW ANGLE, ϕ (DEGREES)
18
54
90
126
162
PROPAGATION DIRECTION, θ (DEGREES)

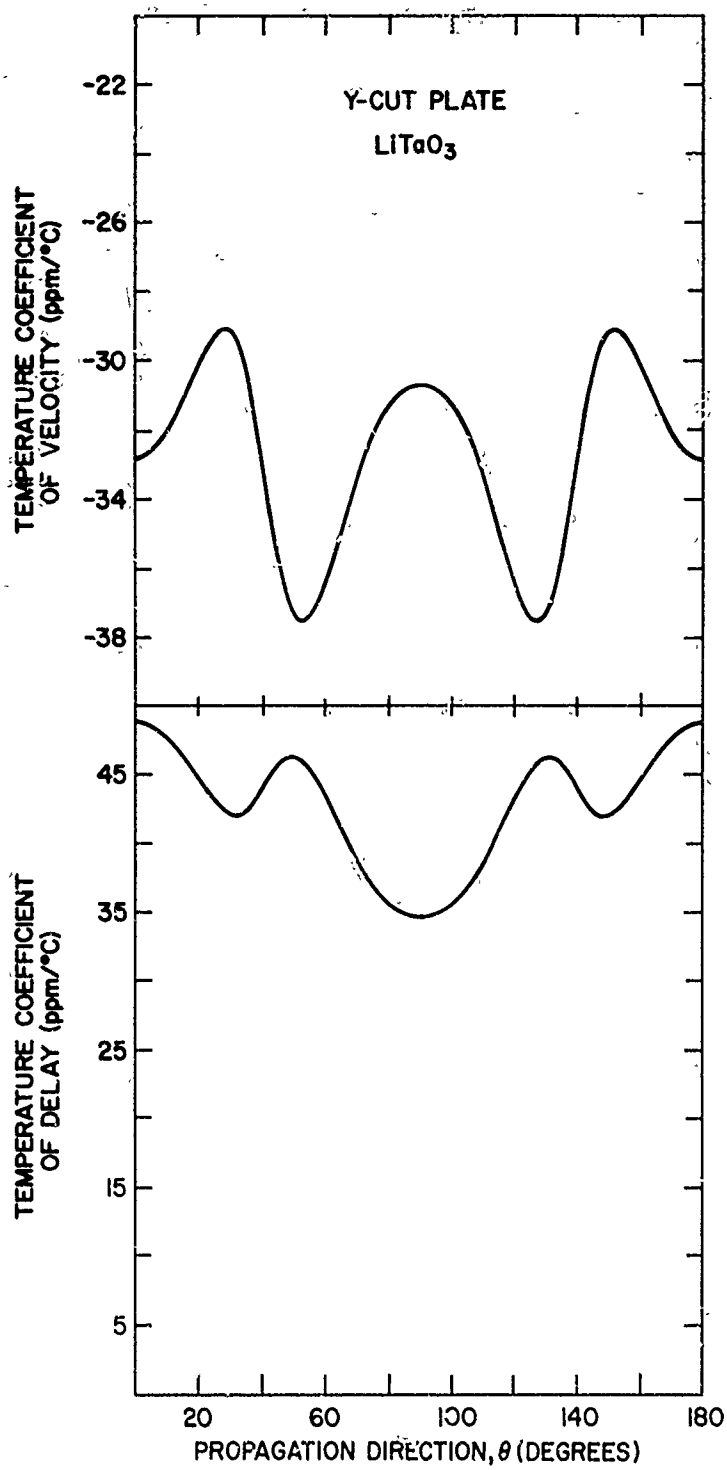
Y-CUT PLATE
LiTaO3
TEMPERATURE COEFFICIENT OF VELOCITY (ppm/°C)
-22
-26
-30
-34
-38
TEMPERATURE COEFFICIENT OF DELAY (ppm/°C)
45
35
25
15
5
20
60
100
140
180
PROPAGATION DIRECTION, θ (DEGREES)

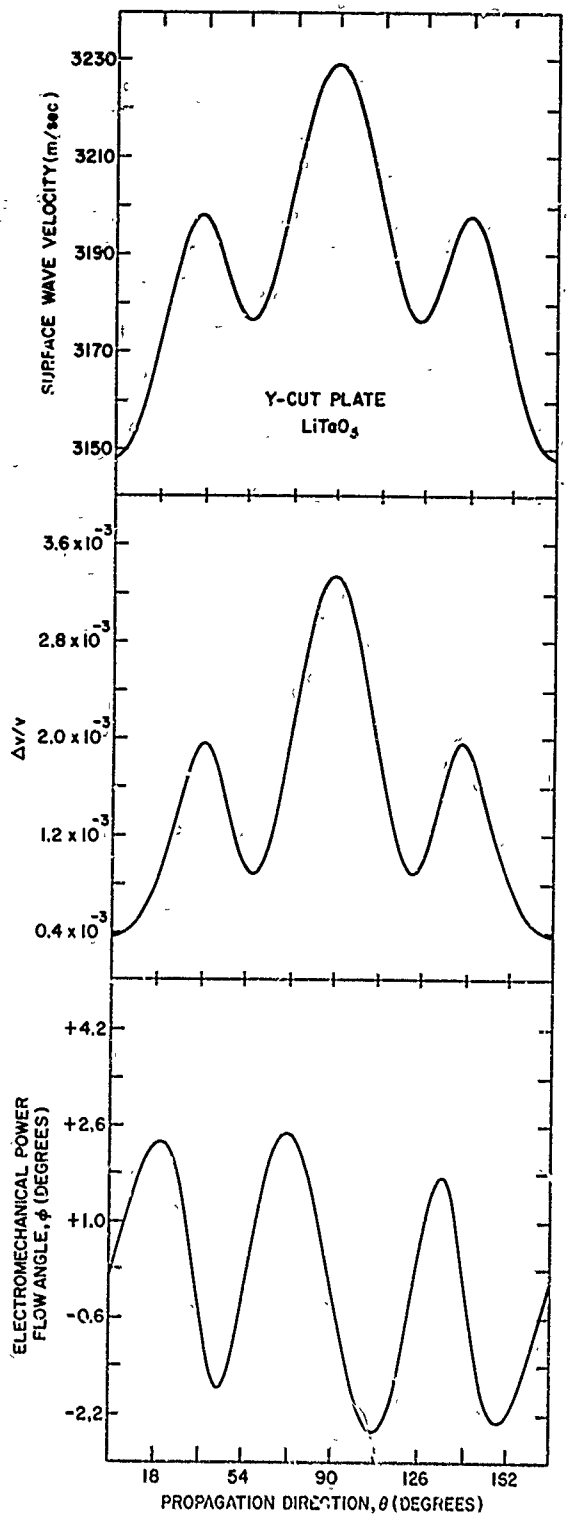
SURFACE WAVE VELOCITY (m/sec)
3230
3210
3190
3170
3150
Y-CUT PLATE
LiTaO3
Δv/v
3.6 x 10-3
2.8 x 10-3
2.0 x 10-3
1.2 x 10-3
0.4 x 10-3
ELECTROMECHANICAL POWER FLOW ANGLE, φ (DEGREES)
+4.2
+2.6
+1.0
-0.6
-2.2
18
54
90
126
152
PROPAGATION DIRECTION, θ (DEGREES)

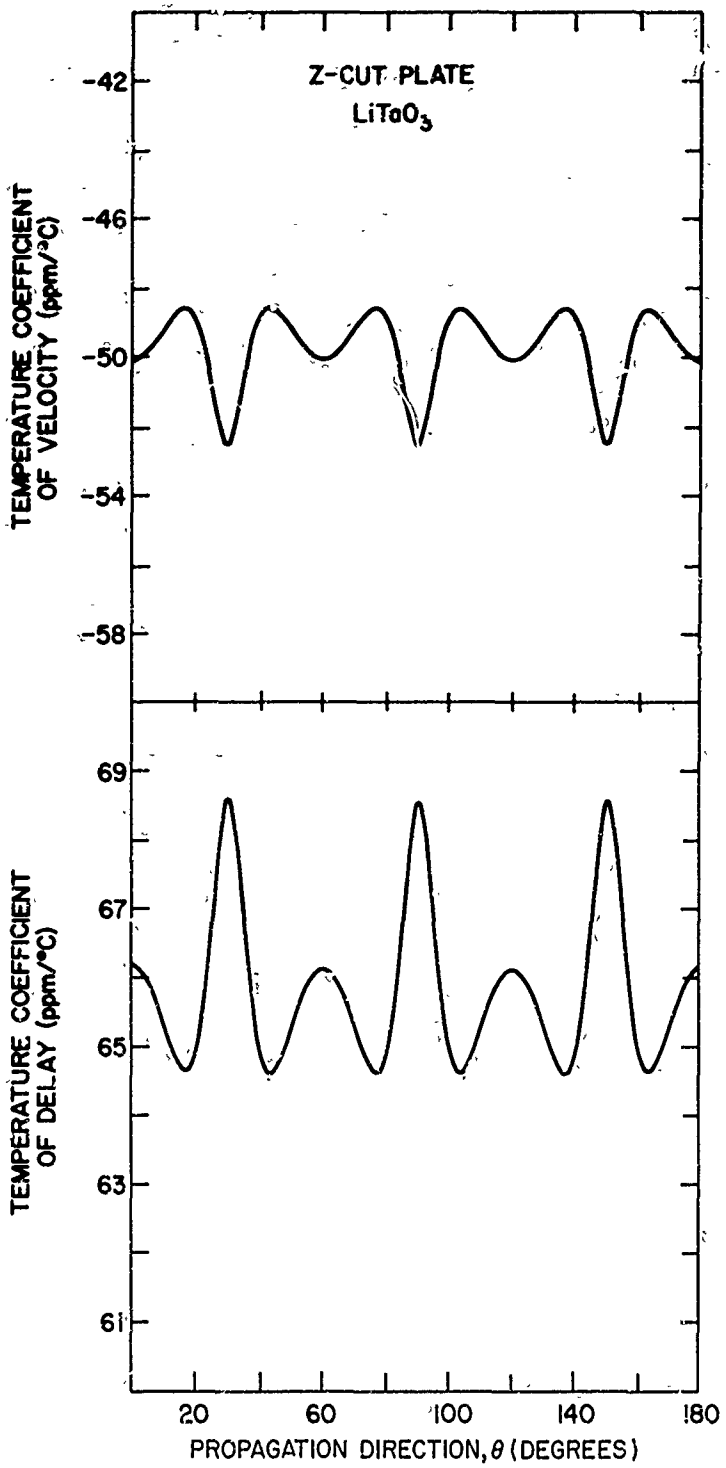
Z-CUT PLATE
LiTaO3
TEMPERATURE COEFFICIENT OF VELOCITY (ppm/°C)
-42
-46
-50
-54
-58
TEMPERATURE COEFFICIENT OF DELAY (ppm/°C)
69
67
65
63
61
20
60
100
140
180
PROPAGATION DIRECTION, θ (DEGREES)

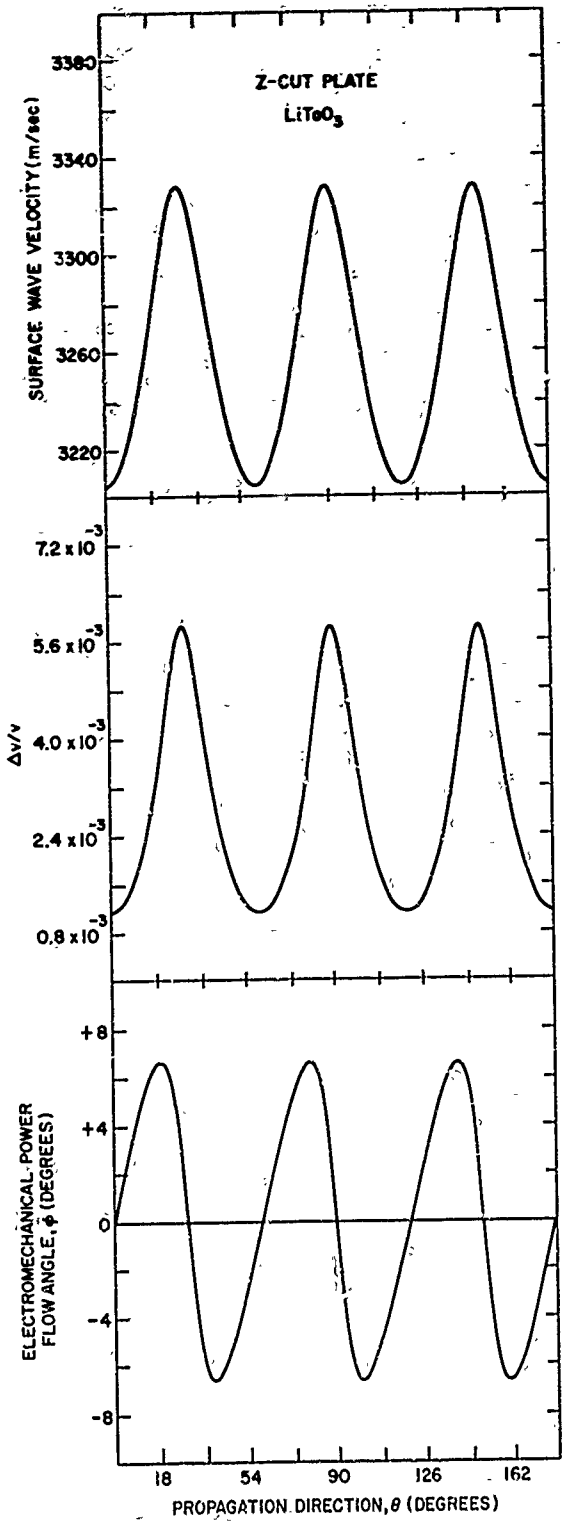
Z-CUT PLATE
LiTaO3
SURFACE WAVE VELOCITY (m/sec)
3380
3340
3300
3260
3220
Δv/v
7.2 x 10-3
5.6 x 10-3
4.0 x 10-3
2.4 x 10-3
0.8 x 10-3
ELECTROMECHANICAL POWER FLOW ANGLE, ϕ (DEGREES)
+8
+4
0
-4
-8
18
54
90
126
162
PROPAGATION DIRECTION, θ (DEGREES)

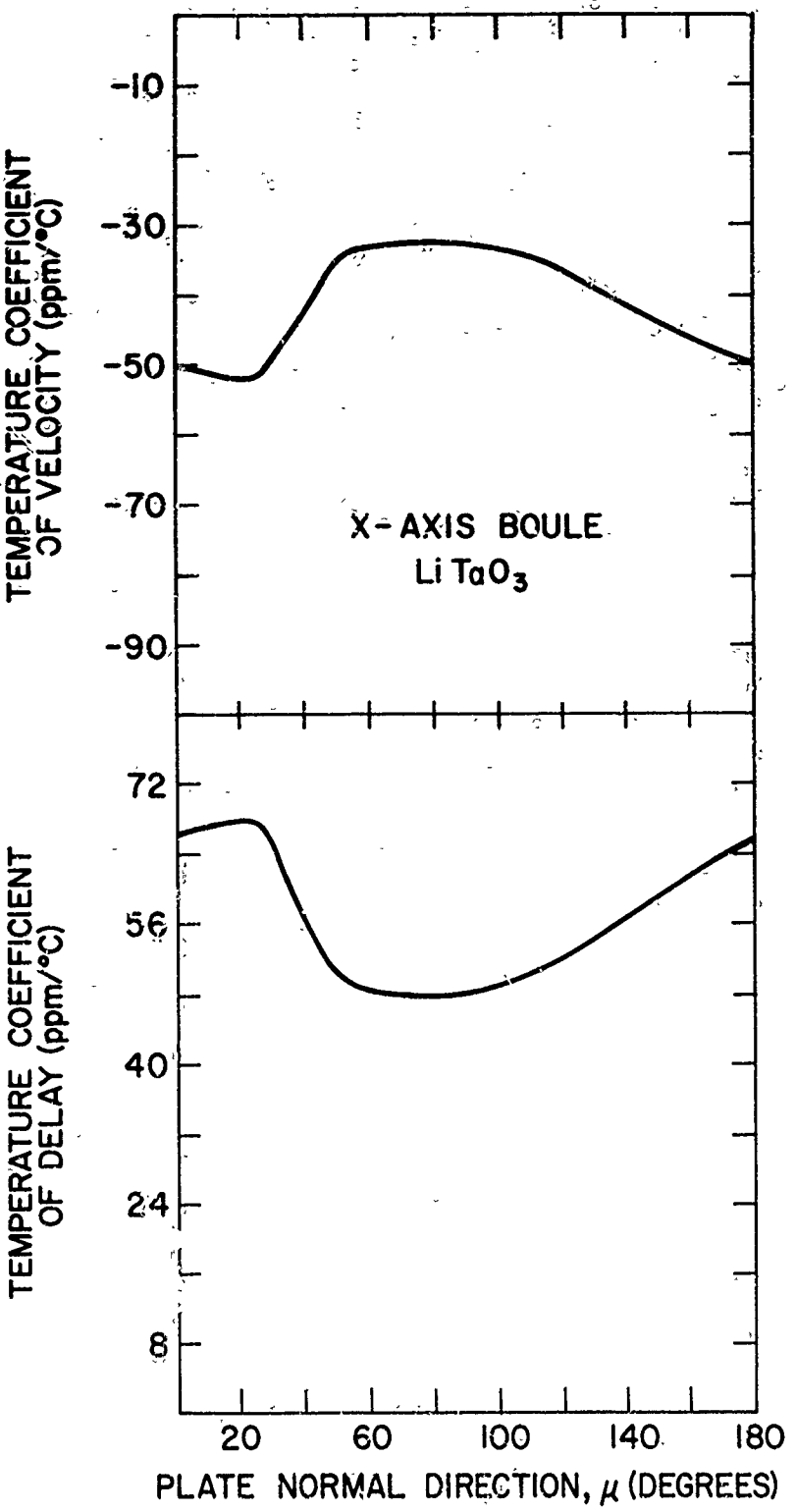
TEMPERATURE COEFFICIENT OF VELOCITY (ppm/°C)
-10
-30
-50
-70
-90
X-AXIS BOULE
LiTaO3
TEMPERATURE COEFFICIENT OF DELAY (ppm/°C)
72
56
40
24
8
20
60
100
140
180
PLATE NORMAL DIRECTION, μ (DEGREES)

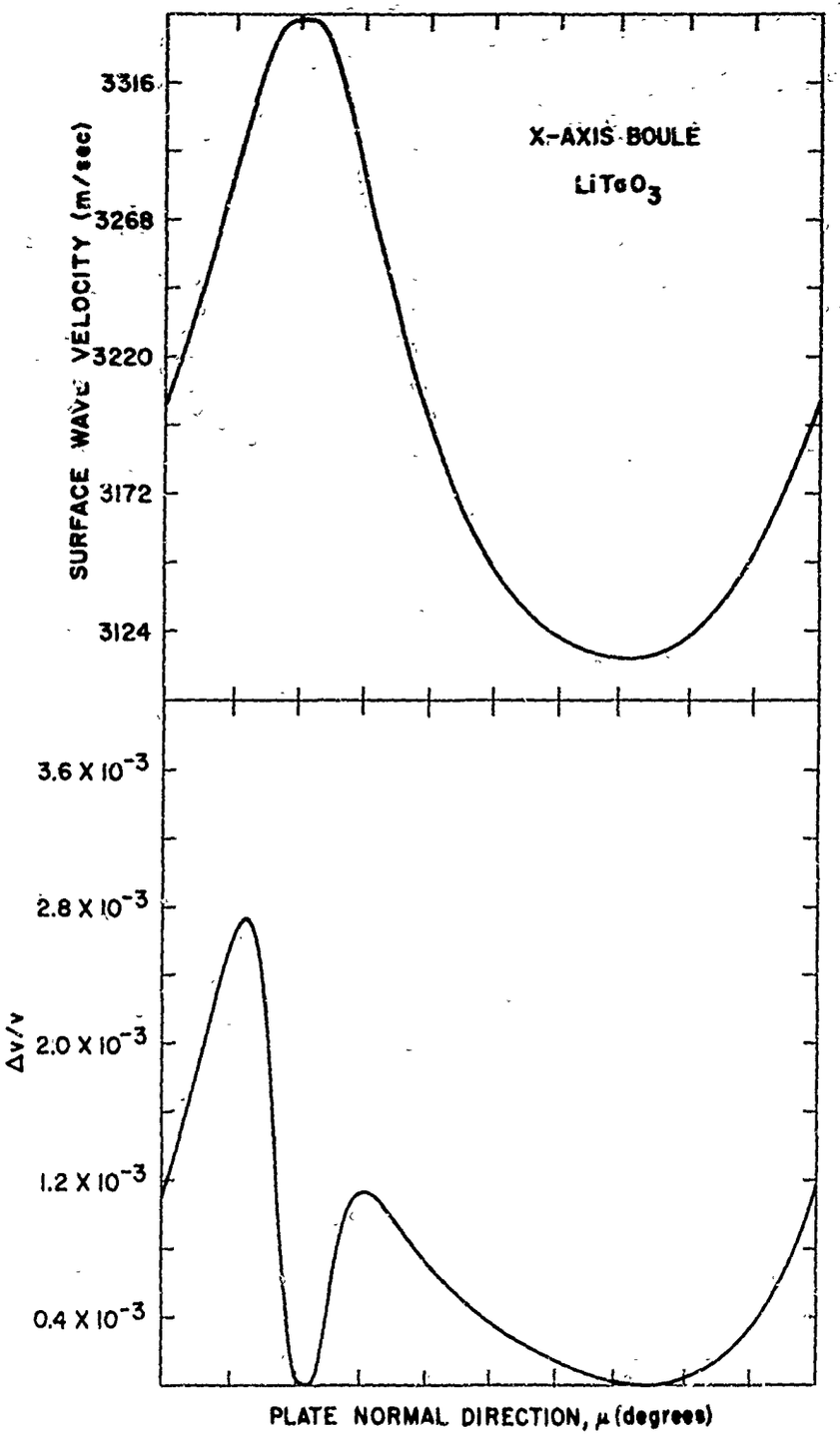

NOTE: TIME AVERAGE POWER FLOW ANGLE IDENTICALLY ZERO.

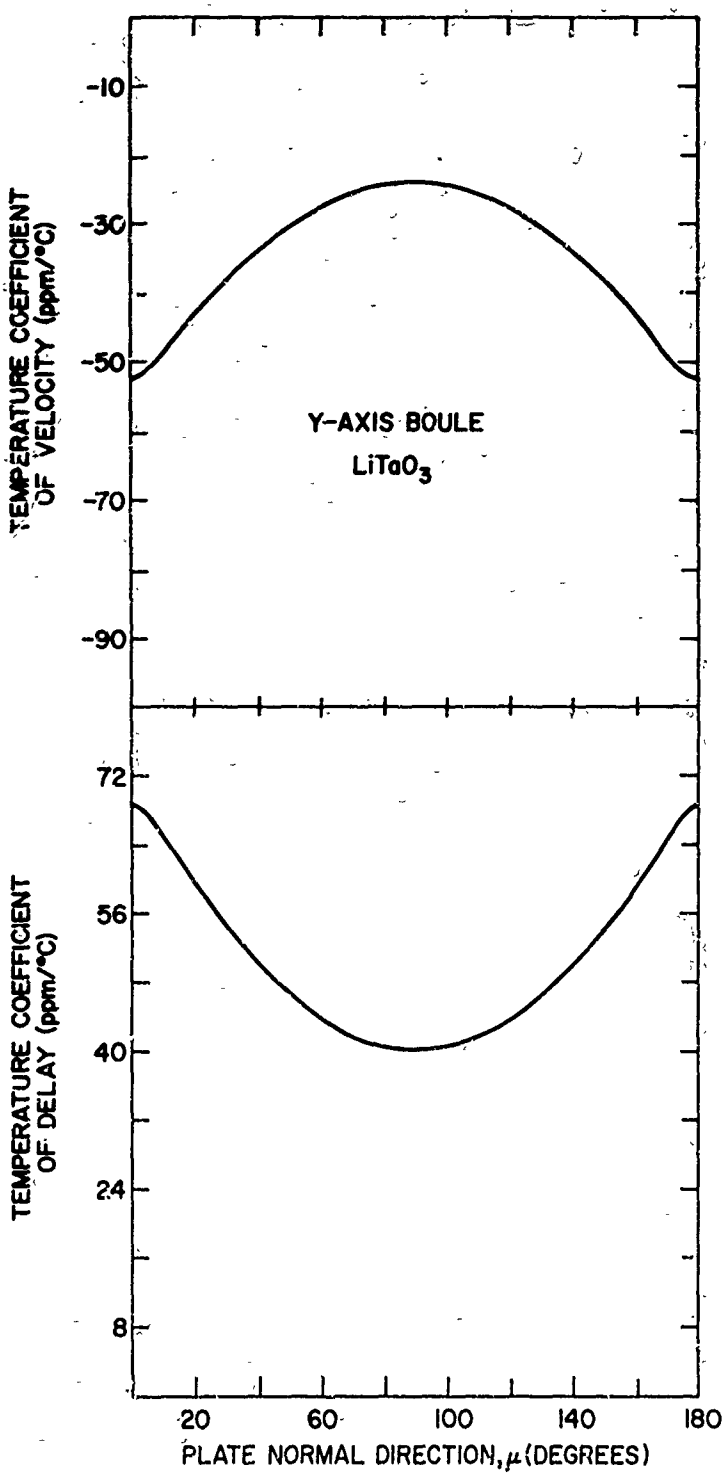
-10
-30
-50
-70
-90
TEMPERATURE COEFFICIENT OF VELOCITY (ppm/°C)
Y-AXIS BOULE
LiTaO3
72
56
40
24
8
TEMPERATURE COEFFICIENT OF DELAY (ppm/°C)
20
60
100
140
180
PLATE NORMAL DIRECTION, μ (DEGREES)

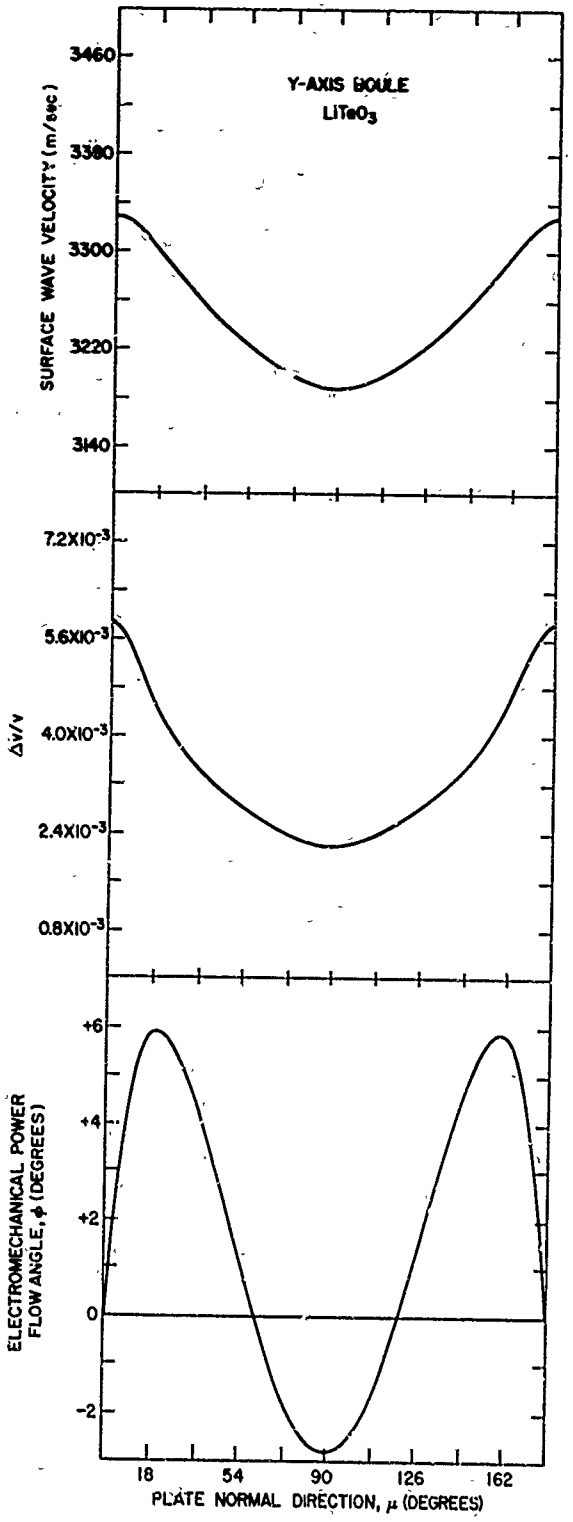
Y-AXIS BOULE
LiTaO3
SURFACE WAVE VELOCITY (m/sec)
3460
3380
3300
3220
3140
Δv/v
7.2X10-3
5.6X10-3
4.0X10-3
2.4X10-3
0.8X10-3
ELECTROMECHANICAL POWER FLOW ANGLE, ϕ (DEGREES)
+6
+4
+2
0
-2
18
54
90
126
162
PLATE NORMAL DIRECTION, μ (DEGREES)

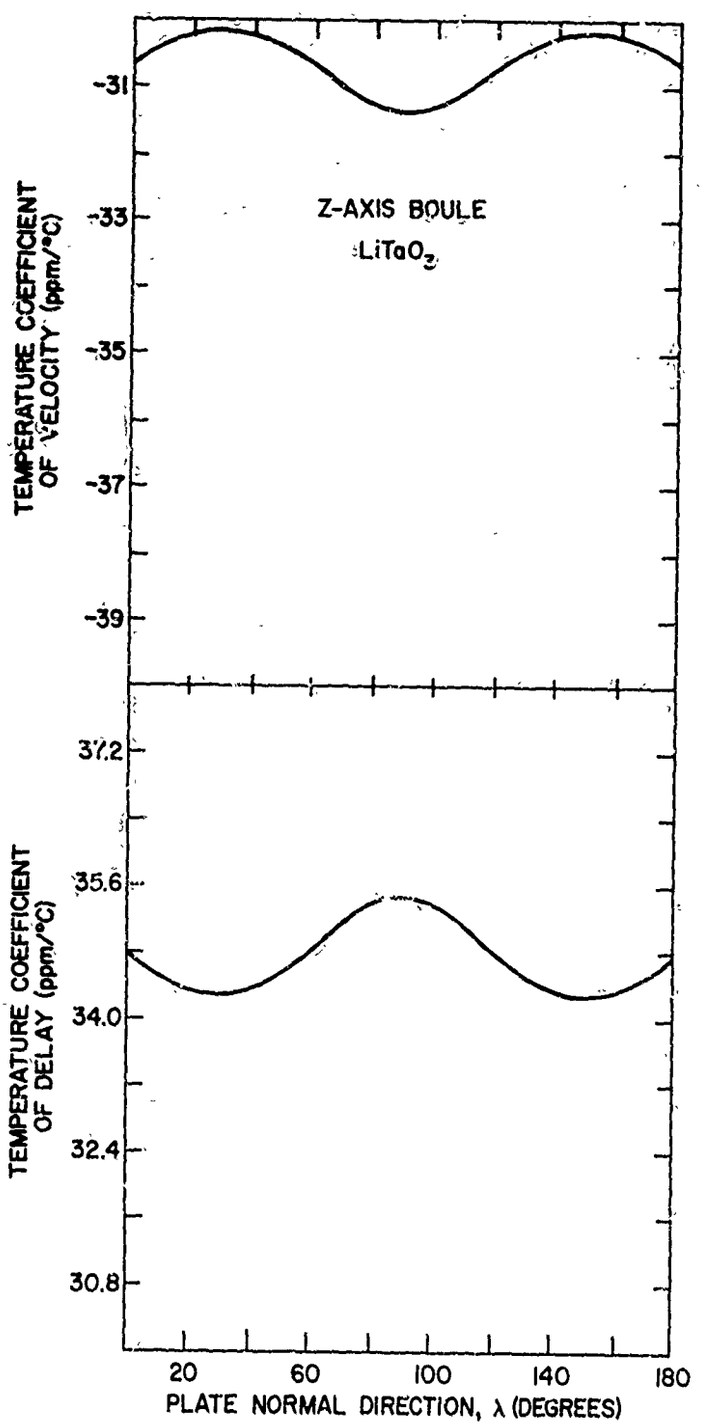
Z-AXIS BOULE
LiTaO3
TEMPERATURE COEFFICIENT OF VELOCITY (ppm/°C)
-31
-33
-35
-37
-39
TEMPERATURE COEFFICIENT OF DELAY (ppm/°C)
37.2
35.6
34.0
32.4
30.8
20
60
100
140
180
PLATE NORMAL DIRECTION, λ (DEGREES)

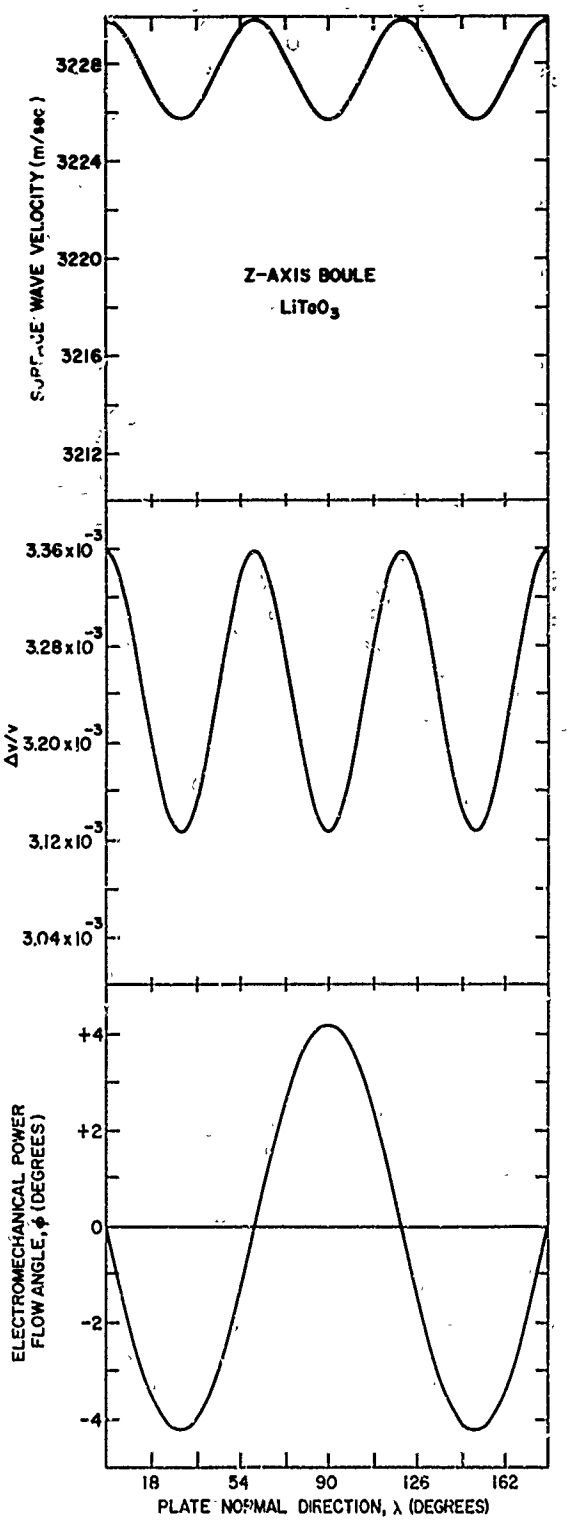
3228
3224
3220
3216
3212
SURFACE WAVE VELOCITY (m/sec)
Z-AXIS BOULE
LiTaO3
3.36x10-3
3.28x10-3
3.20x10-3
3.12x10-3
3.04x10-3
Δv/v
+4
+2
0
-2
-4
ELECTROMECHANICAL POWER FLOW ANGLE, ϕ (DEGREES)
18
54
90
126
162
PLATE NORMAL DIRECTION, λ (DEGREES)

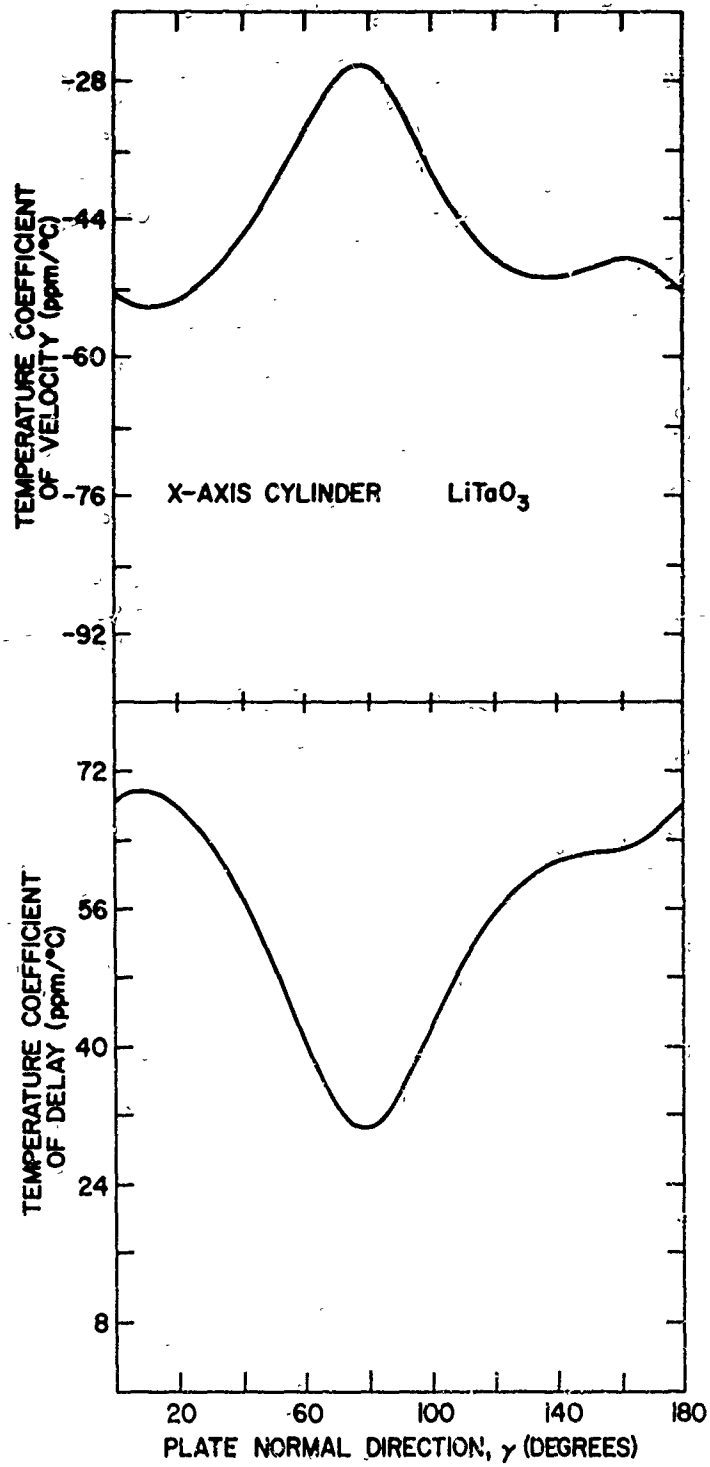
-28
-44
-60
-76
-92
TEMPERATURE COEFFICIENT OF VELOCITY (ppm/°C)
X-AXIS CYLINDER
LiTaO3
72
56
40
24
8
TEMPERATURE COEFFICIENT OF DELAY (ppm/°C)
20
60
100
140
180
PLATE NORMAL DIRECTION, γ (DEGREES)

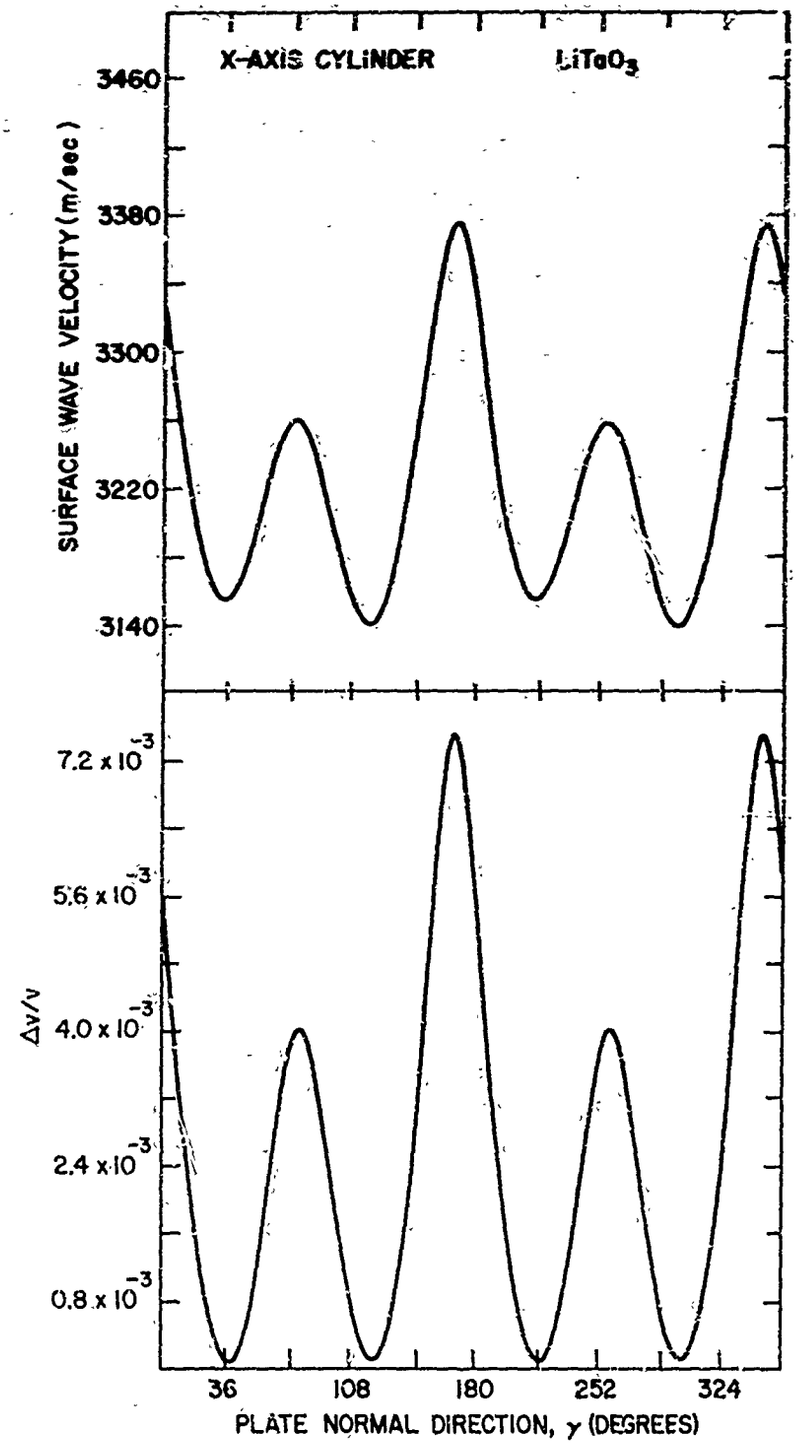

NOTE: TIME AVERAGE POWER FLOW ANGLE IDENTICALLY ZERO.

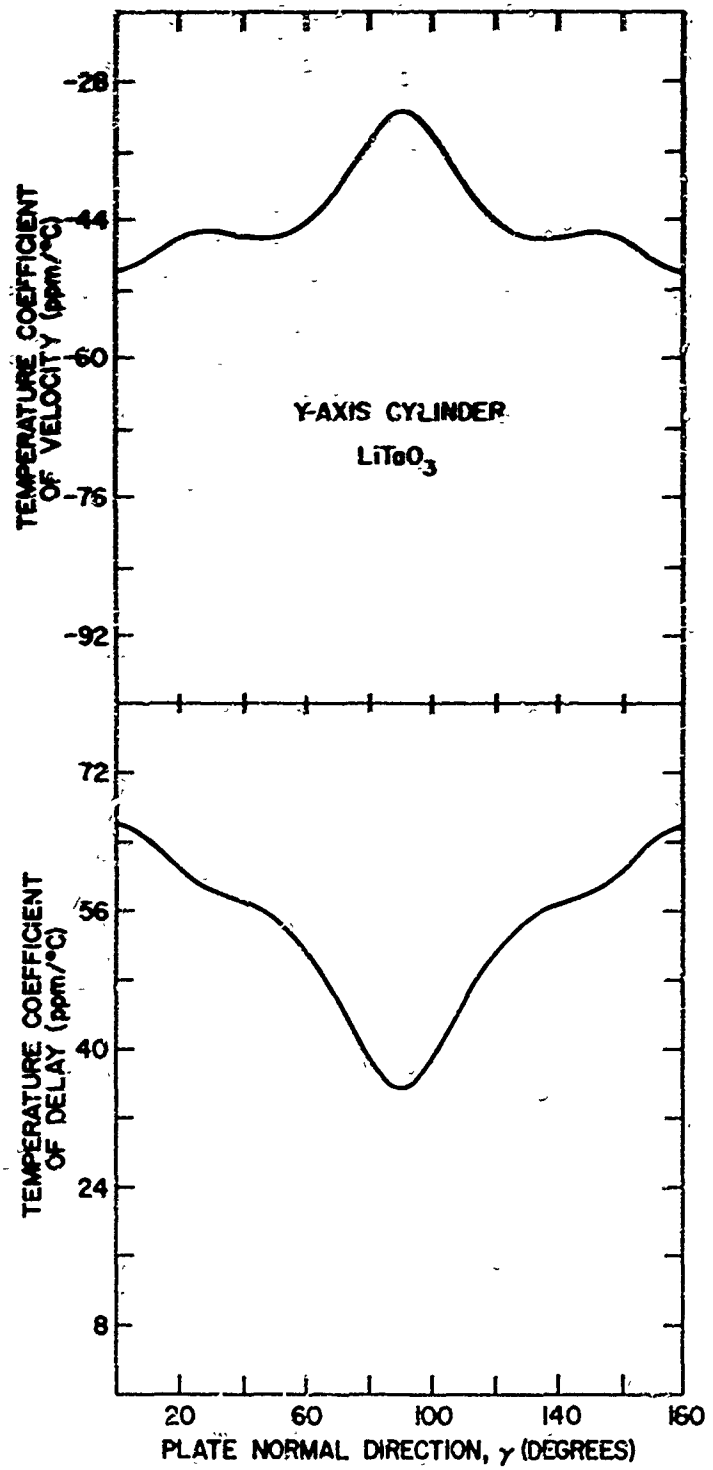
-28
-44
-60
-76
-92
TEMPERATURE COEFFICIENT OF VELOCITY (ppm/°C)
Y-AXIS CYLINDER
LiTaO3
72
56
40
24
8
TEMPERATURE COEFFICIENT OF DELAY (ppm/°C)
20
60
100
140
160
PLATE NORMAL DIRECTION, γ (DEGREES)

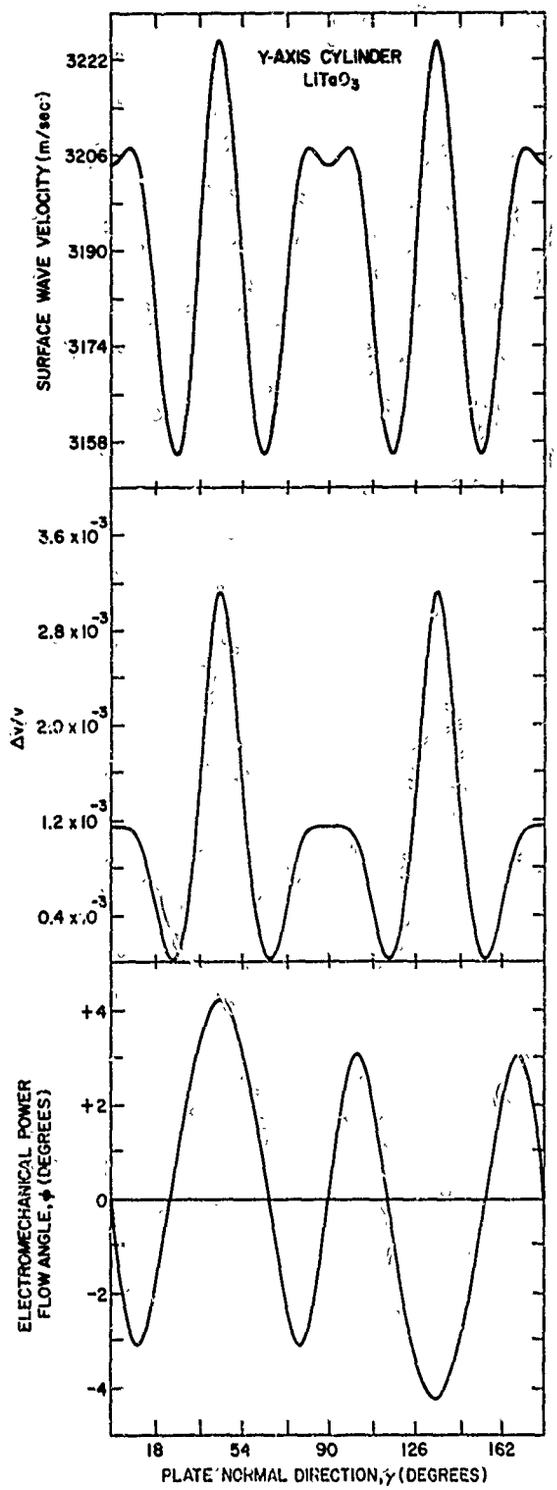
Y-AXIS CYLINDER
LiTaO3
SURFACE WAVE VELOCITY (m/sec)
3222
3206
3190
3174
3158
Δv/v
3.6 x10-3
2.8 x10-3
2.0 x10-3
1.2 x10-3
0.4 x10-3
ELECTROMECHANICAL POWER FLOW ANGLE, ψ (DEGREES)
+4
+2
0
-2
-4
18
54
90
126
162
PLATE NORMAL DIRECTION, γ (DEGREES)

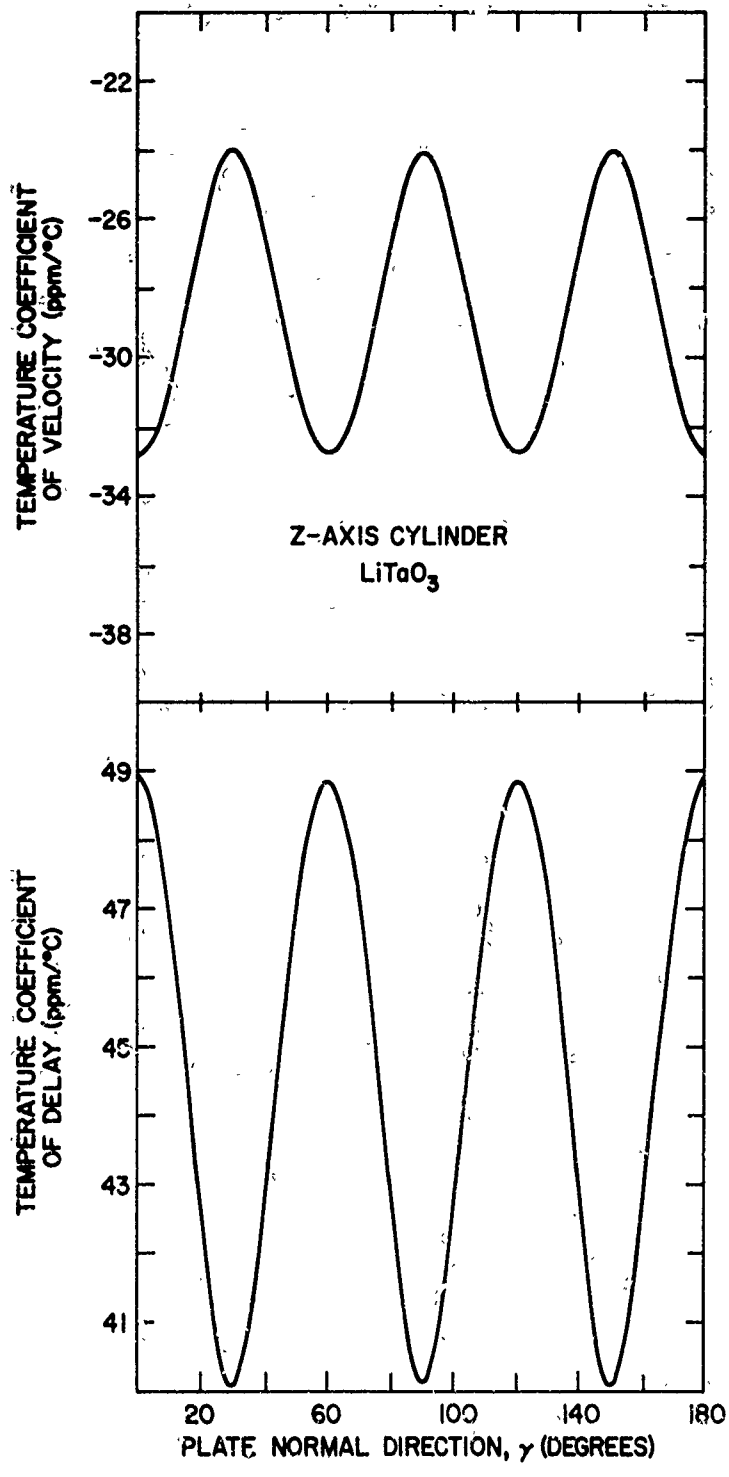
-22
-26
-30
-34
-38
TEMPERATURE COEFFICIENT OF VELOCITY (ppm/°C)
Z-AXIS CYLINDER
LiTaO3
49
47
45
43
41
TEMPERATURE COEFFICIENT OF DELAY (ppm/°C)
20
60
100
140
180
PLATE NORMAL DIRECTION, γ (DEGREES)

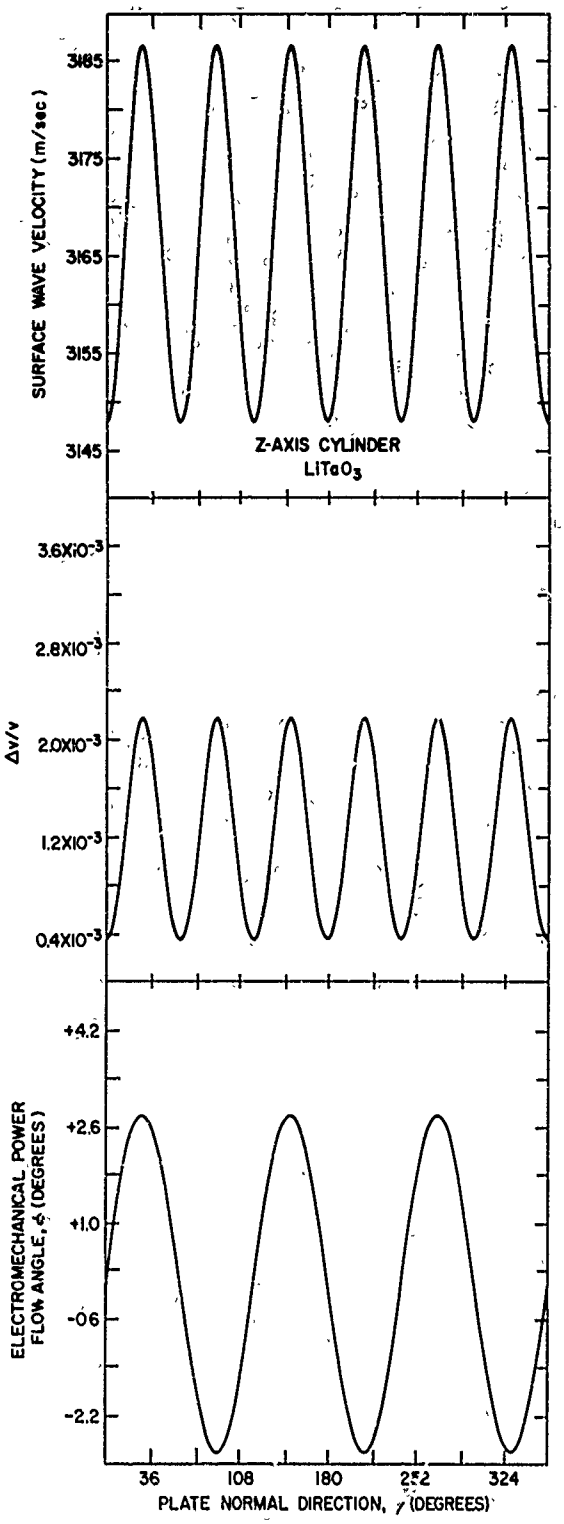
SURFACE WAVE VELOCITY (m/sec)
3185
3175
3165
3155
3145
Z-AXIS CYLINDER
LiTaO3
Δv/v
3.6X10-3
2.8X10-3
2.0X10-3
1.2X10-3
0.4X10-3
ELECTROMECHANICAL POWER FLOW ANGLE, ϕ (DEGREES)
+4.2
+2.6
+1.0
-0.6
-2.2
36
108
180
252
324
PLATE NORMAL DIRECTION, γ (DEGREES)

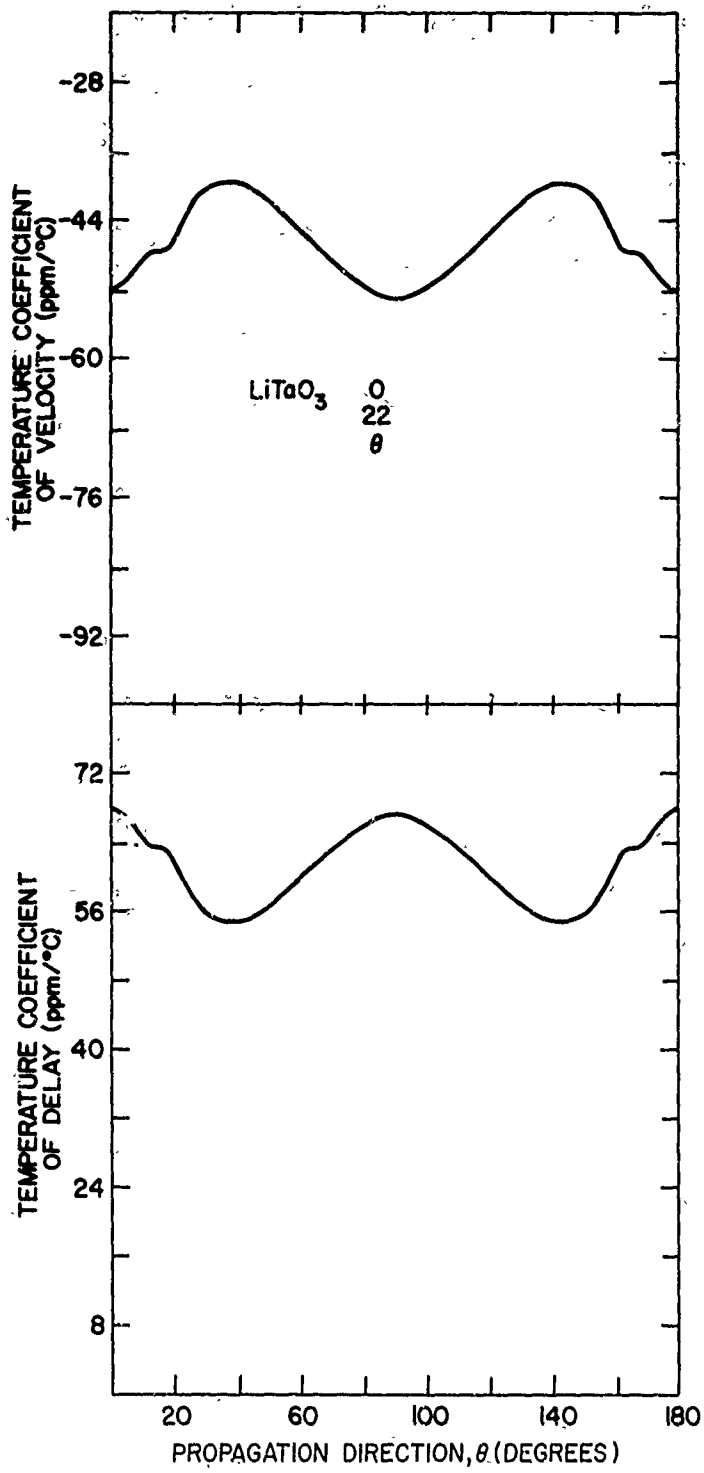
-28
-44
-60
-76
-92
TEMPERATURE COEFFICIENT OF VELOCITY (ppm/°C)
LiTaO3
0
22
θ
72
56
40
24
8
TEMPERATURE COEFFICIENT OF DELAY (ppm/°C)
20
60
100
140
180
PROPAGATION DIRECTION, θ (DEGREES)

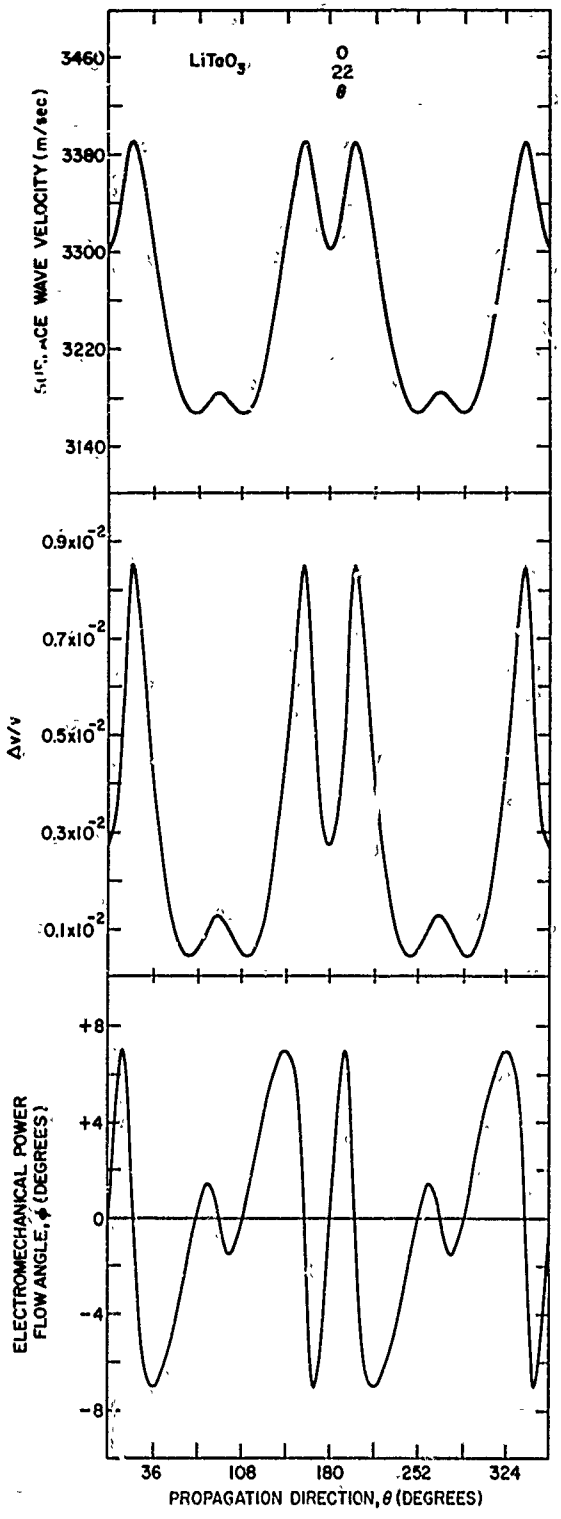
LiTaO3
0
22
θ
SURFACE WAVE VELOCITY (m/sec)
3460
3380
3300
3220
3140
Δv/v
0.9x10⁻²
0.7x10⁻²
0.5x10⁻²
0.3x10⁻²
0.1x10⁻²
ELECTROMECHANICAL POWER FLOW ANGLE, ϕ (DEGREES)
+8
+4
0
-4
-8
36
108
180
252
324
PROPAGATION DIRECTION, θ (DEGREES)

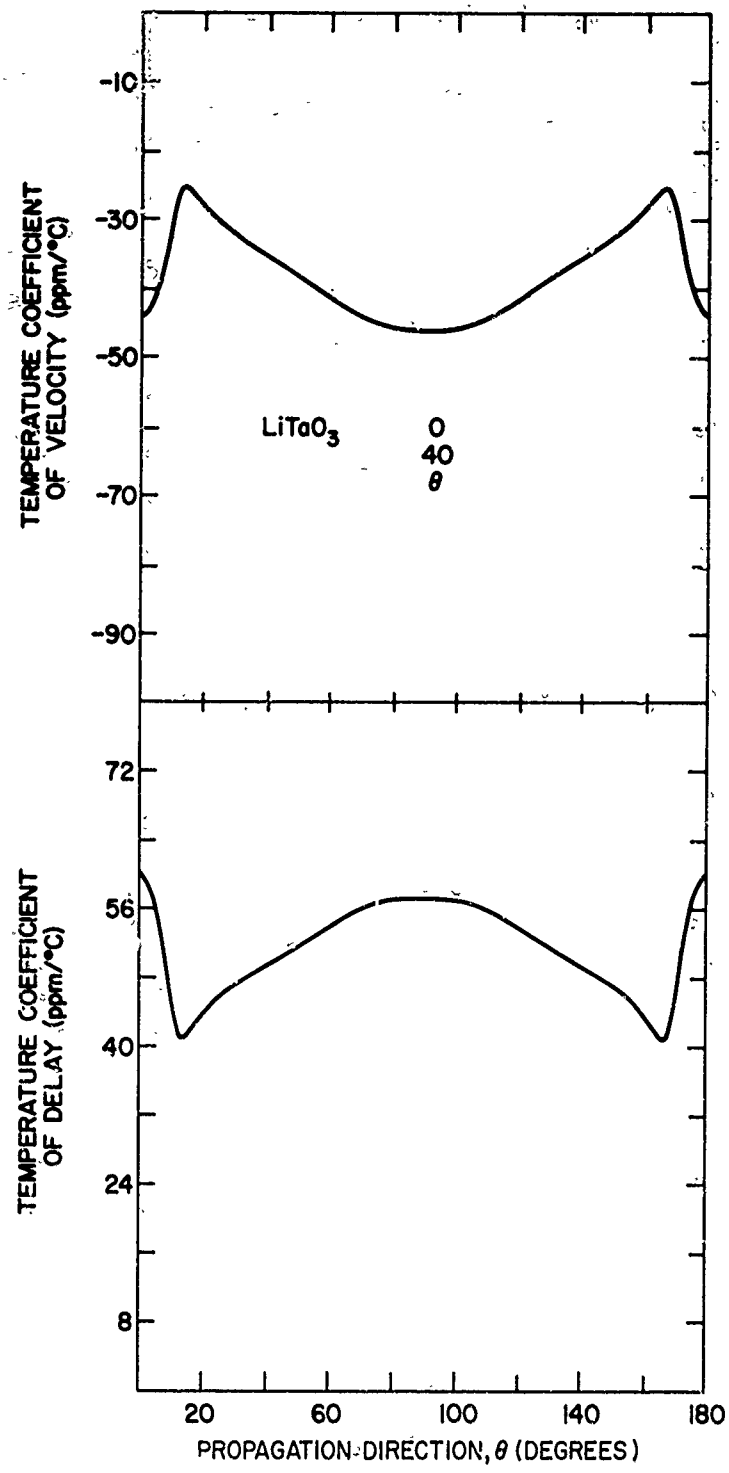
-10
-30
-50
-70
-90
TEMPERATURE COEFFICIENT OF VELOCITY (ppm/°C)
LiTaO3
0
40
θ
72
56
40
24
8
TEMPERATURE COEFFICIENT OF DELAY (ppm/°C)
20
60
100
140
180
PROPAGATION DIRECTION, θ (DEGREES)

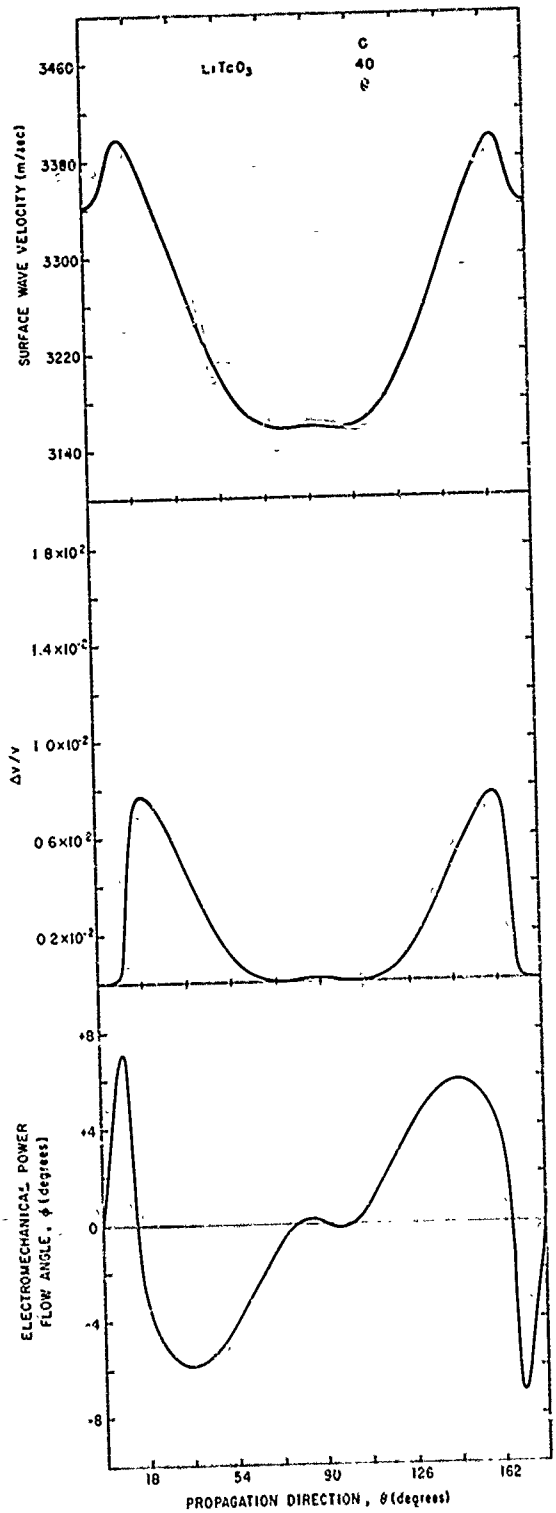
LiTaO3
C
40
SURFACE WAVE VELOCITY (m/sec)
3460
3380
3300
3220
3140
Δv/v
1.8×10-2
1.4×10-2
1.0×10-2
0.6×10-2
0.2×10-2
ELECTROMECHANICAL POWER FLOW ANGLE, φ (degrees)
+8
+4
0
-4
-8
18
54
90
126
162
PROPAGATION DIRECTION, θ (degrees)

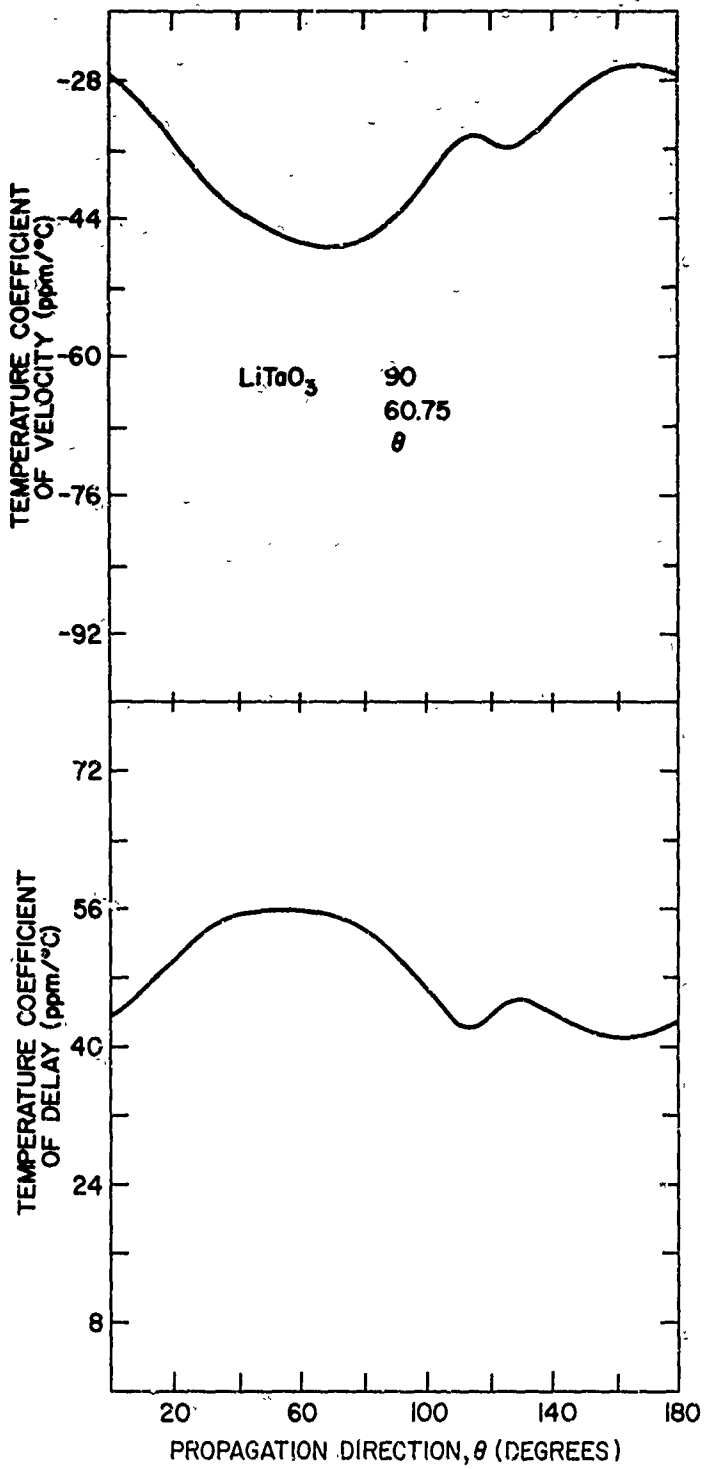
-28
-44
-60
-76
-92
TEMPERATURE COEFFICIENT OF VELOCITY (ppm/°C)
LiTaO3
90
60.75
θ
72
56
40
24
8
TEMPERATURE COEFFICIENT OF DELAY (ppm/°C)
20
60
100
140
180
PROPAGATION DIRECTION, θ (DEGREES)

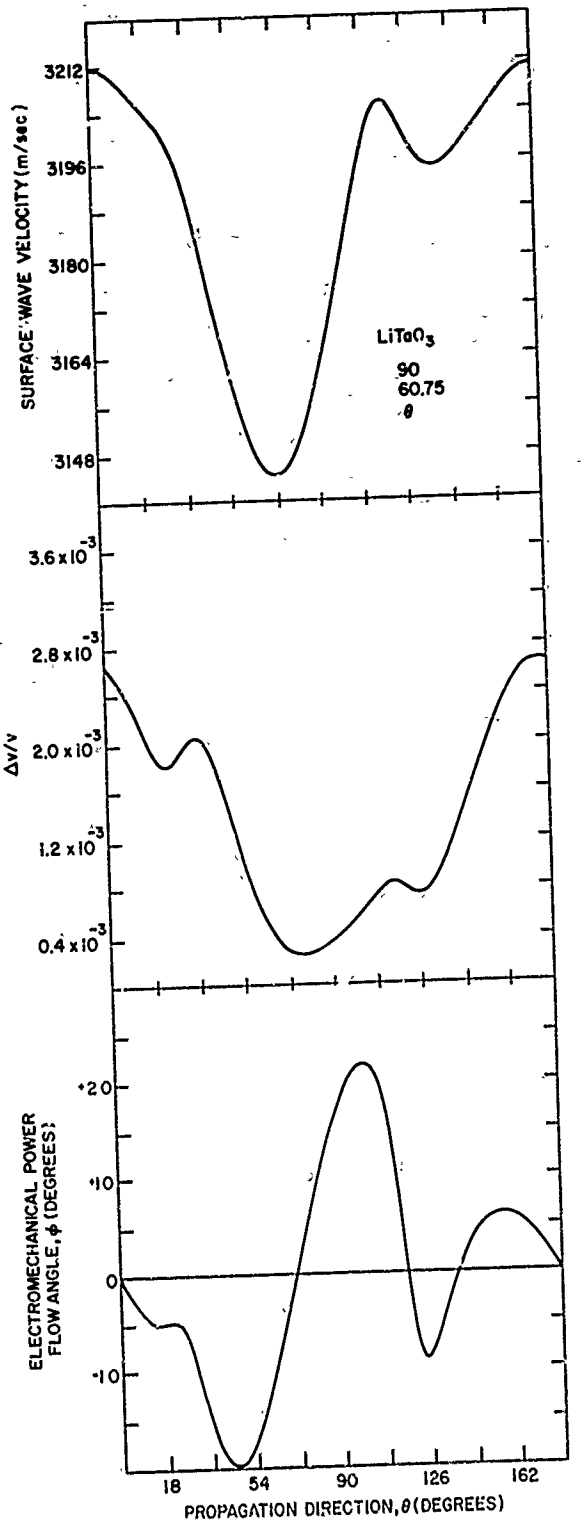
SURFACE WAVE VELOCITY (m/sec)
3212
3196
3180
3164
3148
LiTaO3
90
60.75
θ
3.6 x 10-3
2.8 x 10-3
2.0 x 10-3
1.2 x 10-3
0.4 x 10-3
Δv/v
+20
+10
0
-10
ELECTROMECHANICAL POWER FLOW ANGLE, ϕ (DEGREES)
18
54
90
126
162
PROPAGATION DIRECTION, θ (DEGREES)

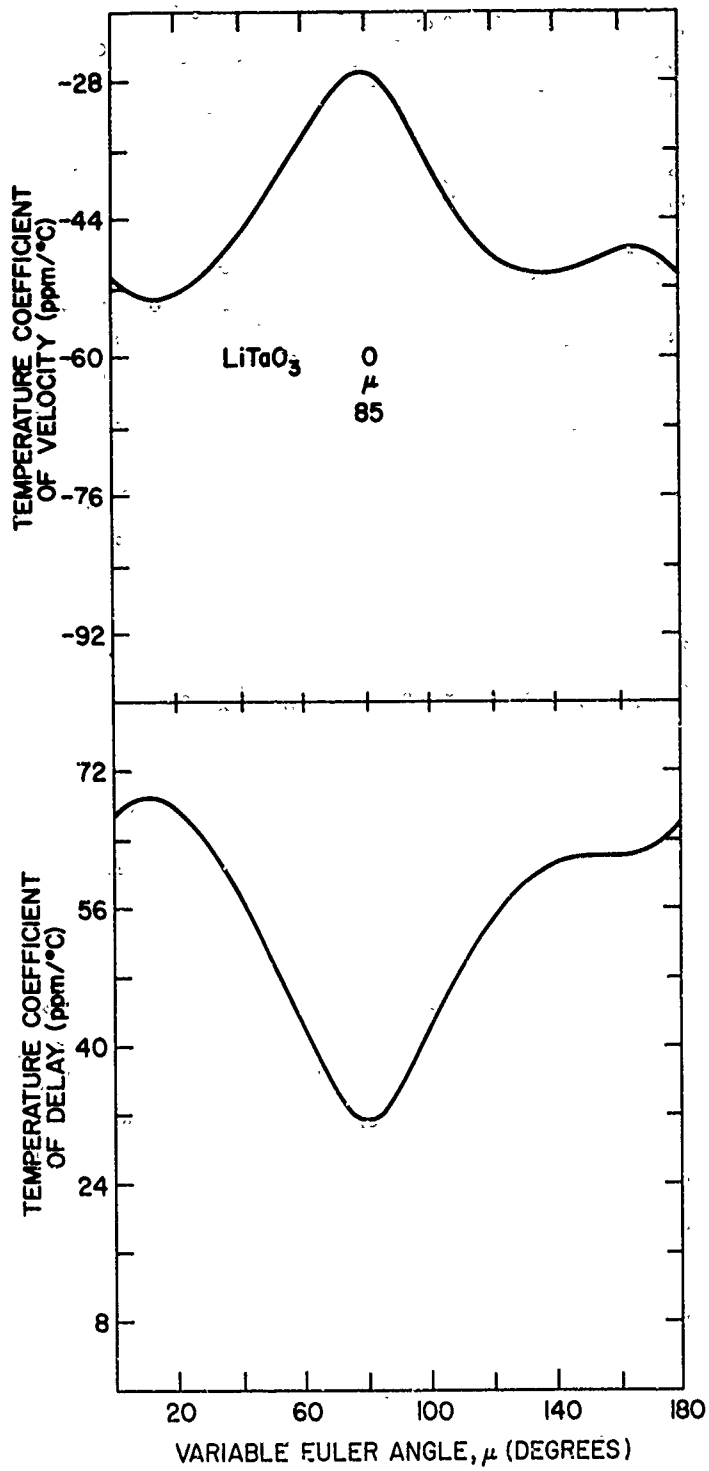
-28
-44
-60
-76
-92
TEMPERATURE COEFFICIENT OF VELOCITY (ppm/°C)
LiTaO3
0
μ
85
72
56
40
24
8
TEMPERATURE COEFFICIENT OF DELAY (ppm/°C)
20
60
100
140
180
VARIABLE EULER ANGLE, μ (DEGREES)

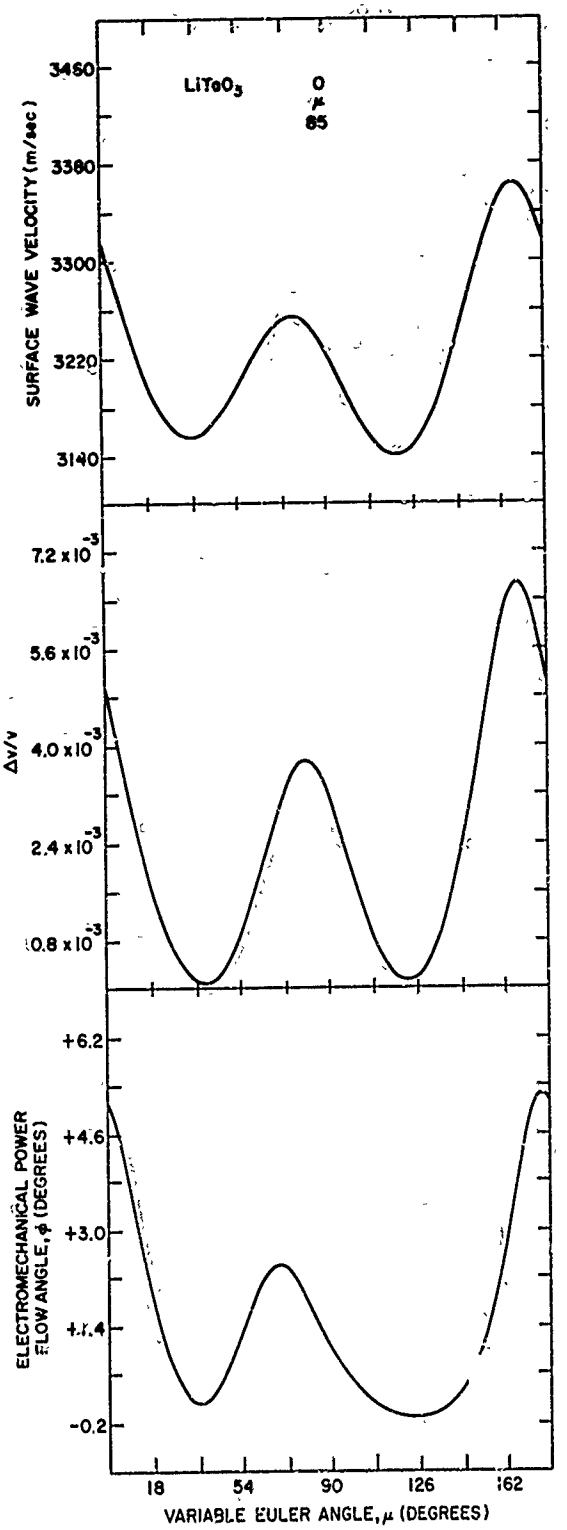
LiTaO3
0
Y
65
SURFACE WAVE VELOCITY (m/sec)
3460
3380
3300
3220
3140
Δv/v
7.2 x 10-3
5.6 x 10-3
4.0 x 10-3
2.4 x 10-3
0.8 x 10-3
ELECTROMECHANICAL POWER FLOW ANGLE, ϕ (DEGREES)
+6.2
+4.6
+3.0
+1.4
-0.2
18
54
90
126
162
VARIABLE EULER ANGLE, μ (DEGREES)

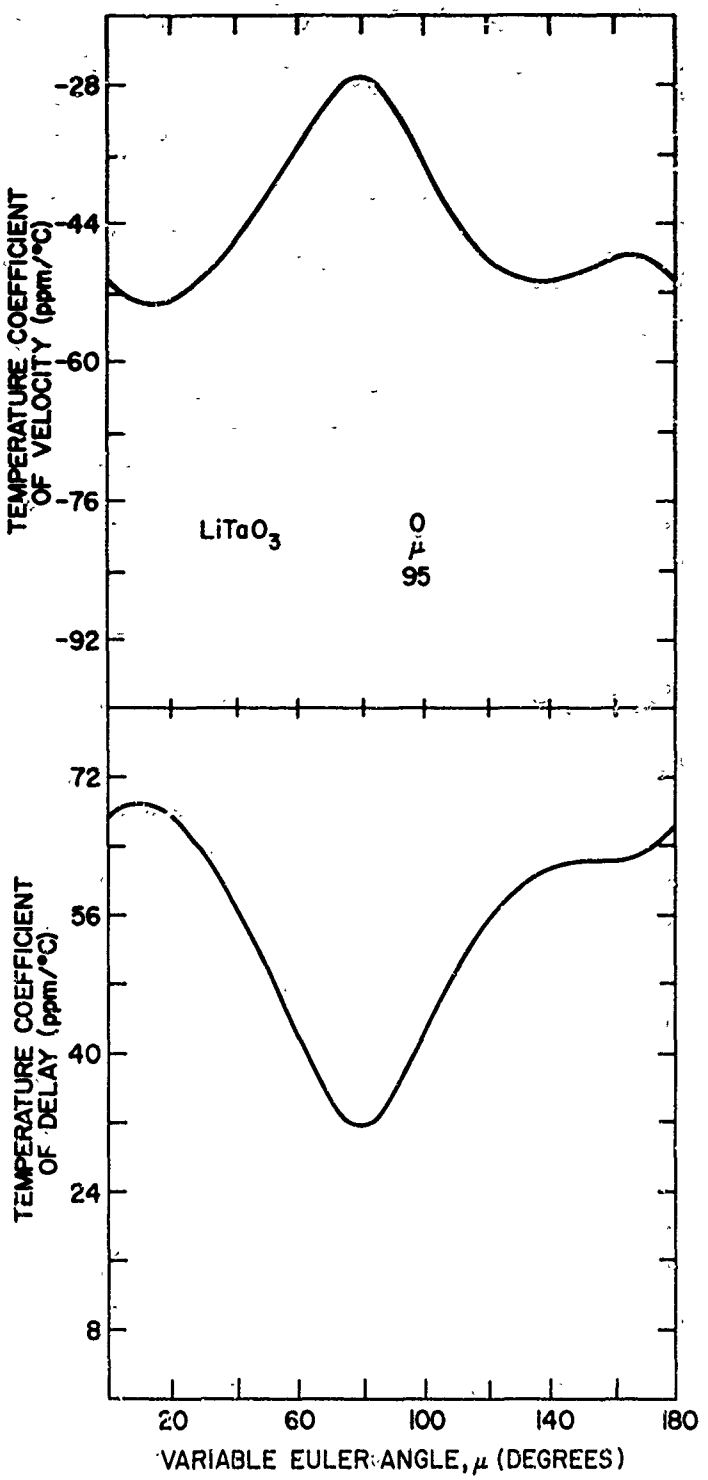
-28
-44
-60
-76
-92
TEMPERATURE COEFFICIENT OF VELOCITY (ppm/°C)
LiTaO3
0
μ
95
72
56
40
24
8
TEMPERATURE COEFFICIENT OF DELAY (ppm/°C)
20
60
100
140
180
VARIABLE EULER ANGLE, μ (DEGREES)

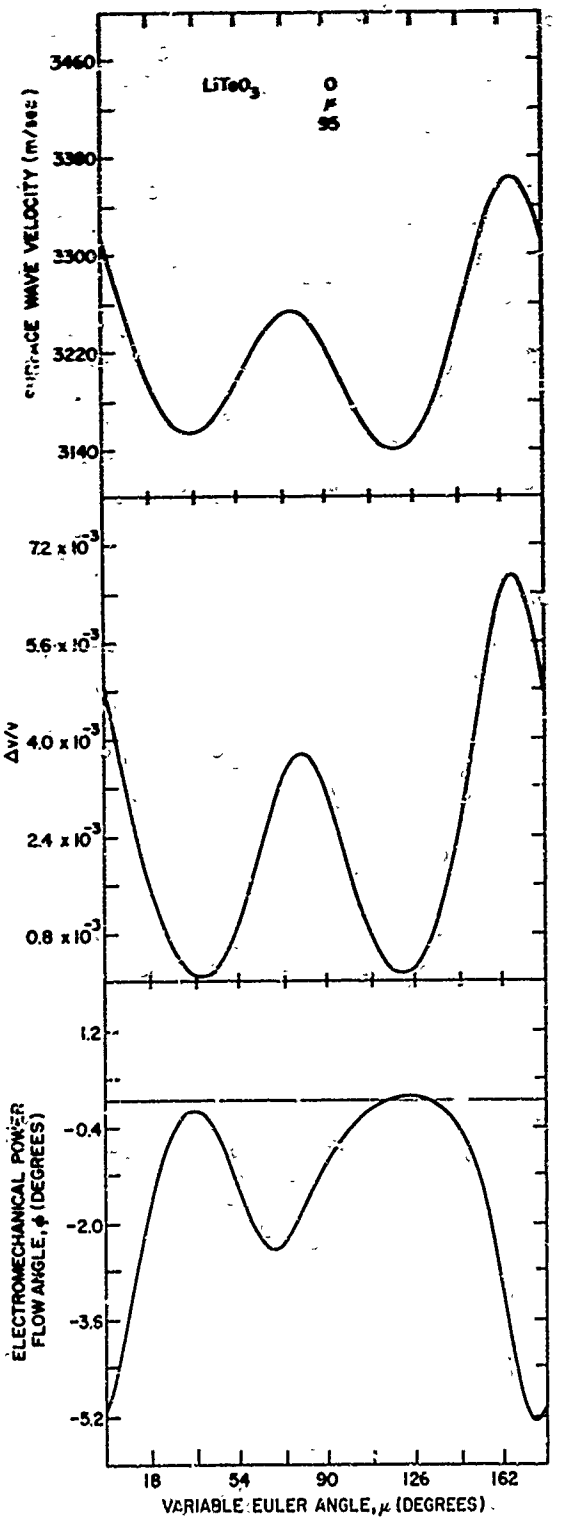
LiTaO3
θ
μ
55
SURFACE WAVE VELOCITY (m/sec)
3460
3380
3300
3220
3140
7.2 x 10-3
5.6 x 10-3
4.0 x 10-3
2.4 x 10-3
0.8 x 10-3
Δv/v
1.2
-0.4
-2.0
-3.6
-5.2
ELECTROMECHANICAL POWER FLOW ANGLE, ϕ (DEGREES)
18
54
90
126
162
VARIABLE EULER ANGLE, μ (DEGREES)

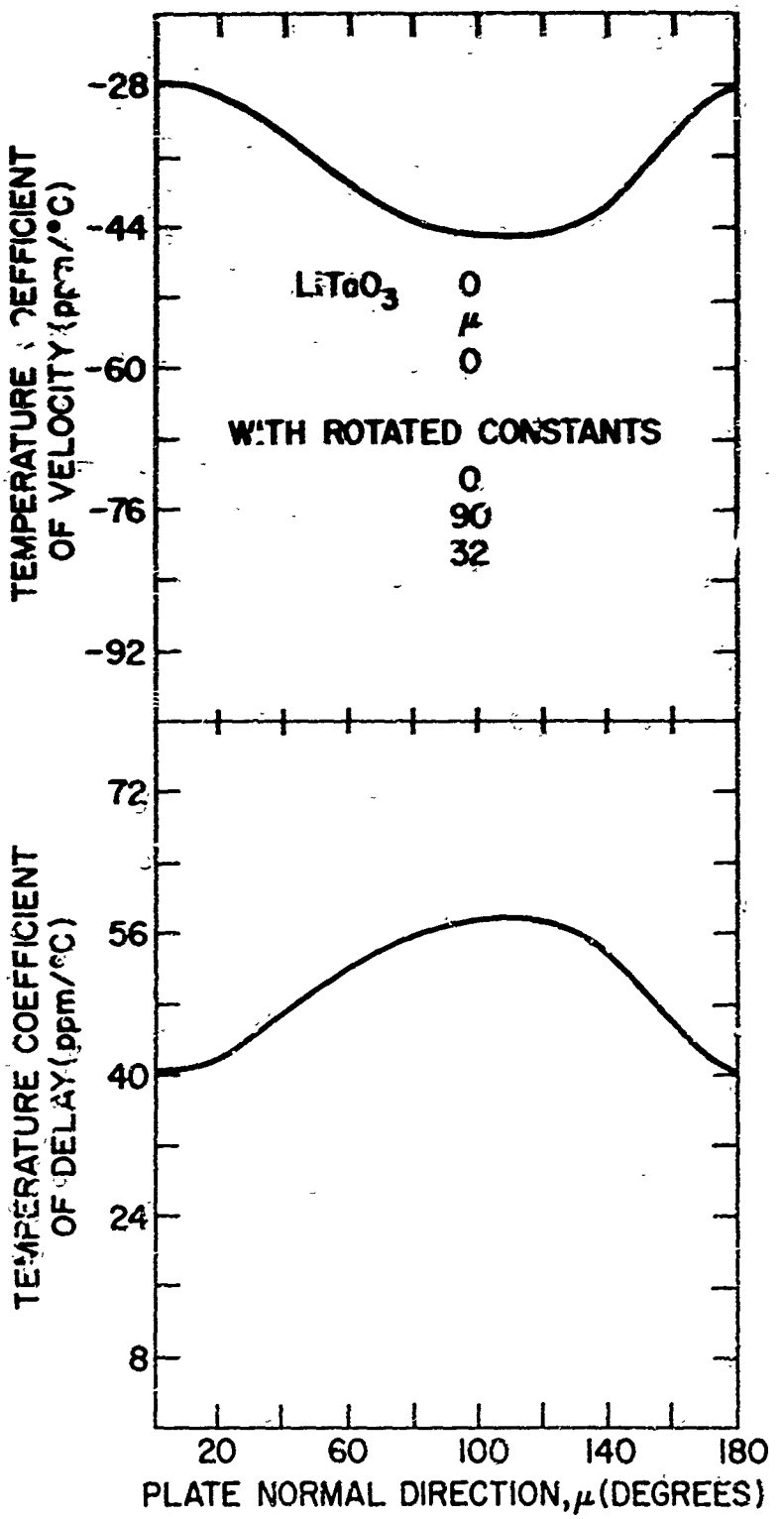
-28
-44
-60
-76
-92
TEMPERATURE COEFFICIENT OF VELOCITY (ppm/°C)
LiTaO3
0
μ
0
WITH ROTATED CONSTANTS
0
90
32
72
56
40
24
8
TEMPERATURE COEFFICIENT OF DELAY (ppm/°C)
20
60
100
140
180
PLATE NORMAL DIRECTION, μ (DEGREES)

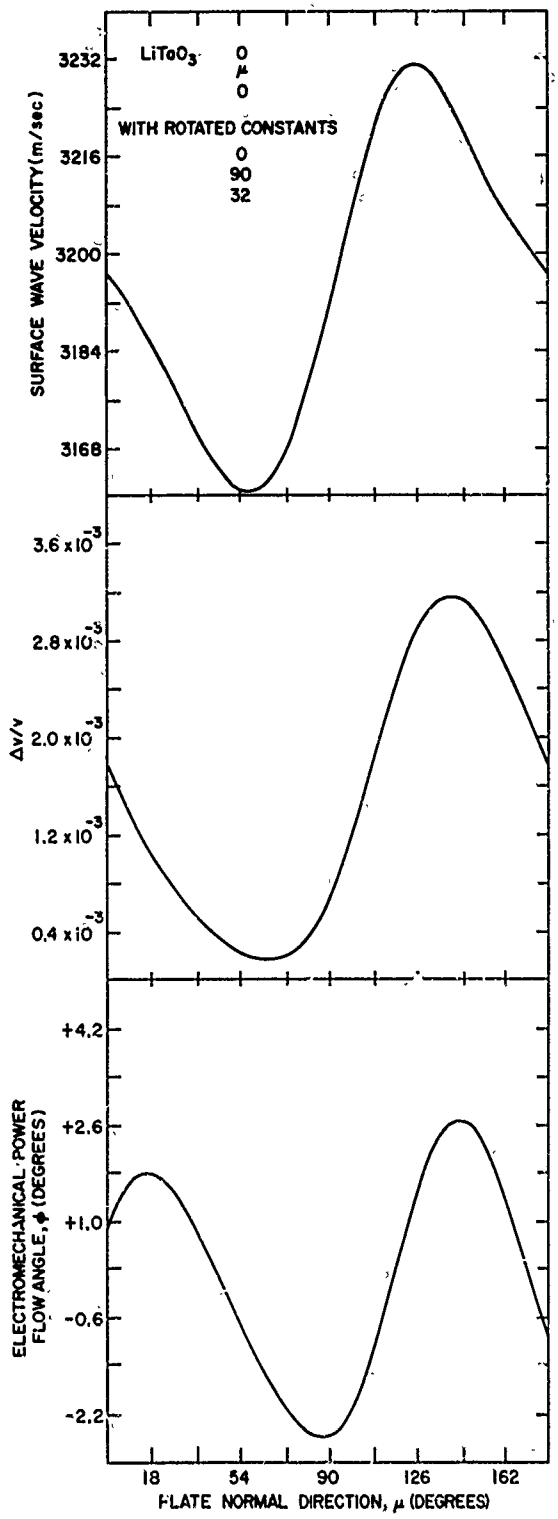
LiTaO3
0
μ
0
WITH ROTATED CONSTANTS
0
90
32
SURFACE WAVE VELOCITY (m/sec)
3232
3216
3200
3184
3168
Δv/v
3.6 x10-3
2.8 x10-3
2.0 x10-3
1.2 x10-3
0.4 x10-3
ELECTROMECHANICAL POWER FLOW ANGLE, ψ (DEGREES)
+4.2
+2.6
+1.0
-0.6
-2.2
18
54
90
126
162
PLATE NORMAL DIRECTION, μ (DEGREES)

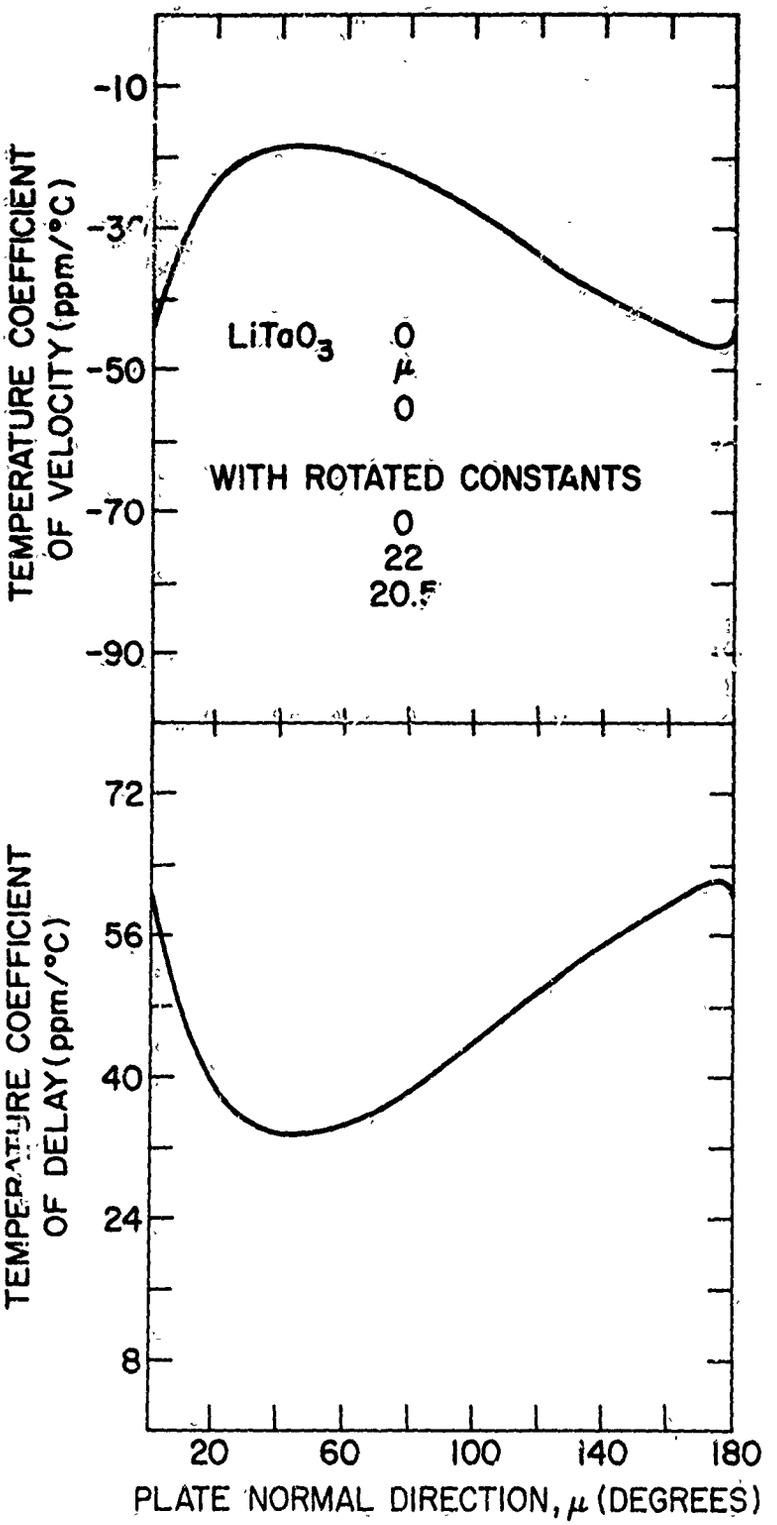
-10
-30
-50
-70
-90
TEMPERATURE COEFFICIENT OF VELOCITY (ppm/°C)
LiTaO3
0
μ
0
WITH ROTATED CONSTANTS
0
22
20.5
72
56
40
24
8
TEMPERATURE COEFFICIENT OF DELAY (ppm/°C)
20
60
100
140
180
PLATE NORMAL DIRECTION, μ (DEGREES)

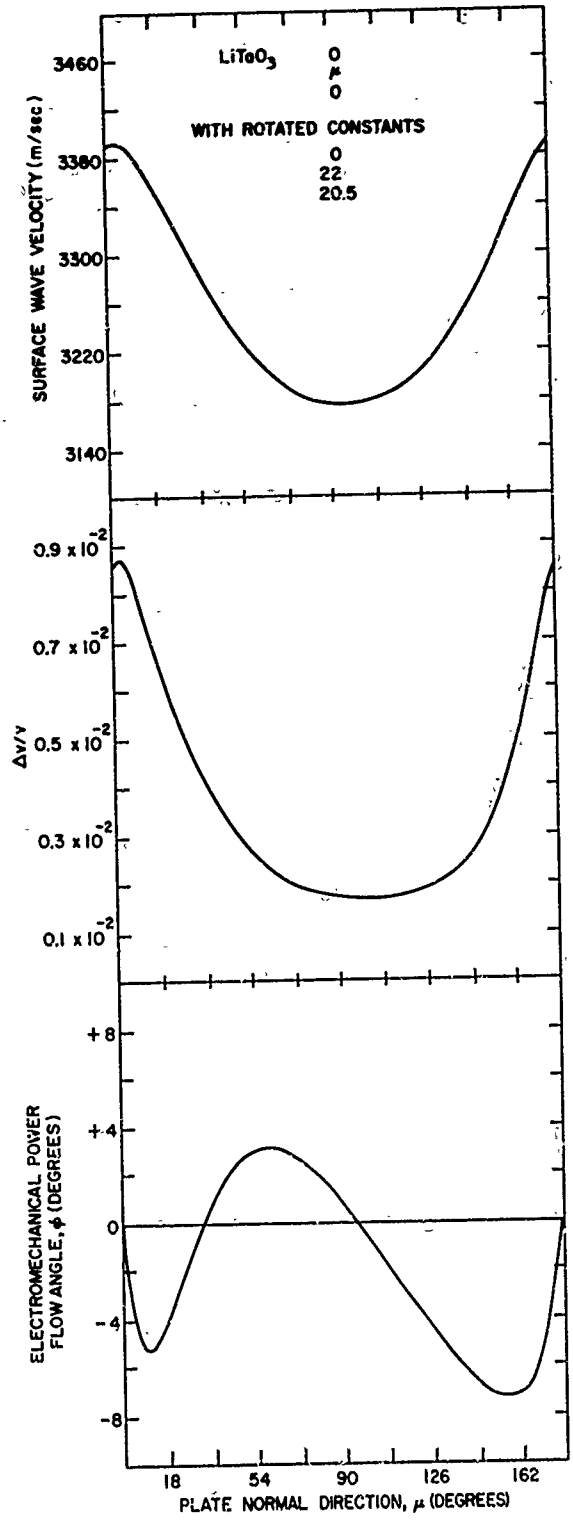
LiTaO3
0
μ
0
WITH ROTATED CONSTANTS
0
22
20.5
SURFACE WAVE VELOCITY (m/sec)
3460
3380
3300
3220
3140
0.9 x 10^-2
0.7 x 10^-2
0.5 x 10^-2
0.3 x 10^-2
0.1 x 10^-2
Δv/v
+8
+4
0
-4
-8
ELECTROMECHANICAL POWER FLOW ANGLE, ϕ (DEGREES)
18
54
90
126
162
PLATE NORMAL DIRECTION, μ (DEGREES)

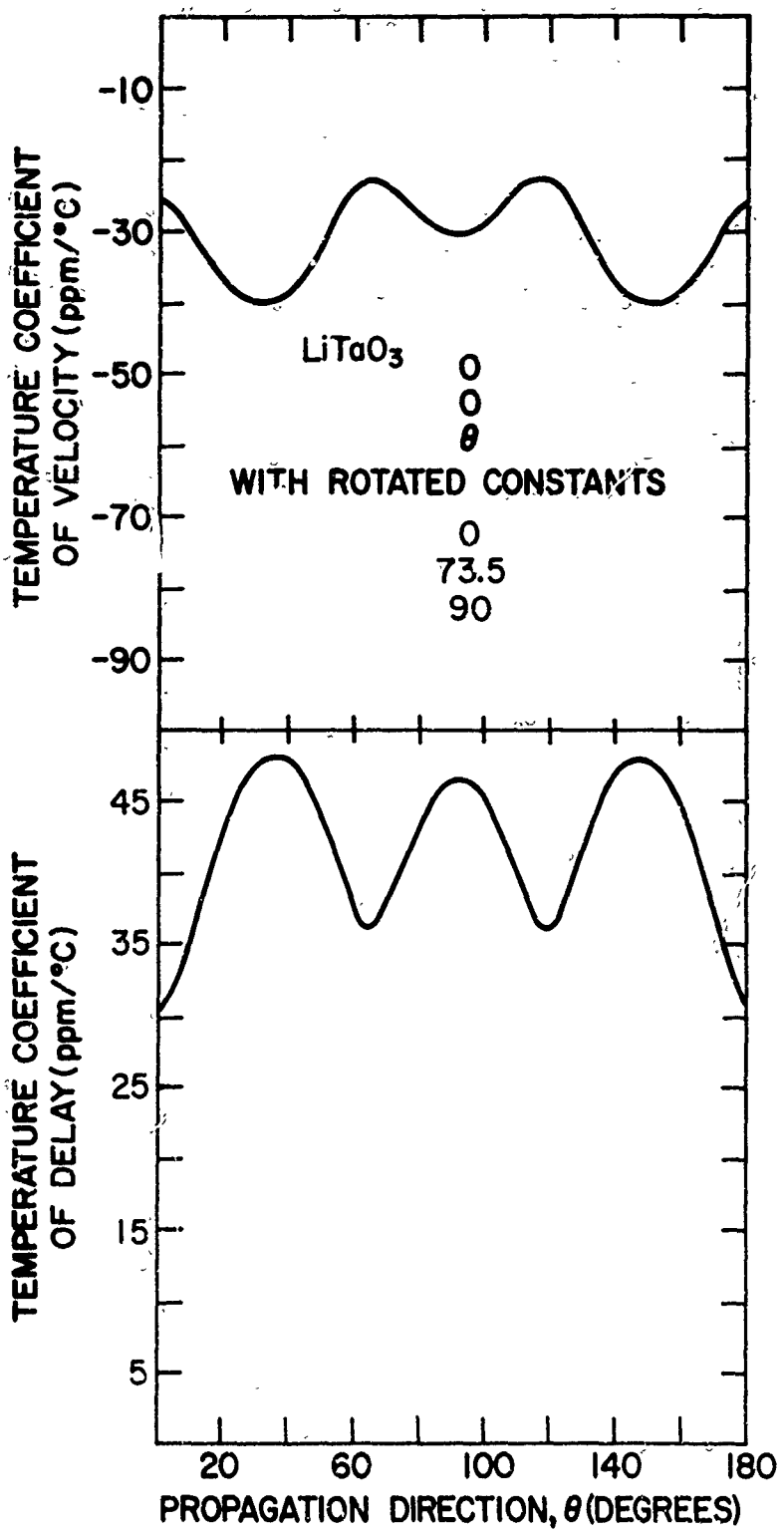
-10
-30
-50
-70
-90
TEMPERATURE COEFFICIENT OF VELOCITY (ppm/°C)
LiTaO3
0
0
θ
WITH ROTATED CONSTANTS
0
73.5
90
45
35
25
15
5
TEMPERATURE COEFFICIENT OF DELAY (ppm/°C)
20
60
100
140
180
PROPAGATION DIRECTION, θ (DEGREES)

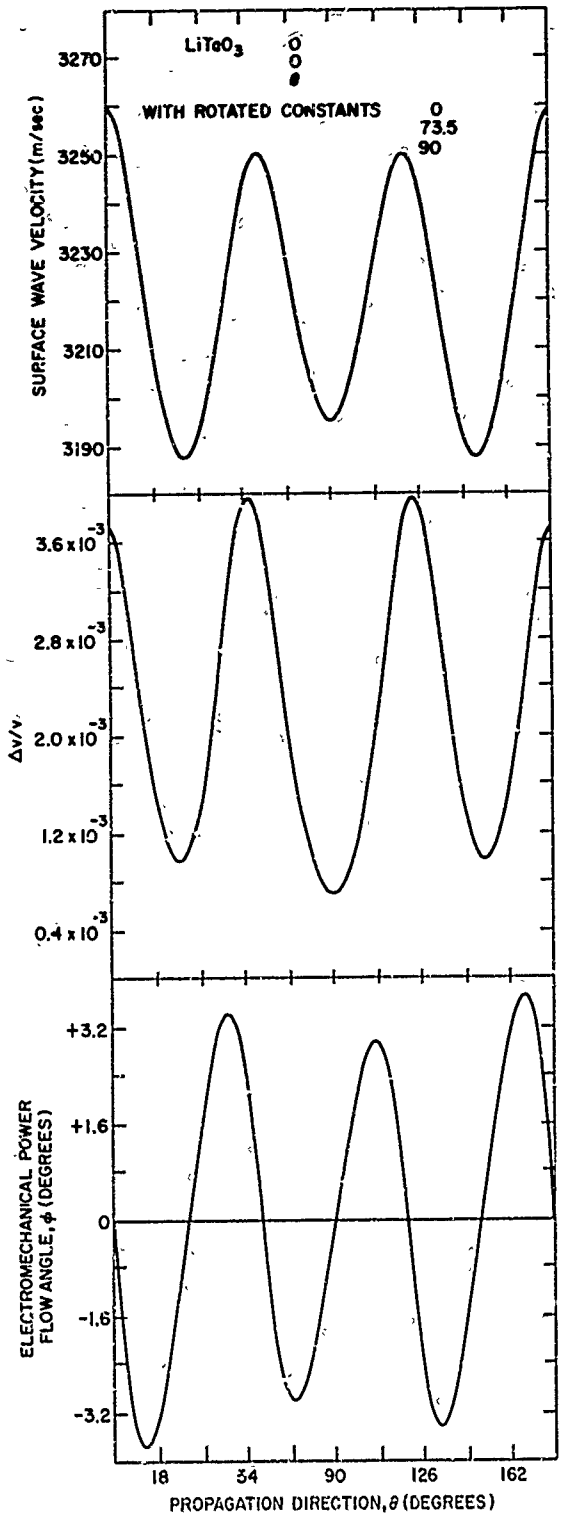
LiTaO3
0
0
θ
WITH ROTATED CONSTANTS
0
73.5
90
SURFACE WAVE VELOCITY (m/sec)
3270
3250
3230
3210
3190
Δv/v
3.6 x 10-3
2.8 x 10-3
2.0 x 10-3
1.2 x 10-3
0.4 x 10-3
ELECTROMECHANICAL POWER FLOW ANGLE, φ (DEGREES)
+3.2
+1.6
0
-1.6
-3.2
18
54
90
126
162
PROPAGATION DIRECTION, θ (DEGREES)

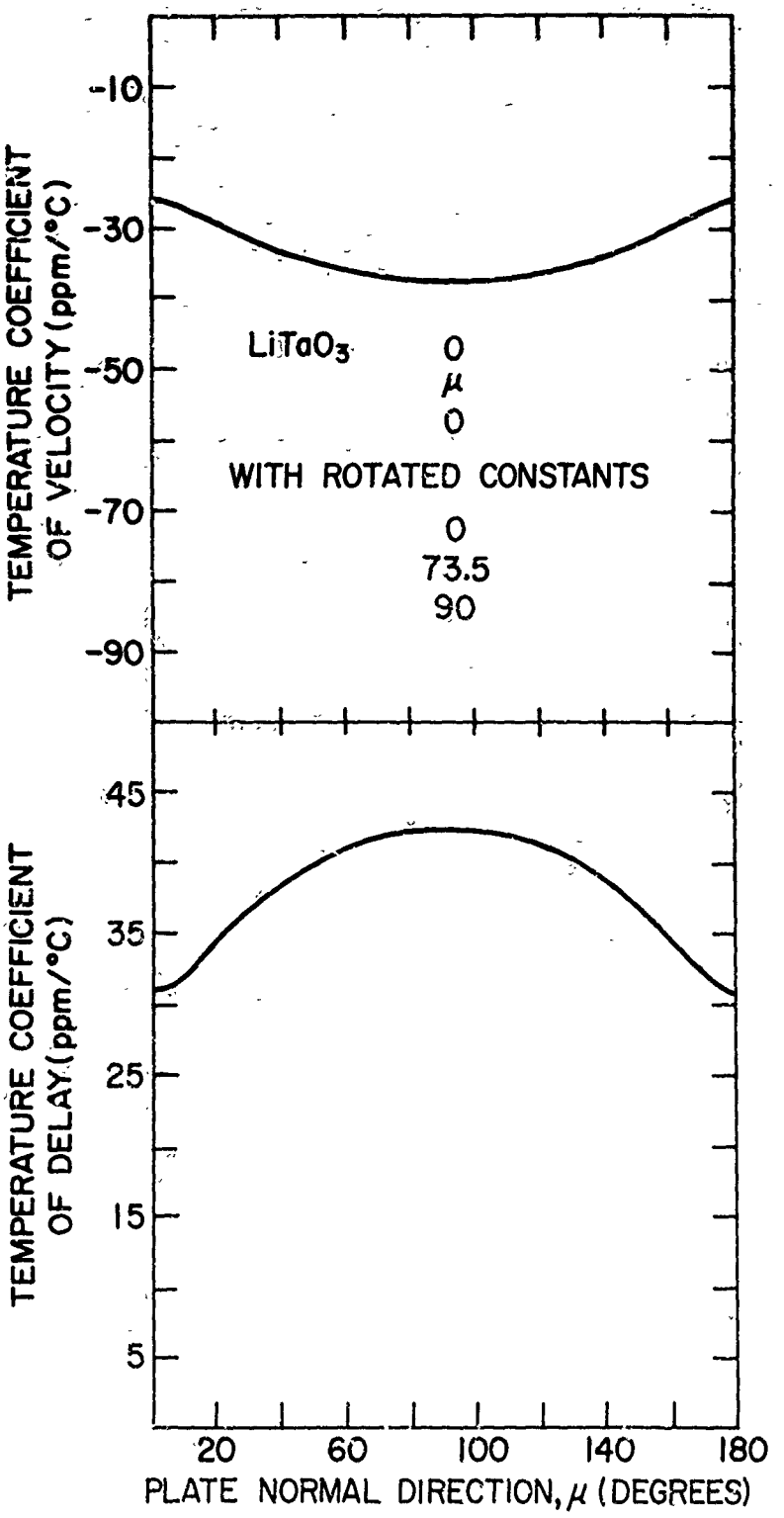
TEMPERATURE COEFFICIENT OF VELOCITY (ppm/°C)
-10
-30
-50
-70
-90
LiTaO3
0
μ
0
WITH ROTATED CONSTANTS
0
73.5
90
TEMPERATURE COEFFICIENT OF DELAY (ppm/°C)
45
35
25
15
5
20
60
100
140
180
PLATE NORMAL DIRECTION, μ (DEGREES)

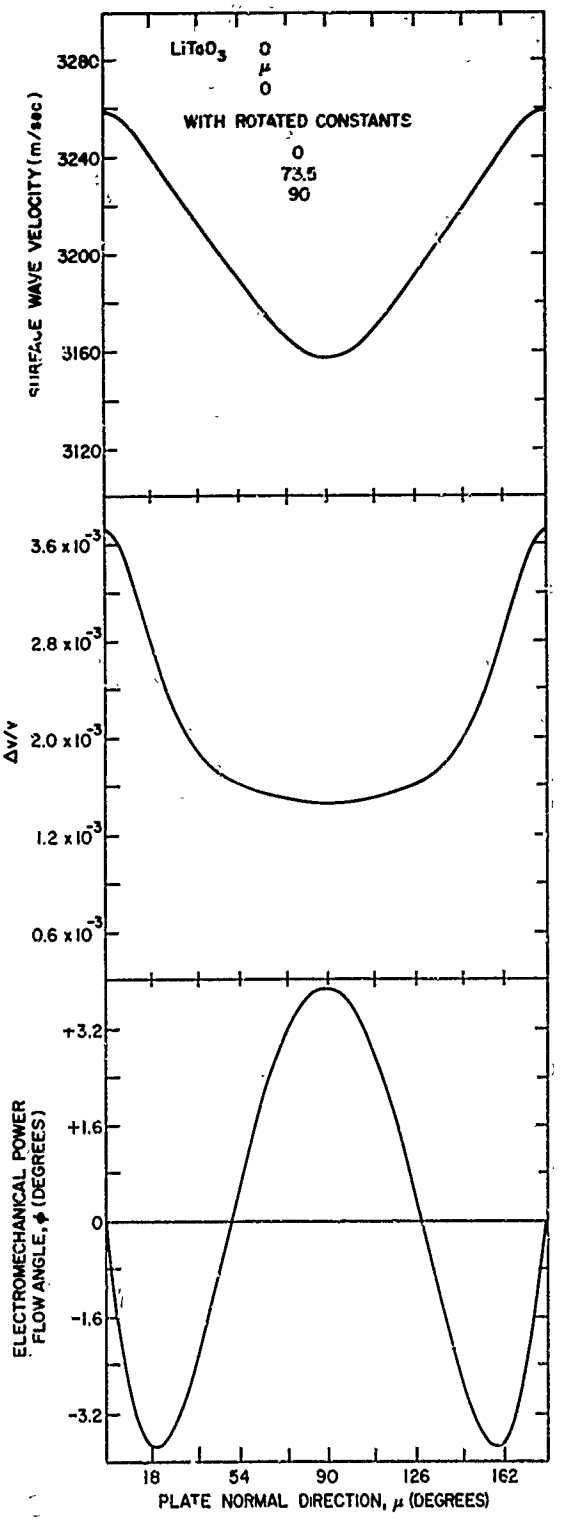
LiTaO3 0 μ 0
WITH ROTATED CONSTANTS
0
73.5
90
SURFACE WAVE VELOCITY (m/sec)
3280
3240
3200
3160
3120
3.6 x 10-3
2.8 x 10-3
2.0 x 10-3
1.2 x 10-3
0.6 x 10-3
Δv/v
+3.2
+1.6
0
-1.6
-3.2
ELECTROMECHANICAL POWER FLOW ANGLE, ϕ (DEGREES)
18
54
90
126
162
PLATE NORMAL DIRECTION, μ (DEGREES)

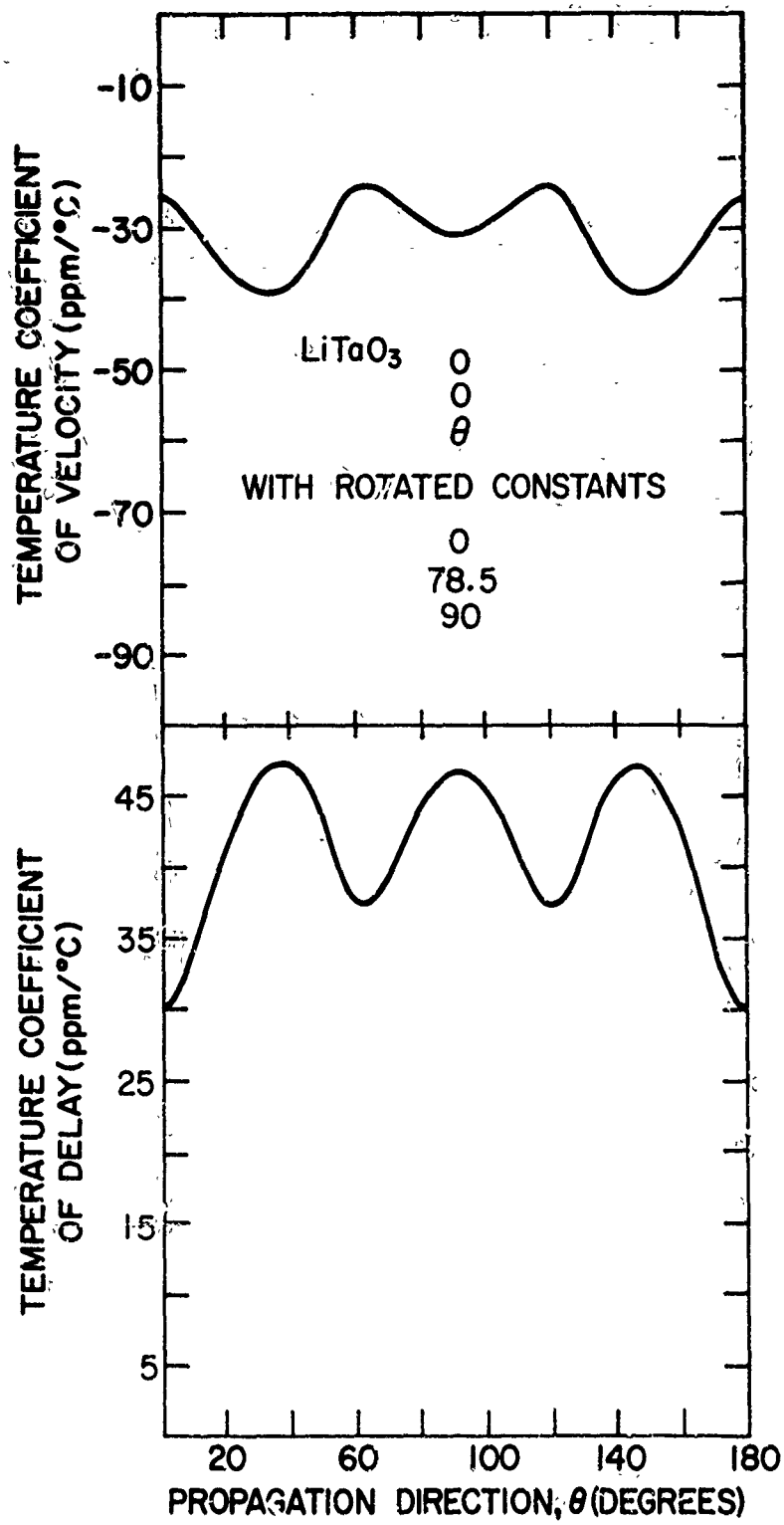
-10
-30
-50
-70
-90
TEMPERATURE COEFFICIENT OF VELOCITY (ppm/°C)
LiTaO3
0
0
θ
WITH ROTATED CONSTANTS
0
78.5
90
45
35
25
15
5
TEMPERATURE COEFFICIENT OF DELAY (ppm/°C)
20
60
100
140
180
PROPAGATION DIRECTION, θ (DEGREES)

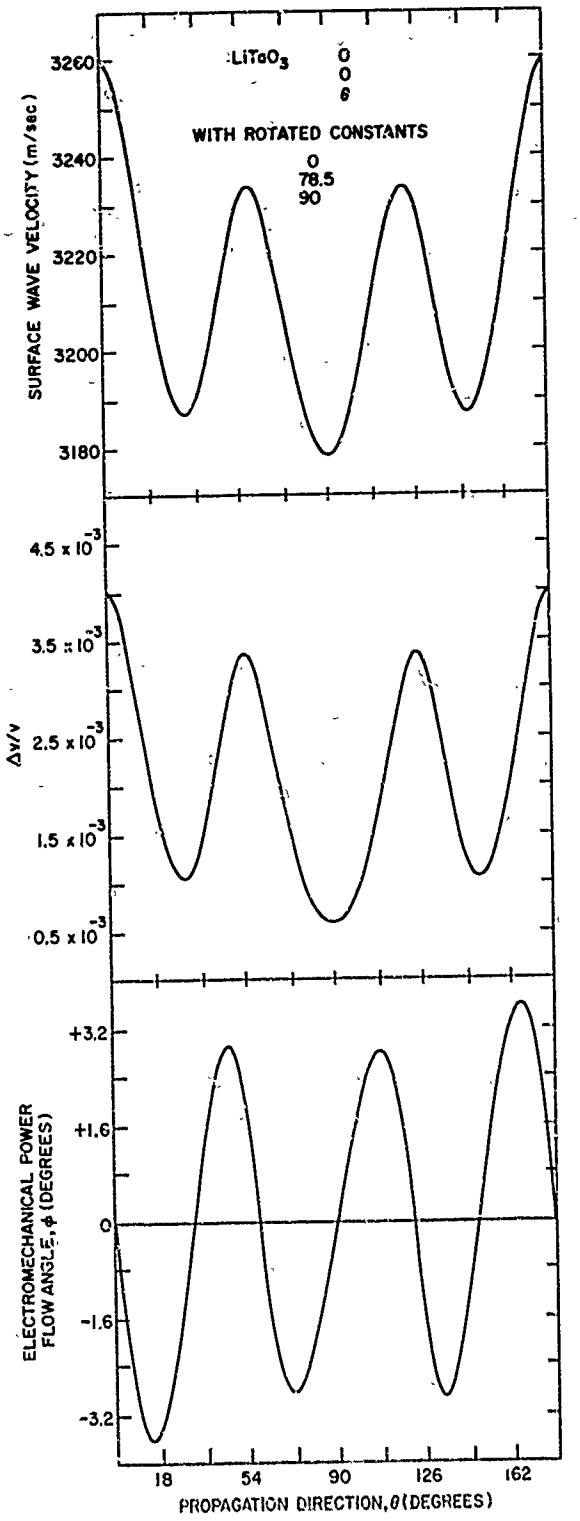
LiTaO3
0
0
θ
WITH ROTATED CONSTANTS
0
78.5
90
SURFACE WAVE VELOCITY (m/sec)
3260
3240
3220
3200
3180
Δv/v
4.5 x 10-3
3.5 x 10-3
2.5 x 10-3
1.5 x 10-3
0.5 x 10-3
ELECTROMECHANICAL POWER FLOW ANGLE, φ (DEGREES)
+3.2
+1.6
0
-1.6
-3.2
18
54
90
126
162
PROPAGATION DIRECTION, θ (DEGREES)

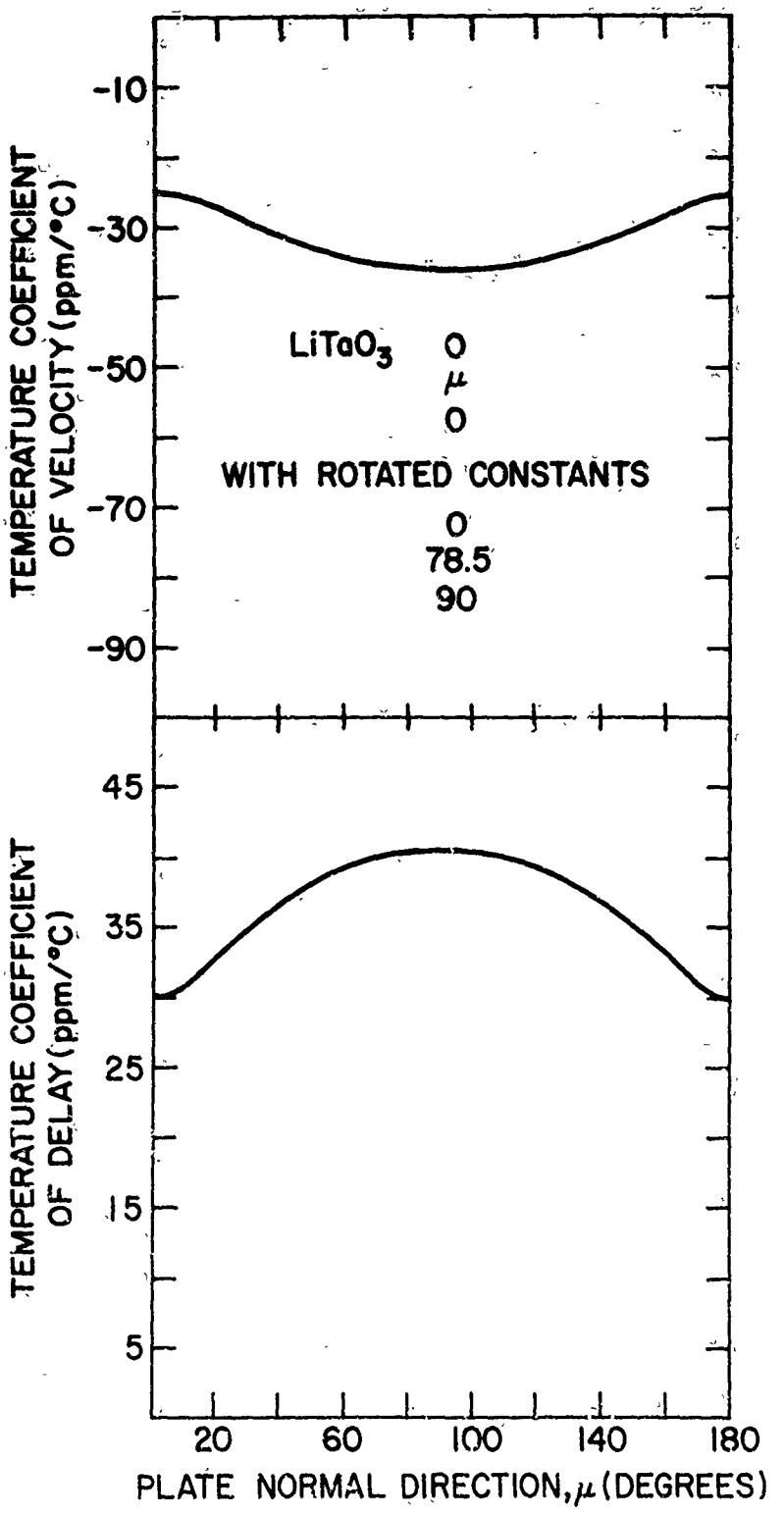
-10
-30
-50
-70
-90
TEMPERATURE COEFFICIENT OF VELOCITY (ppm/°C)
LiTaO3
0
μ
0
WITH ROTATED CONSTANTS
0
78.5
90
45
35
25
15
5
TEMPERATURE COEFFICIENT OF DELAY (ppm/°C)
20
60
100
140
180
PLATE NORMAL DIRECTION, μ (DEGREES)

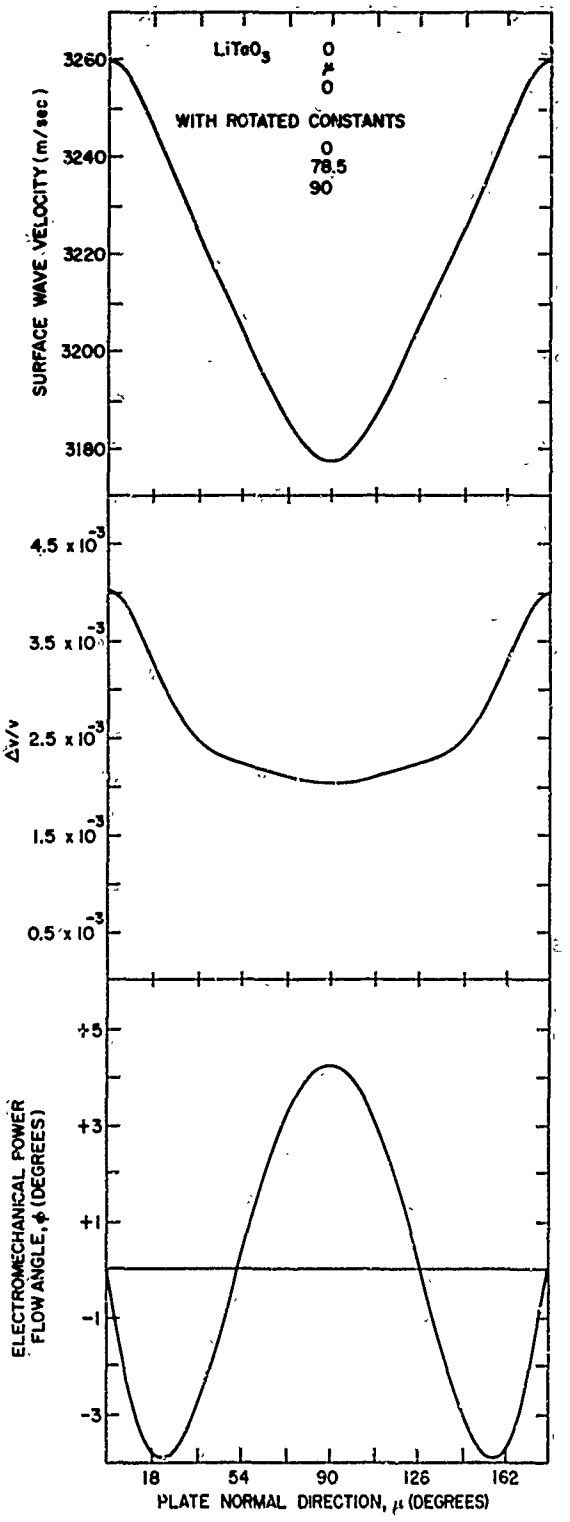
LiTaO3
0
μ
0
WITH ROTATED CONSTANTS
0
78.5
90
SURFACE WAVE VELOCITY (m/sec)
3260
3240
3220
3200
3180
Δv/v
4.5 x 10-3
3.5 x 10-3
2.5 x 10-3
1.5 x 10-3
0.5 x 10-3
ELECTROMECHANICAL POWER FLOW ANGLE, ϕ (DEGREES)
+5
+3
+1
-1
-3
18
54
90
126
162
PLATE NORMAL DIRECTION, μ (DEGREES)

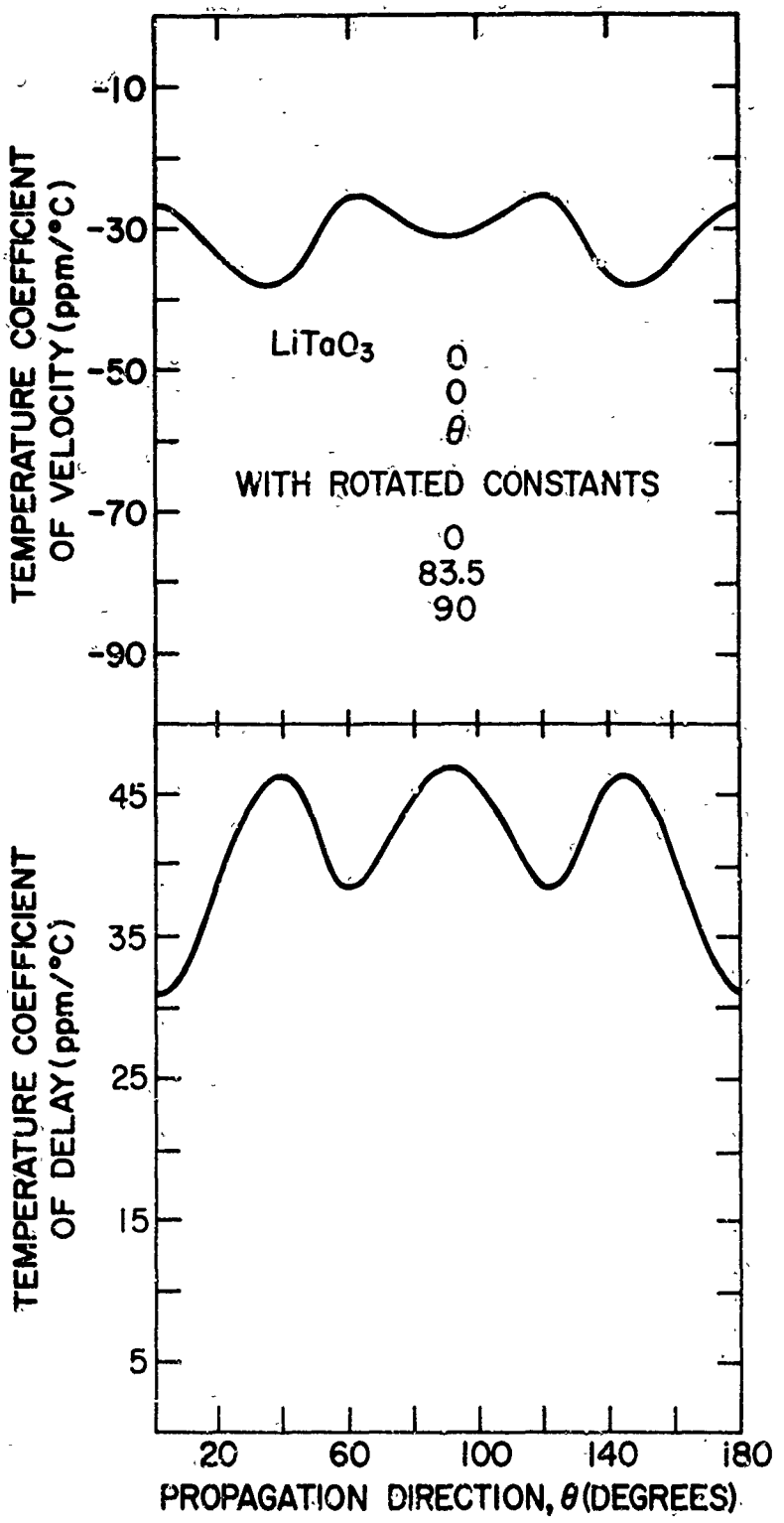
-10
-30
-50
-70
-90
TEMPERATURE COEFFICIENT OF VELOCITY (ppm/°C)
LiTaO3
0
0
θ
WITH ROTATED CONSTANTS
0
83.5
90
45
35
25
15
5
TEMPERATURE COEFFICIENT OF DELAY (ppm/°C)
20
60
100
140
180
PROPAGATION DIRECTION, θ (DEGREES)

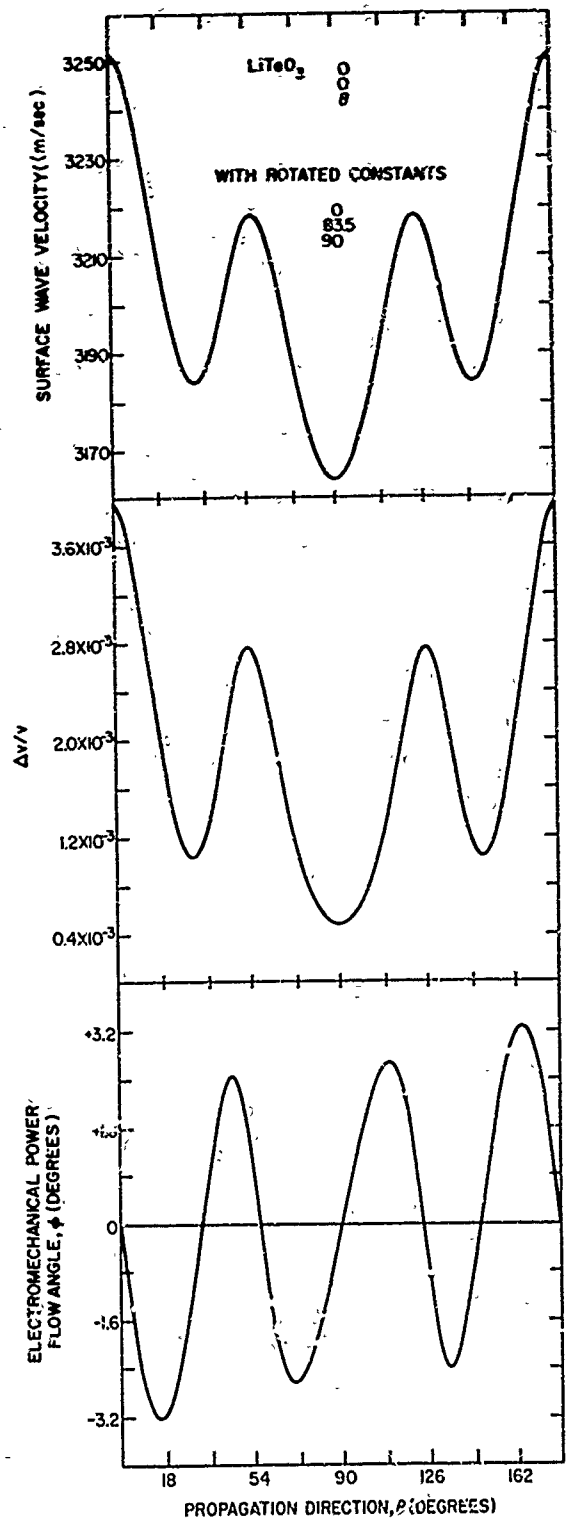
LiTeO3
0
90
0
WITH ROTATED CONSTANTS
0
83.5
90
SURFACE WAVE VELOCITY (m/sec)
3250
3230
3210
3190
3170
Δv/v
3.6X10-3
2.8X10-3
2.0X10-3
1.2X10-3
0.4X10-3
ELECTROMECHANICAL POWER FLOW ANGLE, φ (DEGREES)
+3.2
0
-1.6
-3.2
18
54
90
126
162
PROPAGATION DIRECTION, ρ (DEGREES)

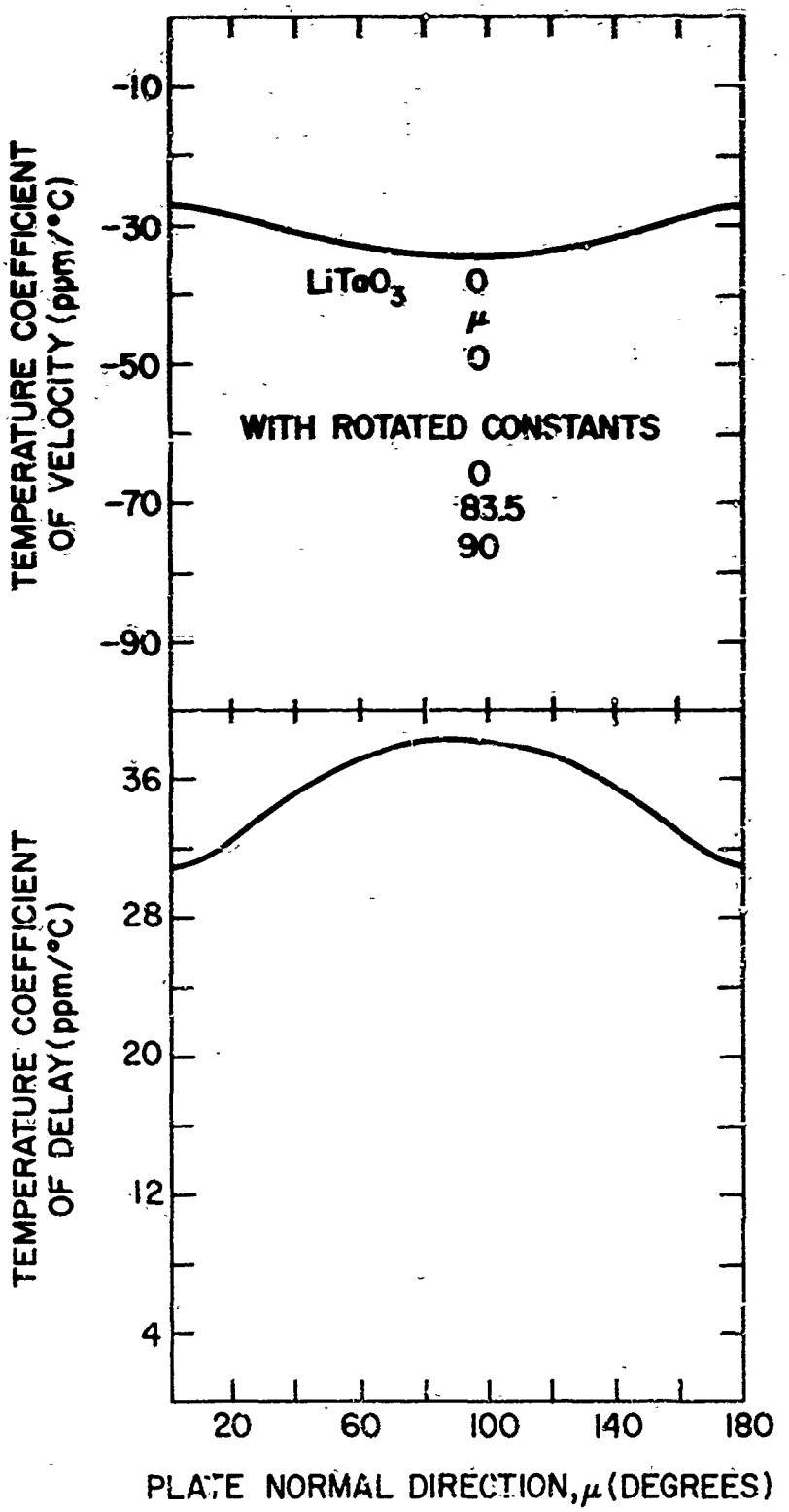
TEMPERATURE COEFFICIENT OF VELOCITY (ppm/°C)
-10
-30
-50
-70
-90
LiTaO3
0
ϕ
0
WITH ROTATED CONSTANTS
0
83.5
90
TEMPERATURE COEFFICIENT OF DELAY (ppm/°C)
36
28
20
12
4
20
60
100
140
180
PLATE NORMAL DIRECTION, μ (DEGREES)

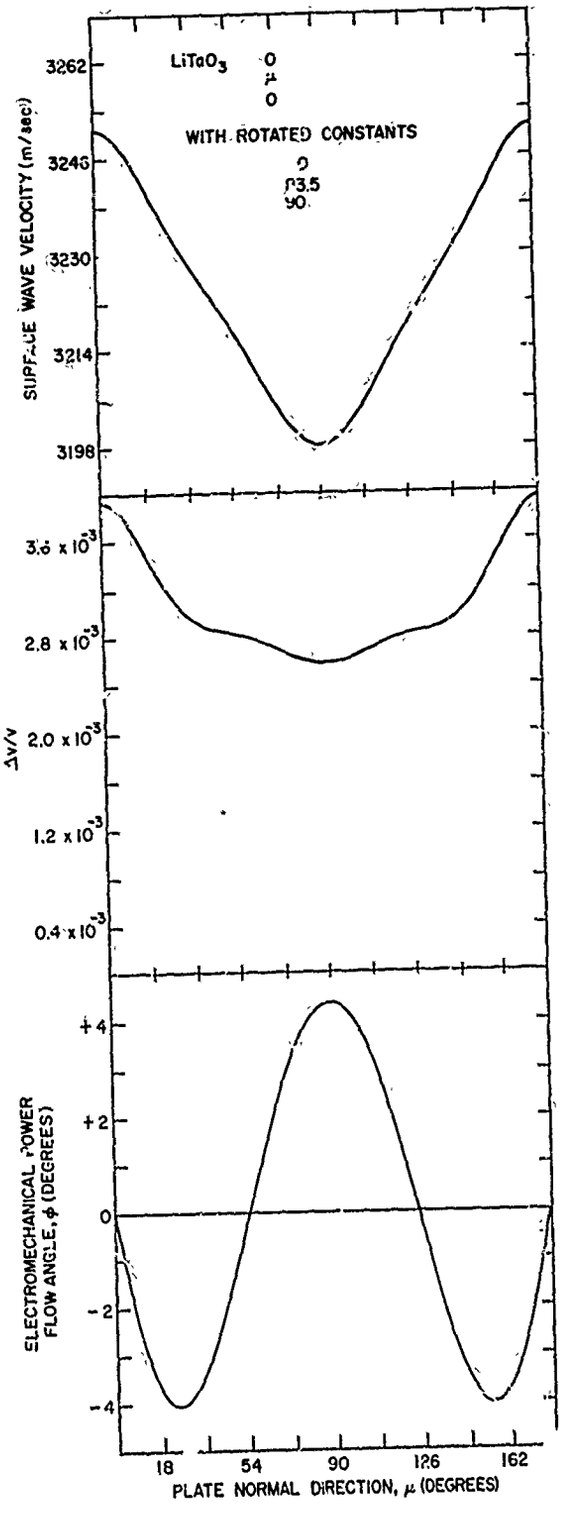
LiTaO3
0
42
0
WITH ROTATED CONSTANTS
0
93.5
90.
SURFACE WAVE VELOCITY (m/sec)
3262
3246
3230
3214
3198
Δv/v
3.6 x 10-3
2.8 x 10-3
2.0 x 10-3
1.2 x 10-3
0.4 x 10-3
ELECTROMECHANICAL POWER FLOW ANGLE, ϕ (DEGREES)
+4
+2
0
-2
-4
18
54
90
126
162
PLATE NORMAL DIRECTION, μ (DEGREES)

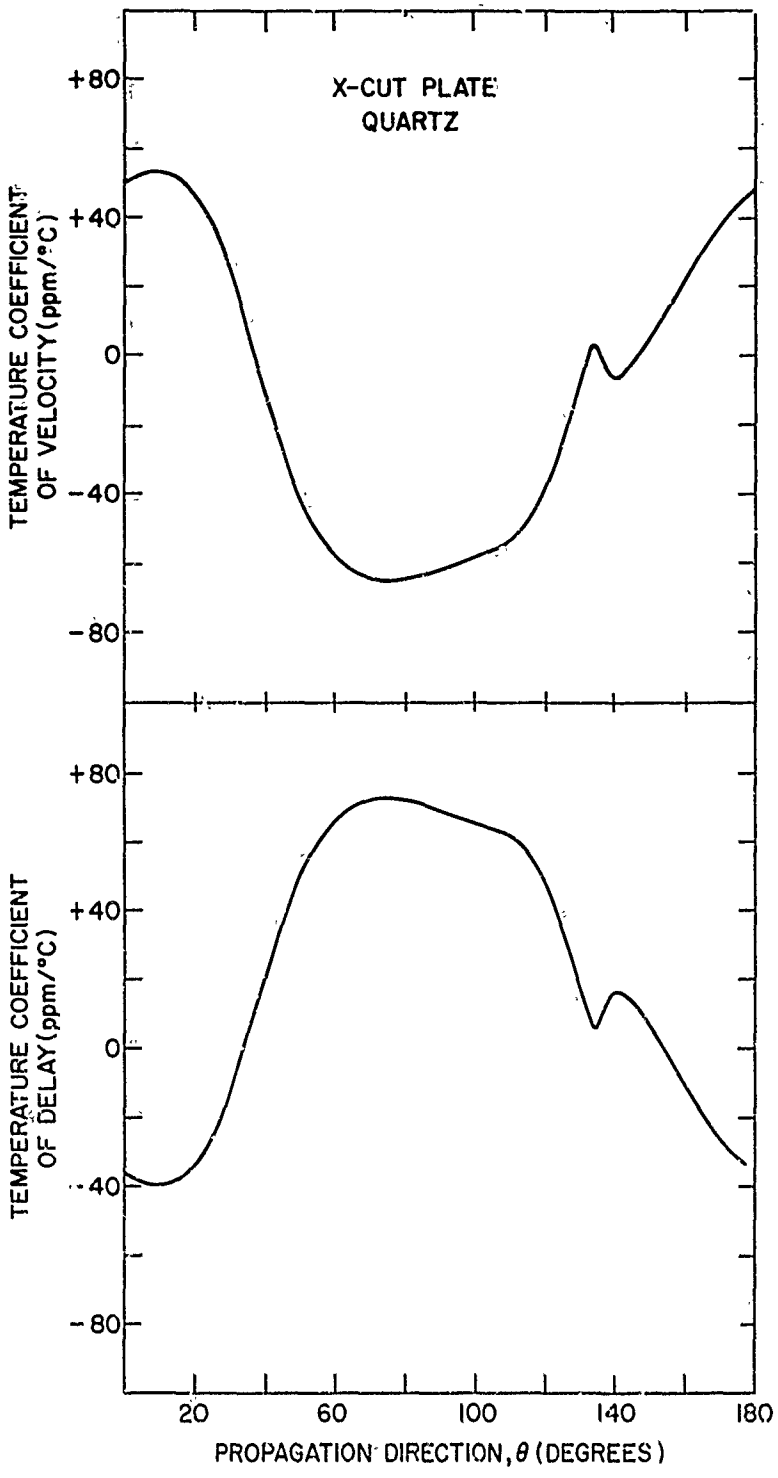
X-CUT PLATE
QUARTZ
TEMPERATURE COEFFICIENT OF VELOCITY (ppm/°C)
+80
+40
0
-40
-80
TEMPERATURE COEFFICIENT OF DELAY (ppm/°C)
+80
+40
0
-40
-80
20
60
100
140
180
PROPAGATION DIRECTION, θ (DEGREES)

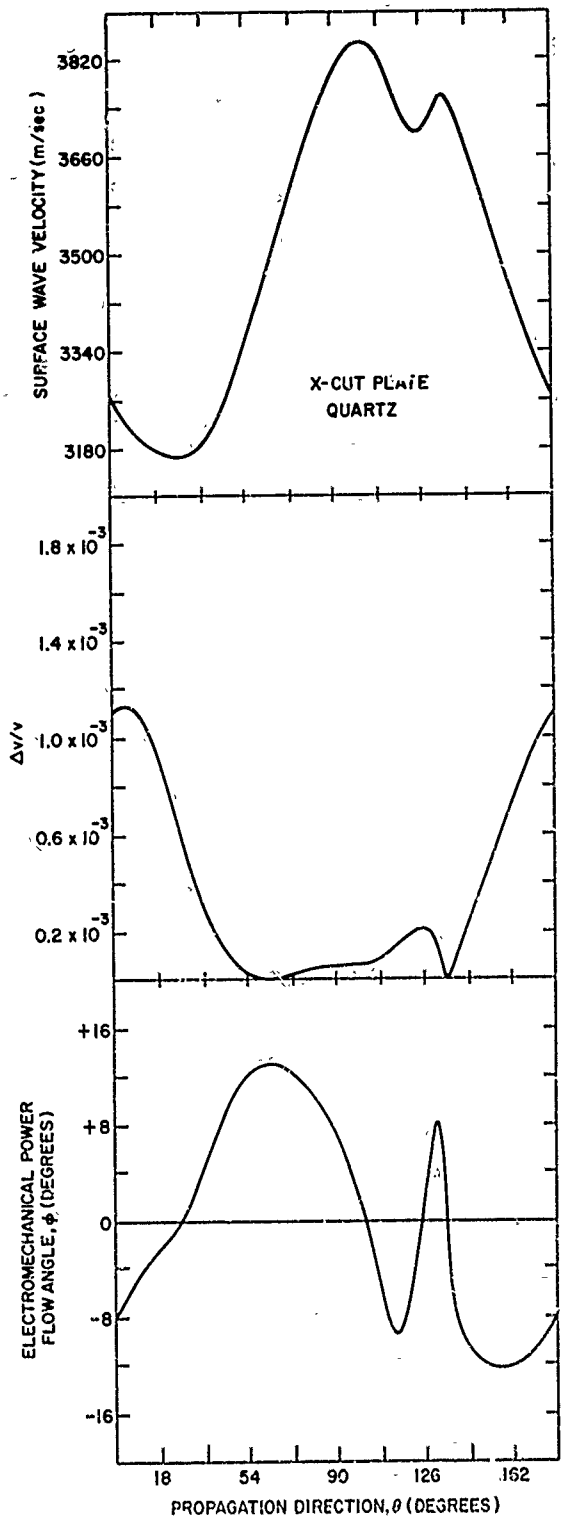
SURFACE WAVE VELOCITY (m/sec)
3820
3660
3500
3340
3180
X-CUT PLATE
QUARTZ
1.8 x 10⁻³
1.4 x 10⁻³
1.0 x 10⁻³
0.6 x 10⁻³
0.2 x 10⁻³
Δv/v
+16
+8
0
-8
-16
ELECTROMECHANICAL POWER FLOW ANGLE, φ (DEGREES)
18
54
90
126
162
PROPAGATION DIRECTION, θ (DEGREES)

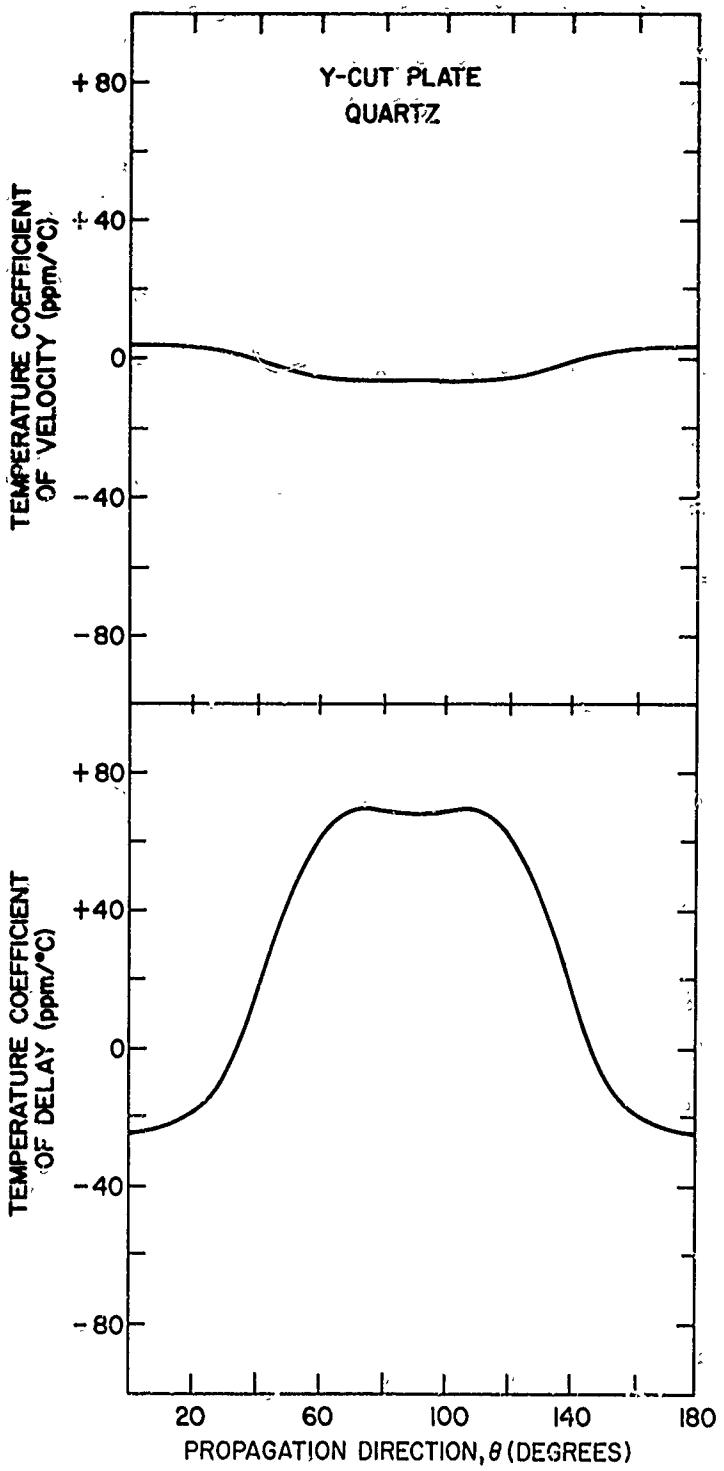
Y-CUT PLATE
QUARTZ
+80
+40
0
-40
-80
TEMPERATURE COEFFICIENT OF VELOCITY (ppm/°C)
+80
+40
0
-40
-80
TEMPERATURE COEFFICIENT OF DELAY (ppm/°C)
20
60
100
140
180
PROPAGATION DIRECTION, θ (DEGREES)

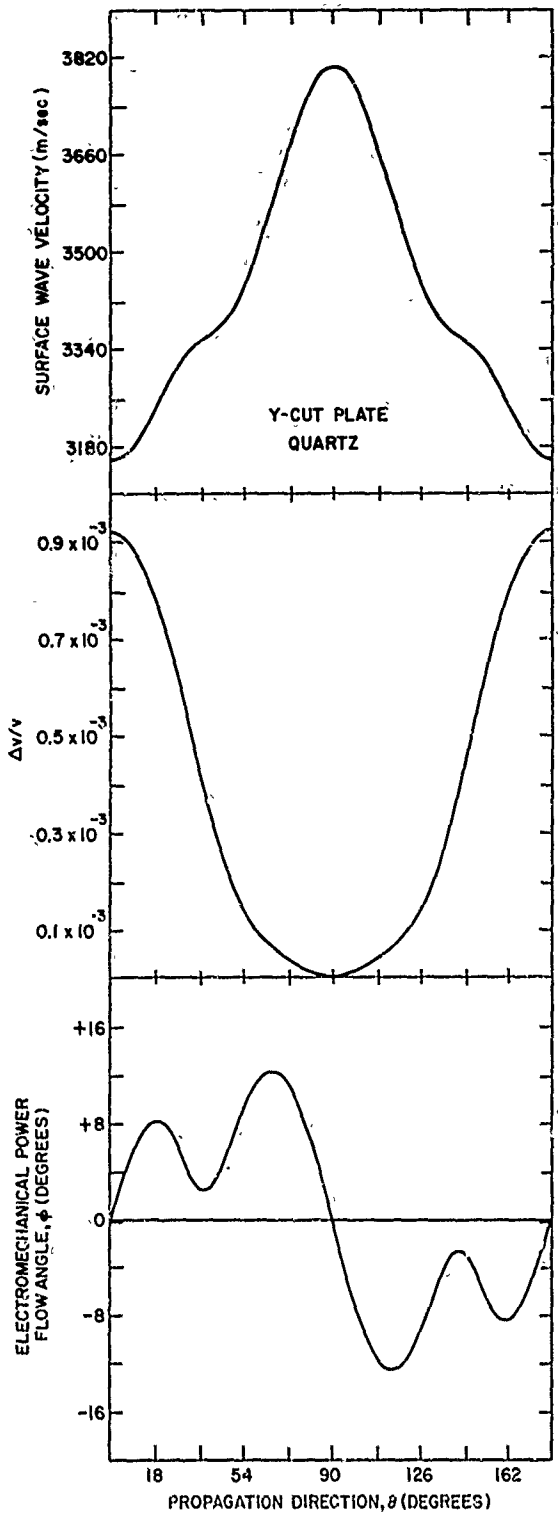
SURFACE WAVE VELOCITY (m/sec)
3820
3660
3500
3340
3180
Y-CUT PLATE
QUARTZ
Δv/v
0.9 x 10⁻³
0.7 x 10⁻³
0.5 x 10⁻³
0.3 x 10⁻³
0.1 x 10⁻³
ELECTROMECHANICAL POWER FLOW ANGLE, ϕ (DEGREES)
+16
+8
0
-8
-16
18
54
90
126
162
PROPAGATION DIRECTION, θ (DEGREES)

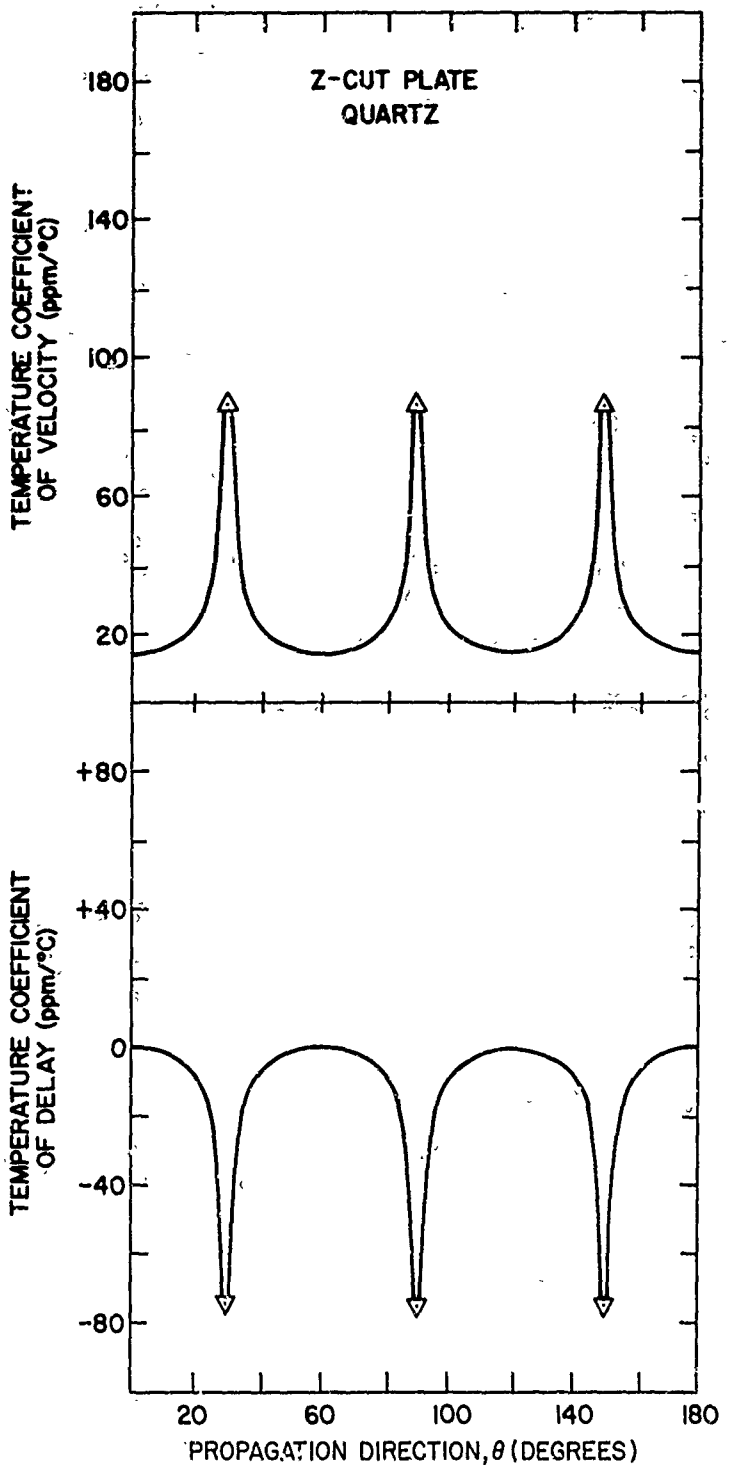

NOTE: FOR SIGNIFICANCE OF THE
Δ SEE FACING PAGE.

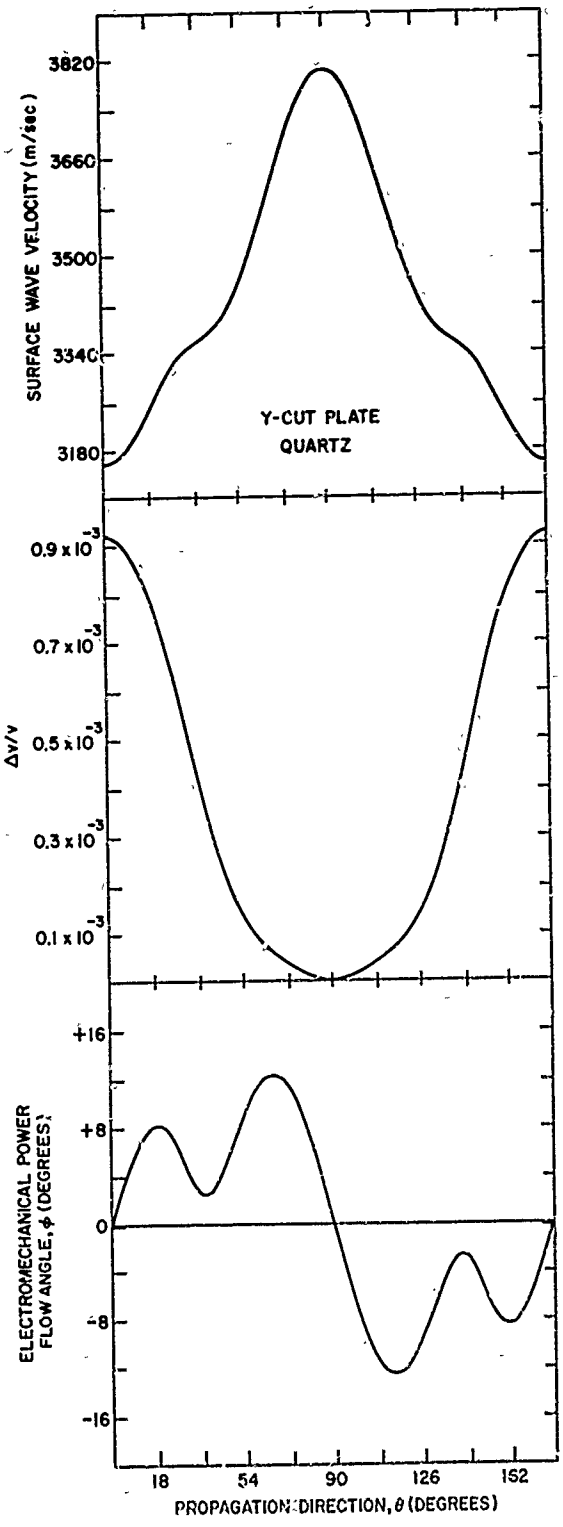
SURFACE WAVE VELOCITY (m/sec)
3820
3660
3500
3340
3180
Y-CUT PLATE
QUARTZ
Δv/v
0.9 x 10⁻³
0.7 x 10⁻³
0.5 x 10⁻³
0.3 x 10⁻³
0.1 x 10⁻³
ELECTROMECHANICAL POWER FLOW ANGLE, ϕ (DEGREES)
+16
+8
0
-8
-16
18
54
90
126
152
PROPAGATION DIRECTION, θ (DEGREES)

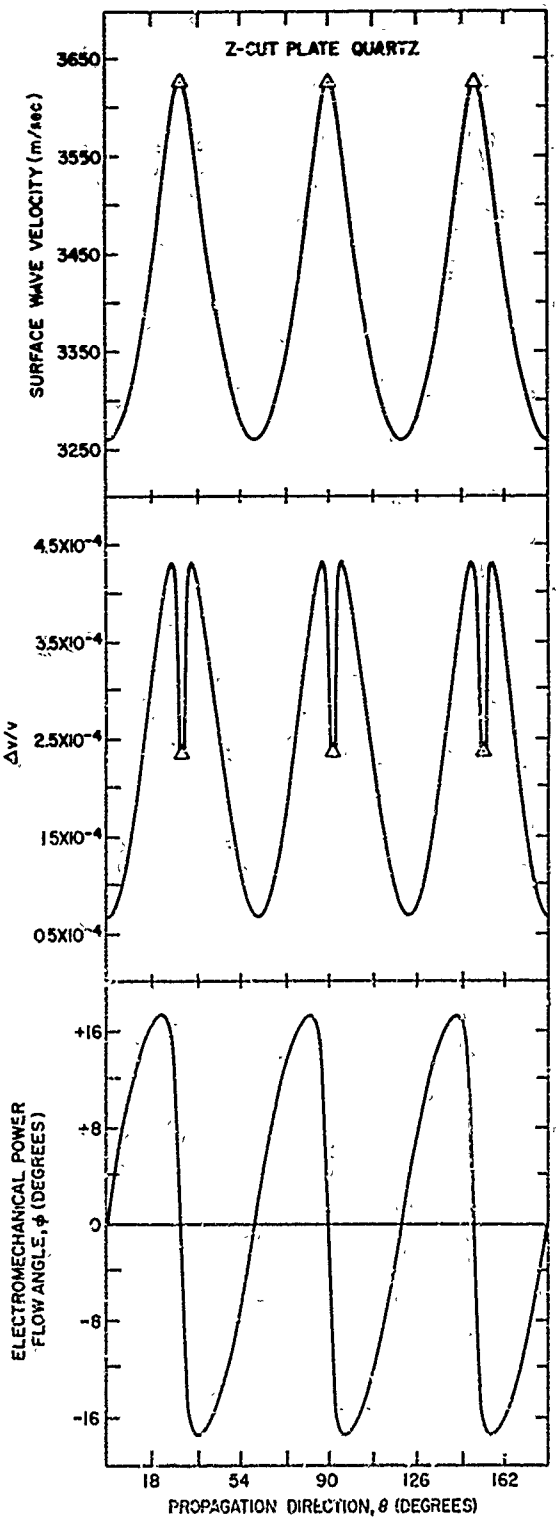

△NOTE AT θ=45°,90° AND 135° THE SURFACE WAVE DEGENERATES INTO A TILTED BULK WAVE. HOWEVER, A RAYLEIGH LIKE WAVE LIES AT 368507 M/SEC ON THE PSEUDO SURFACE WAVE BRANCH. (SEE FARNELL, 1970)

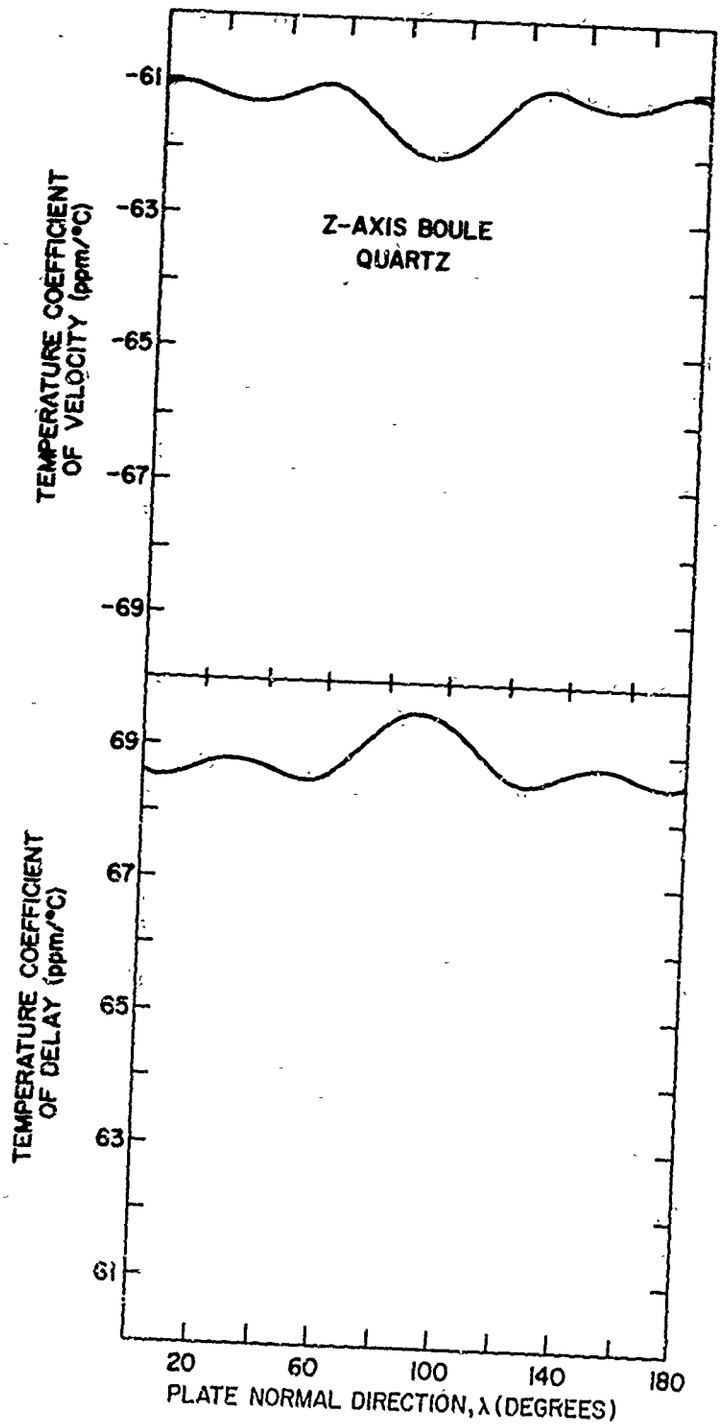
-61
-63
-65
-67
-69
TEMPERATURE COEFFICIENT OF VELOCITY (ppm/°C)
Z-AXIS BOULE
QUARTZ
69
67
65
63
61
TEMPERATURE COEFFICIENT OF DELAY (ppm/°C)
20
60
100
140
180
PLATE NORMAL DIRECTION, λ (DEGREES)

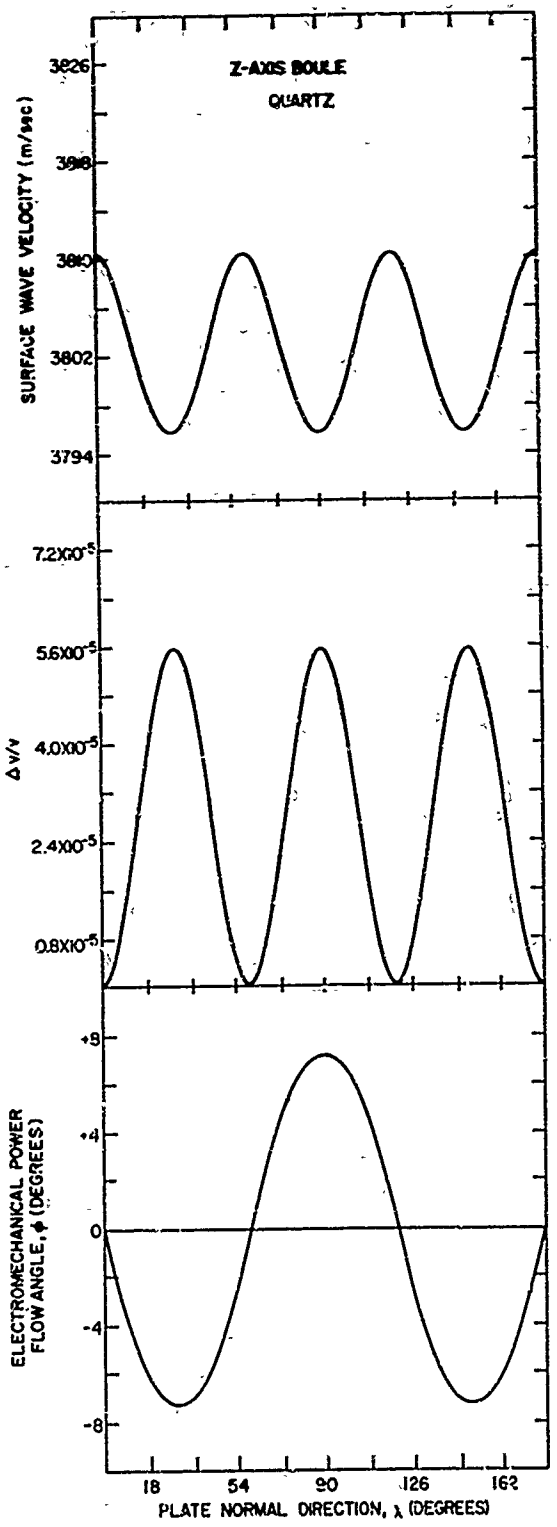
Z-AXIS BOULE
QUARTZ
SURFACE WAVE VELOCITY (m/sec)
3826
3798
3780
3802
3794
Δv/v
7.2X10⁻⁵
5.6X10⁻⁵
4.0X10⁻⁵
2.4X10⁻⁵
0.8X10⁻⁵
ELECTROMECHANICAL POWER FLOW ANGLE, φ (DEGREES)
+8
+4
0
-4
-8
18
54
90
126
162
PLATE NORMAL DIRECTION, λ (DEGREES)

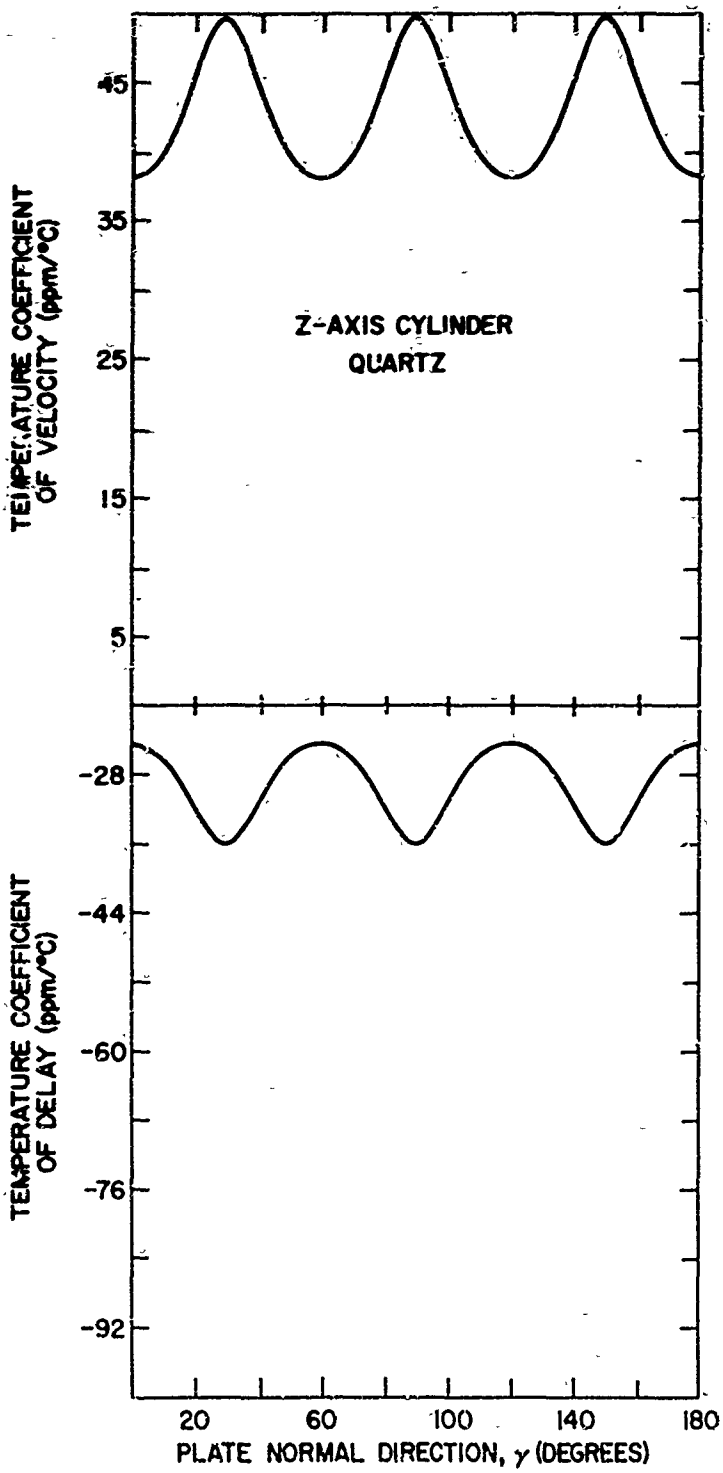
45
35
25
15
5
Z-AXIS CYLINDER
QUARTZ
TEMPERATURE COEFFICIENT
OF VELOCITY (ppm/°C)
-28
-44
-60
-76
-92
TEMPERATURE COEFFICIENT
OF DELAY (ppm/°C)
20
60
100
140
180
PLATE NORMAL DIRECTION, γ (DEGREES)

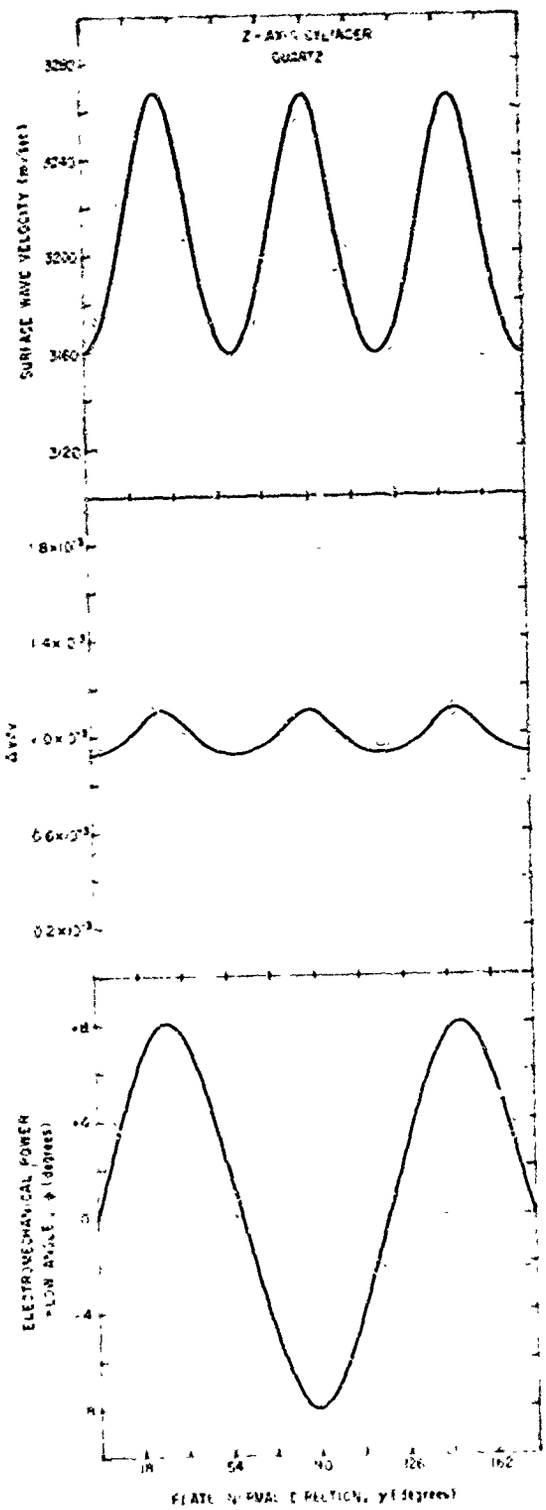
Z-AXIS CYLINDER
QUARTZ
SURFACE WAVE VELOCITY (m/sec)
3280
3240
3200
3160
3120
Δv/v
ELECTROMECHANICAL POWER FLOW ANGLE, Φ (degrees)
+8
+4
0
-4
-8
18
54
90
126
162
PLATE NORMAL DIRECTION, γ (degrees)

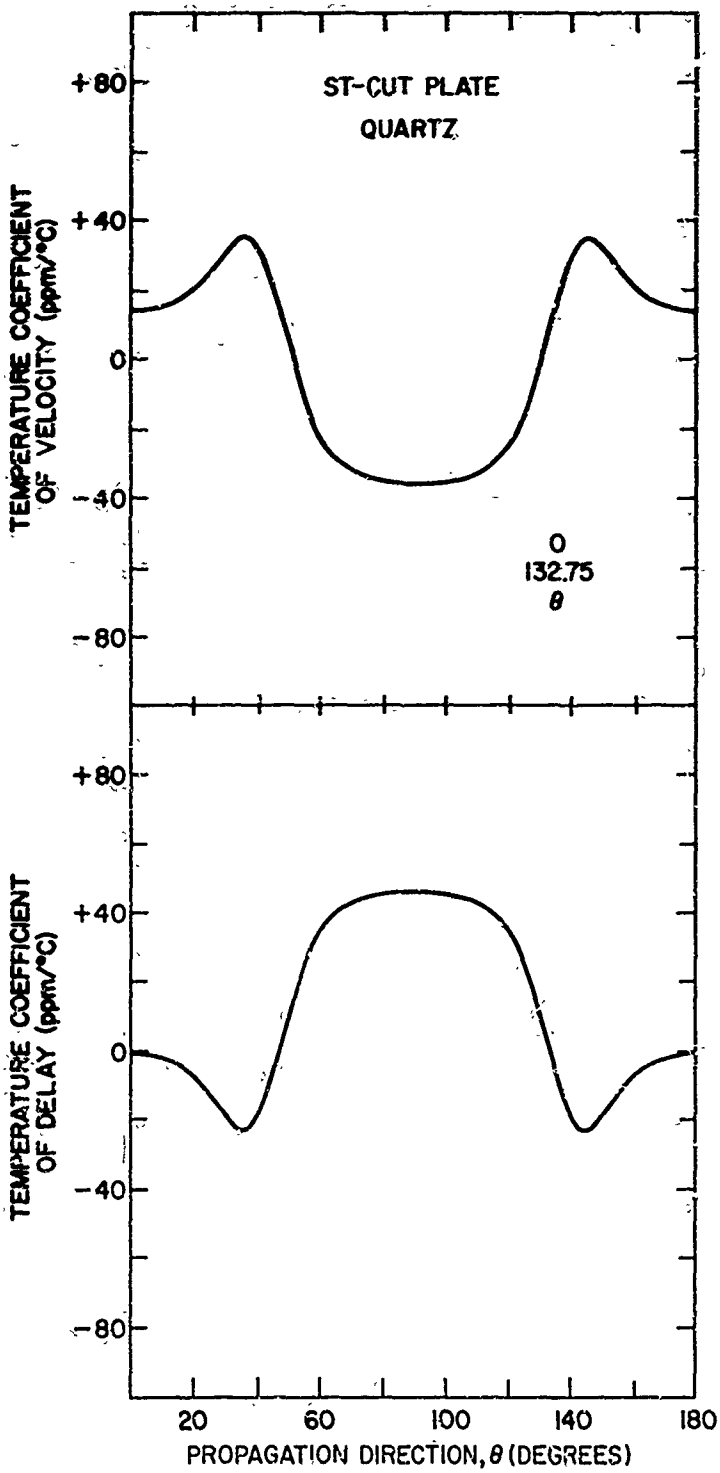
ST-CUT PLATE
QUARTZ
+80
+40
0
-40
-80
TEMPERATURE COEFFICIENT OF VELOCITY (ppm/°C)
0
132.75
θ
+80
+40
0
-40
-80
TEMPERATURE COEFFICIENT OF DELAY (ppm/°C)
20
60
100
140
180
PROPAGATION DIRECTION, θ (DEGREES)

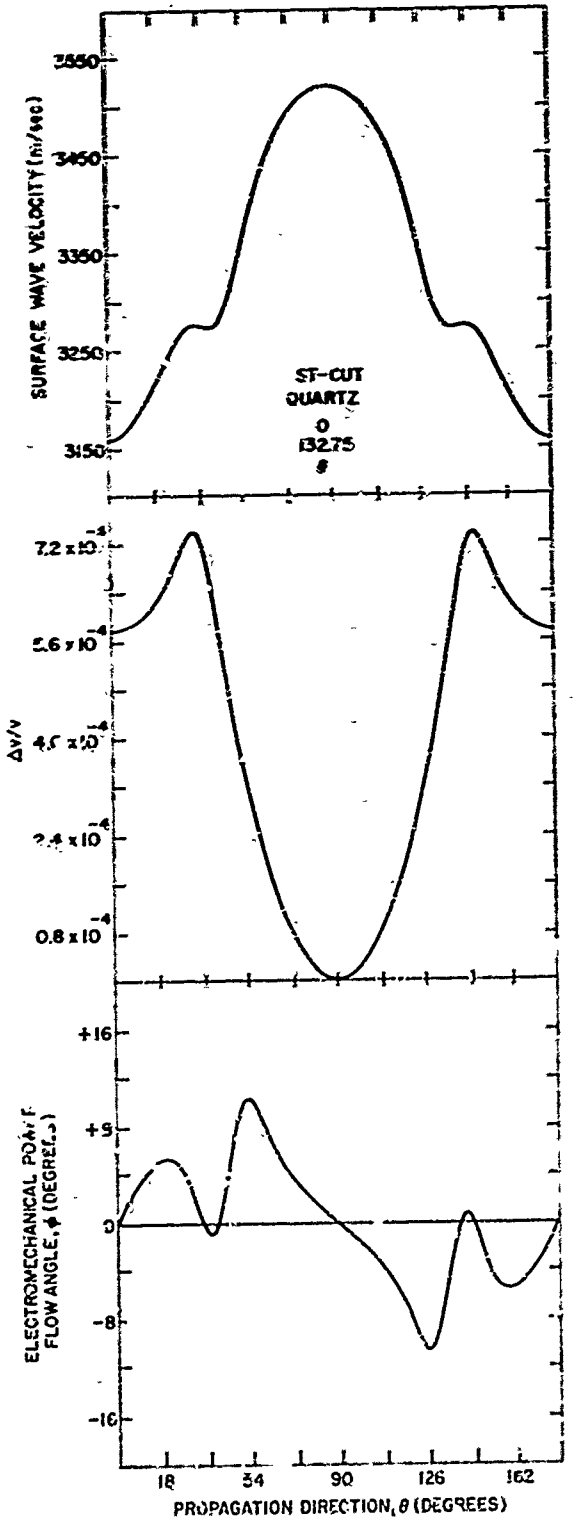
SURFACE WAVE VELOCITY (m/sec)
3550
3450
3350
3250
3150
ST-CUT
QUARTZ
θ
132.75
φ
7.2 x10⁻⁴
5.6 x10⁻⁴
4.8 x10⁻⁴
2.4 x10⁻⁴
0.8 x10⁻⁴
Δv/v
+16
+8
0
-8
-16
ELECTROMECHANICAL POWER FLOW ANGLE, ψ (DEGREES)
18
54
90
126
162
PROPAGATION DIRECTION, θ (DEGREES)

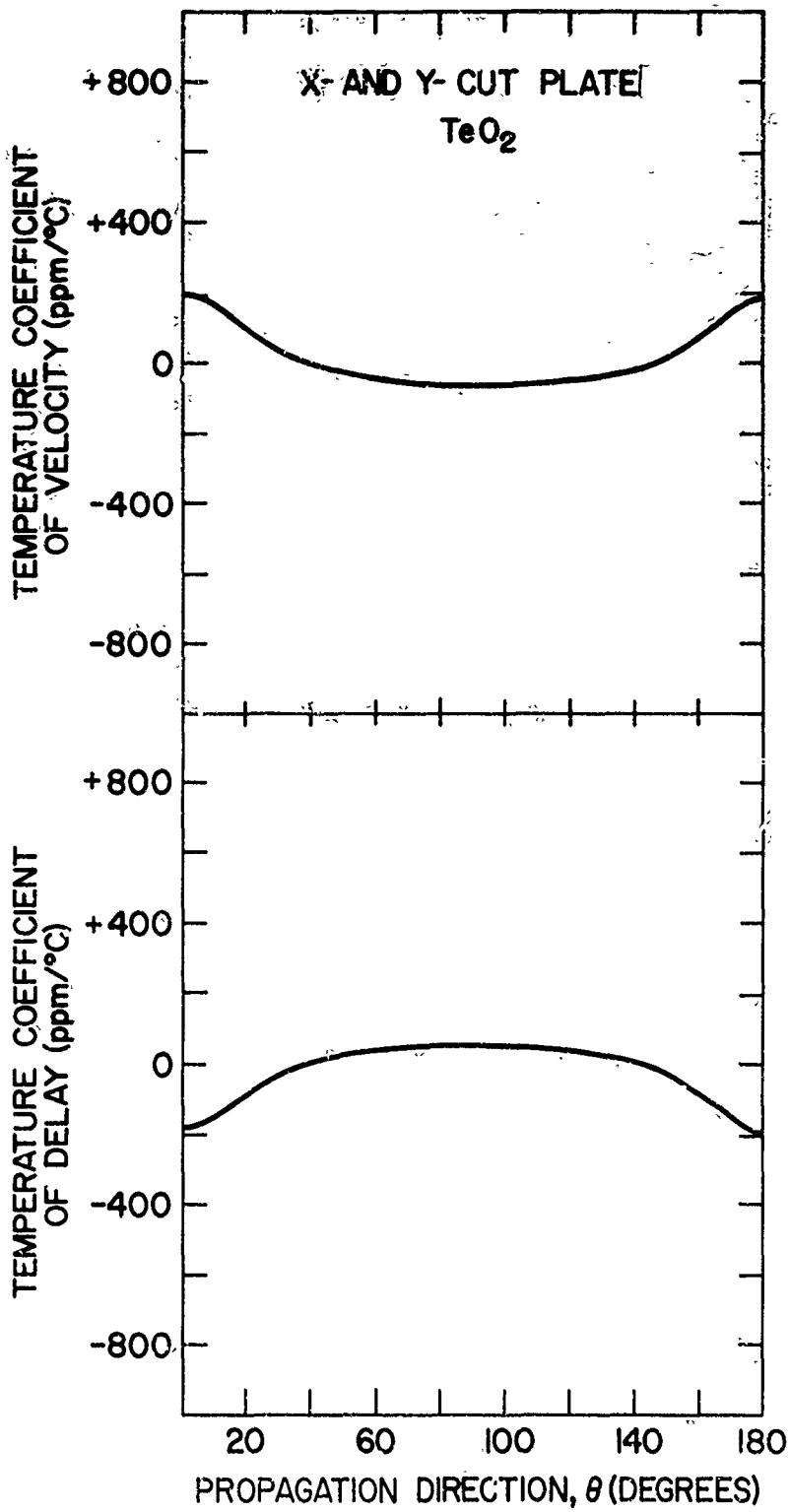
X- AND Y- CUT PLATE
TeO_2
TEMPERATURE COEFFICIENT OF VELOCITY (ppm/°C)
+800
+400
0
-400
-800
TEMPERATURE COEFFICIENT OF DELAY (ppm/°C)
+800
+400
0
-400
-800
20
60
100
140
180
PROPAGATION DIRECTION, θ (DEGREES)

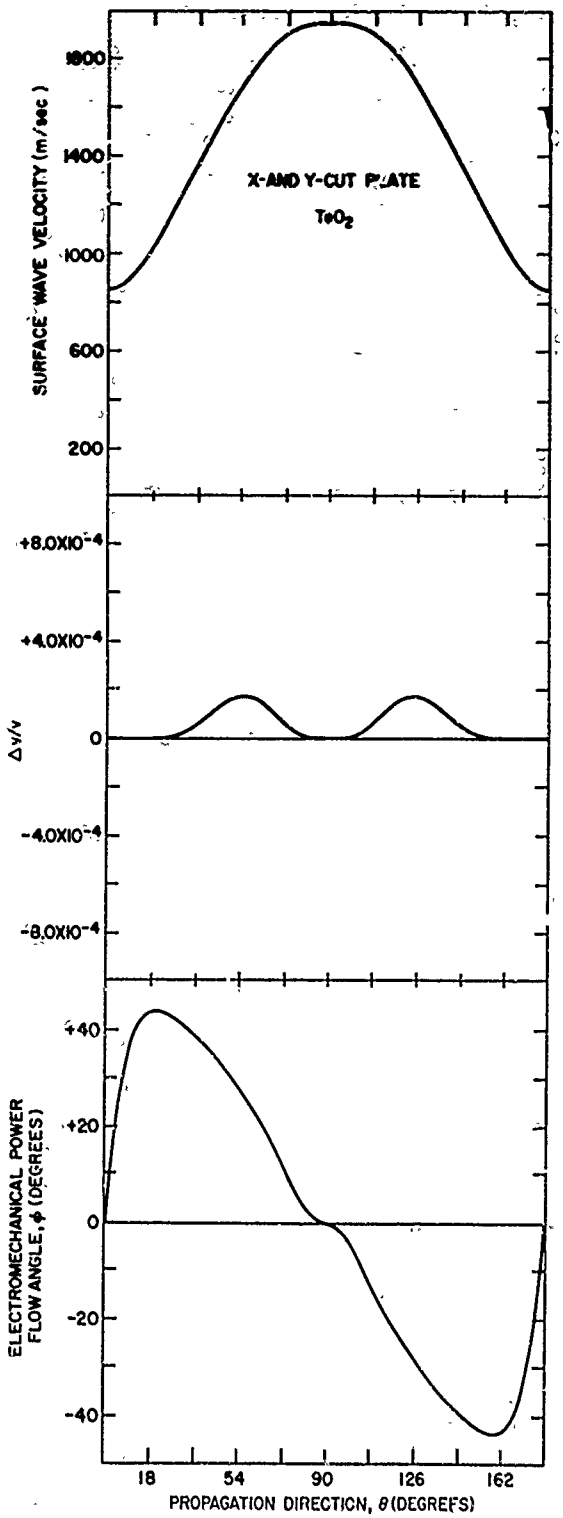
SURFACE WAVE VELOCITY (m/sec)
1800
1400
1000
600
200
X-AND Y-CUT PLATE
TeO_2
+8.0X10⁻⁴
+4.0X10⁻⁴
0
-4.0X10⁻⁴
-8.0X10⁻⁴
Δv/v
ELECTROMECHANICAL POWER FLOW ANGLE, ϕ (DEGREES)
+40
+20
0
-20
-40
18
54
90
126
162
PROPAGATION DIRECTION, θ (DEGREES)

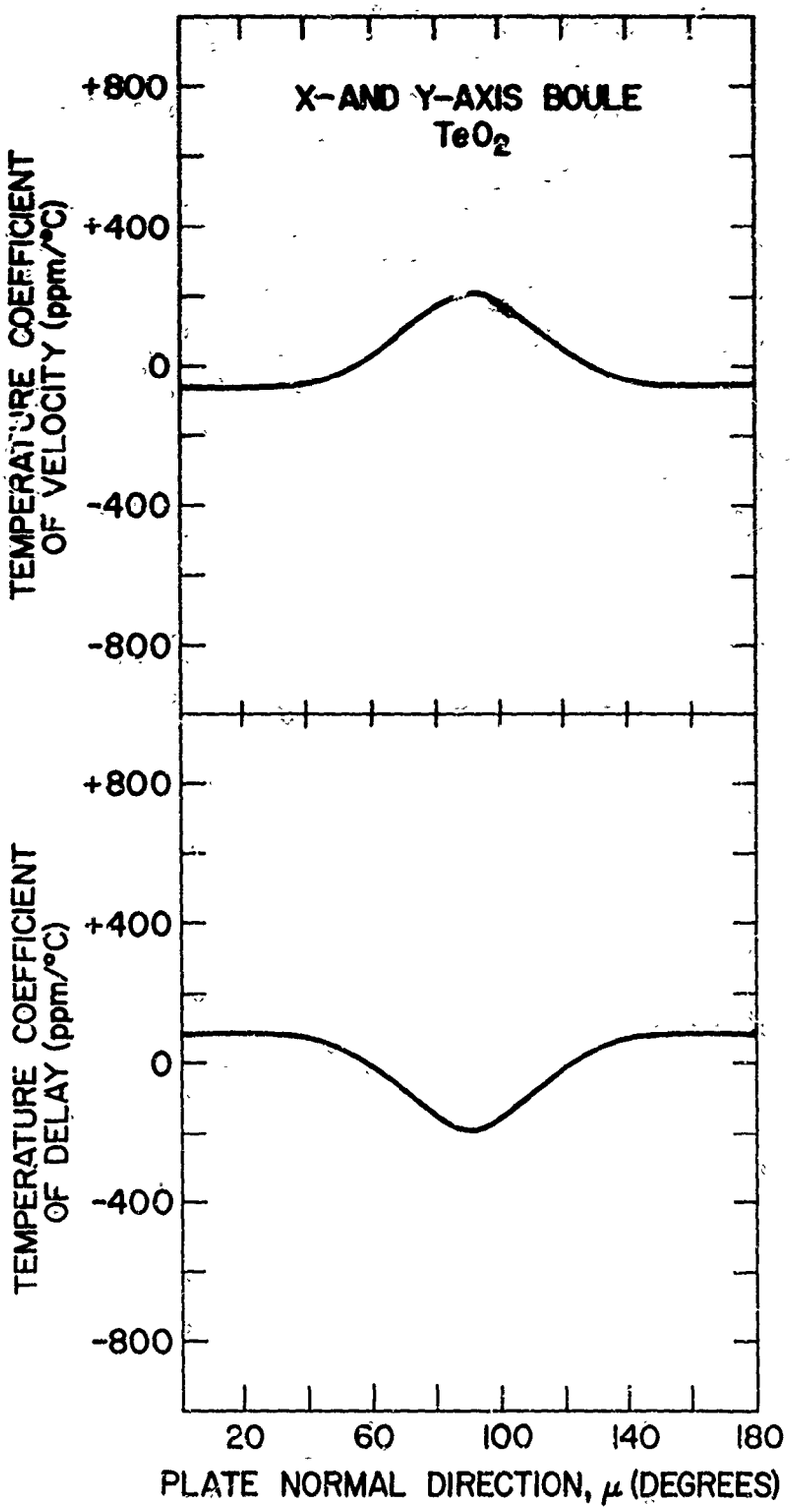
X-AND Y-AXIS BOULE
TeO_2
TEMPERATURE COEFFICIENT OF VELOCITY (ppm/°C)
+800
+400
0
-400
-800
TEMPERATURE COEFFICIENT OF DELAY (ppm/°C)
+800
+400
0
-400
-800
20
60
100
140
180
PLATE NORMAL DIRECTION, μ (DEGREES)

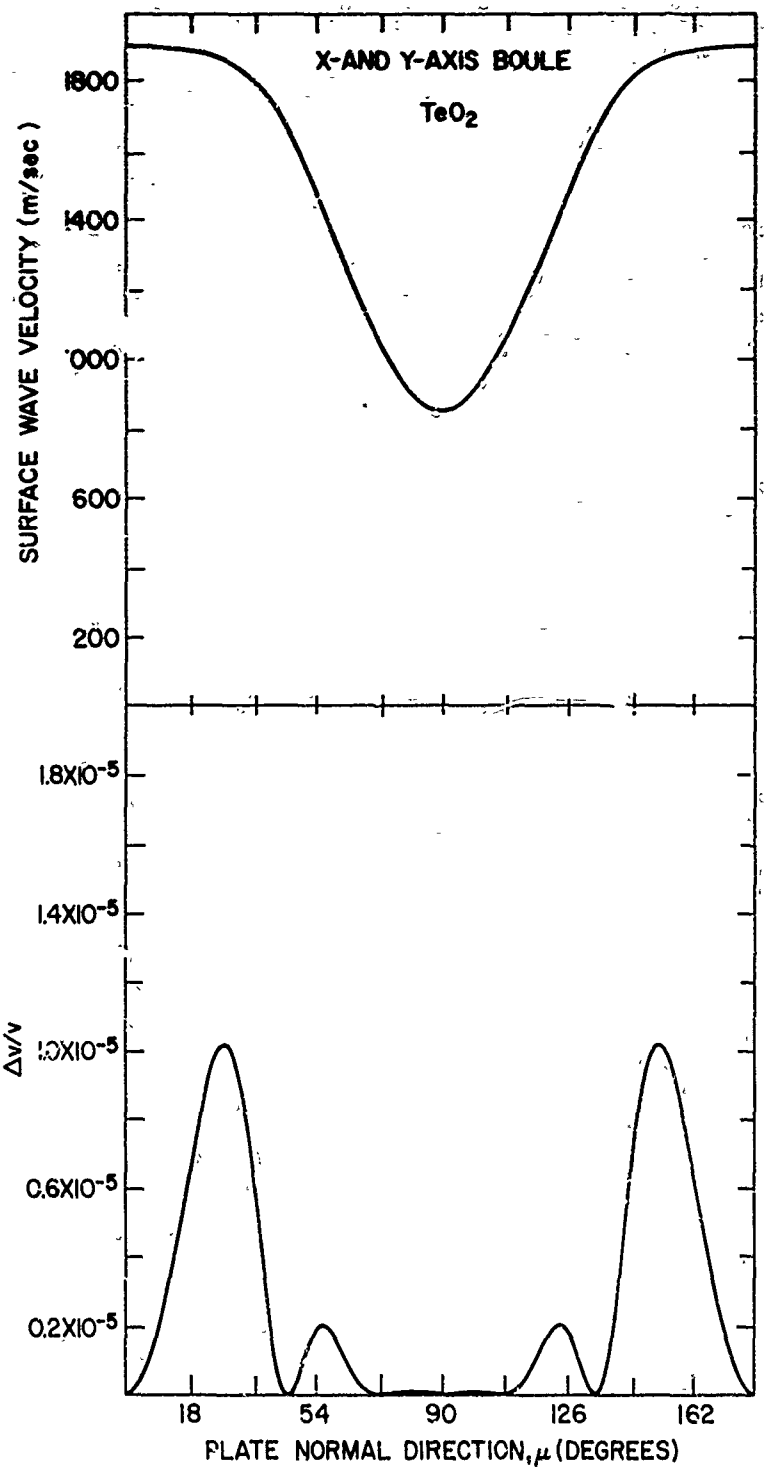

NOTE: TIME AVERAGE POWER FLOW ANGLE IDENTICALLY ZERO.

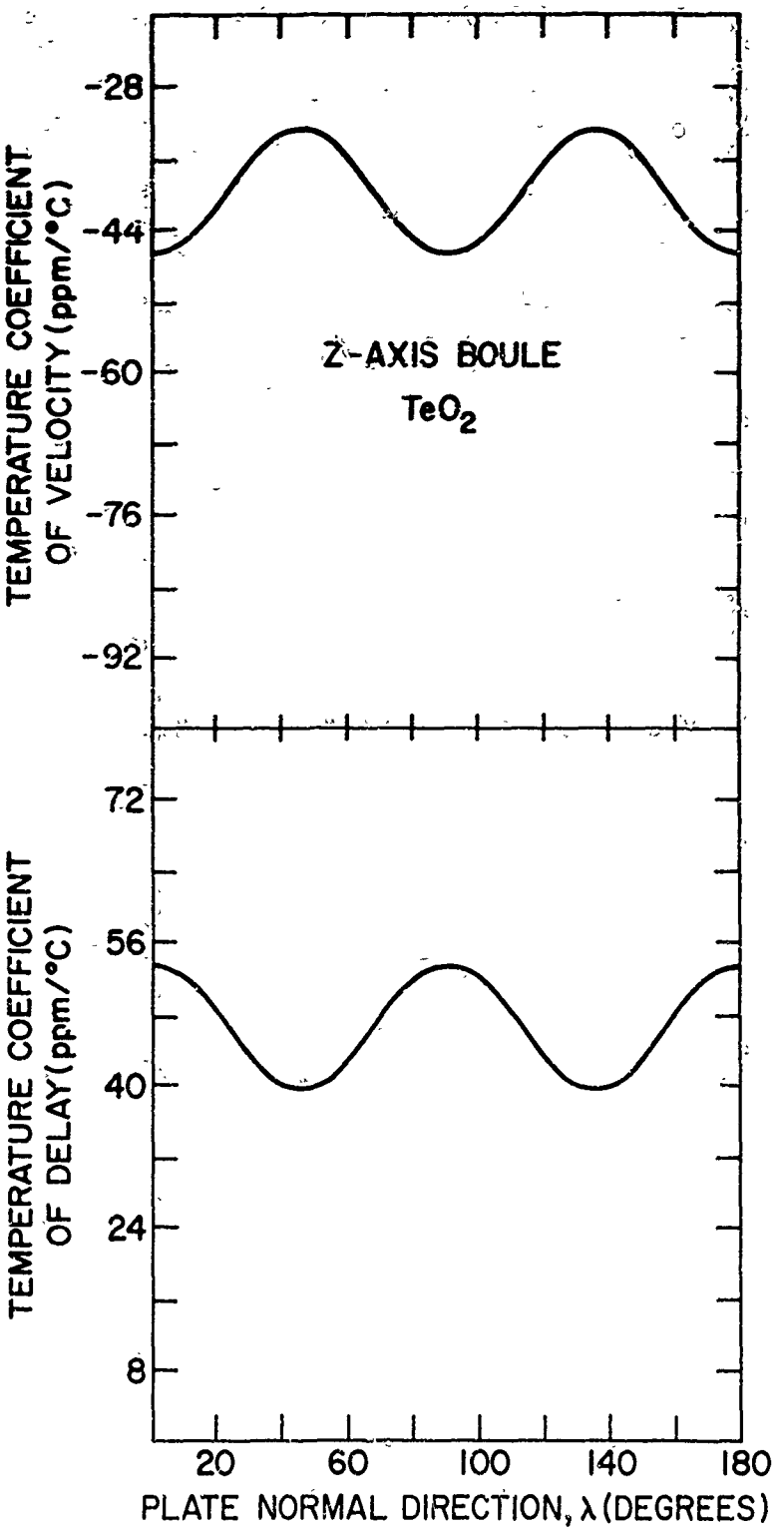
-28
-44
-60
-76
-92
TEMPERATURE COEFFICIENT OF VELOCITY (ppm/°C)
Z-AXIS BOULE
TeO2
72
56
40
24
8
TEMPERATURE COEFFICIENT OF DELAY (ppm/°C)
20
60
100
140
180
PLATE NORMAL DIRECTION, λ (DEGREES)

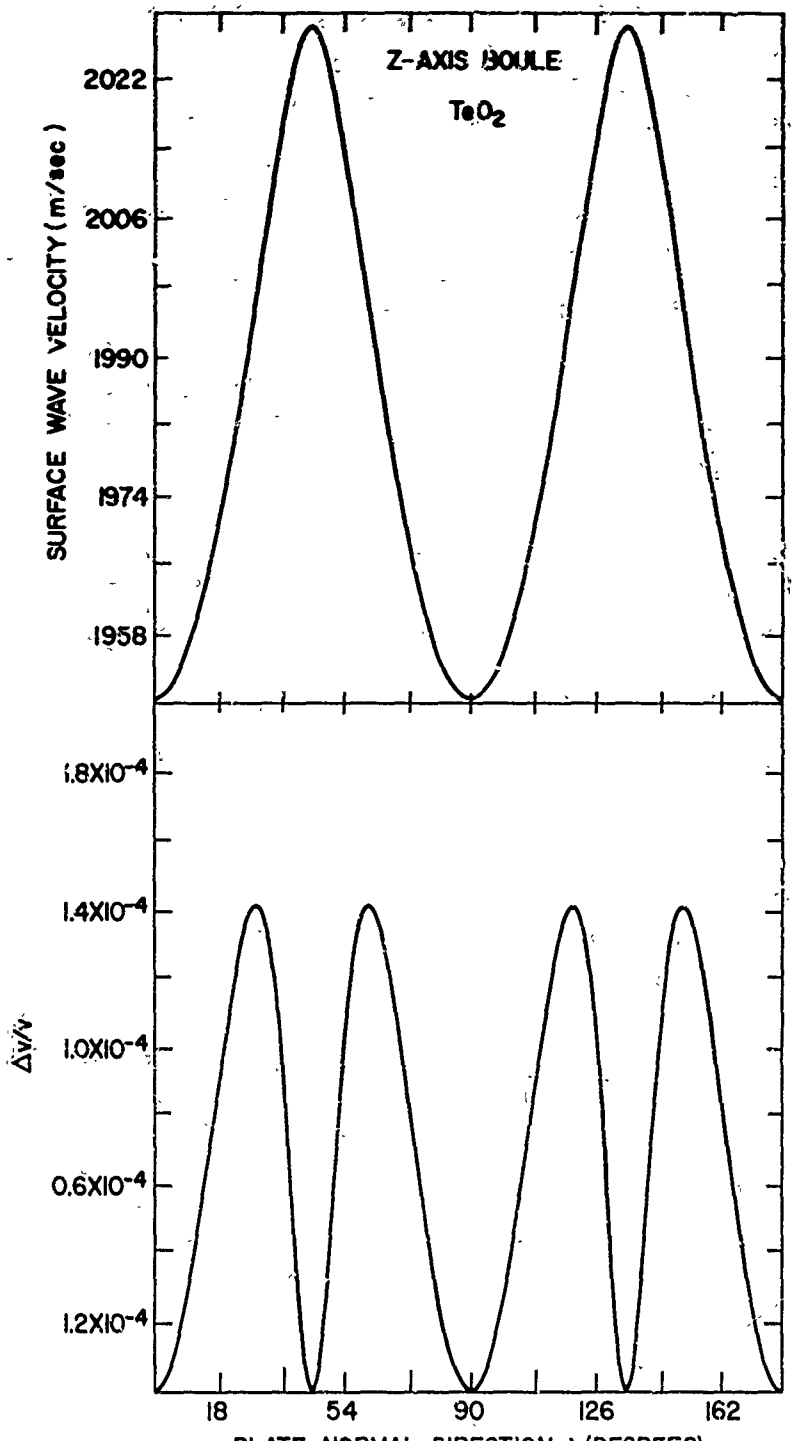

NOTE: TIME AVERAGE POWER FLOW ANGLE IDENTICALLY ZERO.

4. SUMMARY AND CONCLUSIONS

Analysis of the data presented in section 3 yields several interesting surface wave orientations, the more significant of which are listed in Table 1. As expected no zero temperature coefficient of delay cut was found for $LiNbO_3$. However, very fortuitously, the 41-1/2° rotated cut, X propagating orientation (Slobodnik and Conway, 1970b) previously determined to yield excellent, low loss, wide bandwidth devices also possesses the lowest temperature coefficient of delay yet found on this material.

The biggest disappointment was $LiTaO_3$ since, contrary to expectations no zero temperature orientation was found here either. The absolute lowest value of 23 ppm was unfortunately associated with an orientation having some 1.55° of beam steering (Schulz and Holland, 1971). As can also be seen from Table 1, the sacrifice of several parts per million in temperature dependence yields two pure mode axes orientations having velocities of 3300 m/sec. Both of these cuts also have moderately high coupling ($\Delta v/v$). The next to last orientation given in the $LiTaO_3$ column is listed not for its low temperature coefficient but for its very high coupling which is substantially higher than any previously known.

For an exhaustive list of the zero temperature cuts of quartz, the reader is referred to Schulz, Matsinger and Holland (1970). Table 1 merely gives the popular ST cut along with ZX orientation not mentioned by Schulz et al (1970).

It is the two TeO_2 orientations given in Table 1 which show the most unusual and perhaps the most potentially useful properties. Shown here for the first time is a simultaneous combination of zero temperature coefficient of delay, zero power flow angle, ϕ and ultra-low surface wave velocity. This last property allows, of course, long time delays in short spaces and the consequent reduction in size and weight. The low coupling associated with these orientations will probably require enhancement through thin films (Solie, 1971; Reeder et al, 1971; and Smith, 1971) or surface wave generation scheines other than interdigital transducers (Bertoni, 1969; Li and Yen, 1971; and Bertoni and Tamir, 1971). In addition, the high acoustic propagation loss (Ohmachi and Uchida, 1970) of TeO_2 will probably limit its use to the VHF frequency range.

Table 1. Summary of Data of Temperature Coefficients of Velocity and Delay for Newly Discovered Orientations of Interest as Well as Many Popular Surface Wave Cuts

Material	Orientation	Euler Angles	Rotated Constants	Velocity (m/sec)	$\Delta v/v_\infty$	$\frac{1}{v}\frac{\partial v}{\partial T}$ (ppm/°C)	$\frac{1}{\tau}\frac{\partial \tau}{\partial T}$ (ppm/°C)	ϕ (Degrees)
$LiNbO_3$	41-1/2,X	0,41-1/2,0	-	4000	0.0277	-57	72	0
	Y,Z	0,90,90	-	3488	0.0241	-87	94	0
	16-1/2 Double Rotated	0,73-1/2,90	-	3503	0.0268	-88	96	0
$LiTaO_3$	-	90,90,112	-	3295	0.0035	-17	23	1.55
	-	90,90,119.5	-	3300	0.0037	-24	30	0
	-	0,33,0	0,22,20.5	3300	0.0045	-17	33	0
	Y,Z	0,90,90	-	3230	0.0033	-31	35	0
	-	0,78.5,90	-	3260	0.0040	-25	41	0
	-	0,179.5,0	0,22,20.5	3391	0.0084	-42	68	0
	Z,Y	0,0,90	-	3329	0.0059	-52	69	0
Quartz	Z,X	0,0,0	-	3260	0.00006	14	0	0
	ST,X	0,132-3/4,0	-	3158	0.00058	14	0	0
TeO	-	90,90,39	-	1424	0.00008	14	0	0
	-	0,58.2,0	-	1387	0.00002	20	0	0

Acknowledgments

The author is deeply indebted to B. J. Welch of RDP, Inc. for his very capable and extensive computer programming assistance. Without him this report could not have been written. Mr. Welch was supported by the Analysis and Simulation Branch of AFCRL under contract and the author wishes to thank Miss E. Cronin, Chief of that branch, and Mr. P. Tsipouras for their assistance. The author also wishes to thank J. J. Campbell and W. R. Jones of the Hughes Aircraft Company for providing a copy of their basic velocity calculating program. The author also gratefully acknowledges the programming assistance of R. W. Mack and finally wishes to thank M. B. Schulz of the Raytheon Company for bringing the material TeO_2 to his attention.

References

Bechmann, R., Ballato, A.D., and Lukaszek, T.J. (1962) Higher-order temperature coefficients of the elastic stiffnesses and compliances of alpha-quartz, Proc. IEEE 50:1812-1822.

Berlincourt, D.A., Curran, D.R., and Jaffe, H. (1964) Piezoelectric and Piezoelectric Materials and Their Function in Transducers, Physical Acoustics 1A: 169-270, New York, Academic Press.

Bertoni, H.L. (1969) Piezoelectric Rayleigh wave excitation by bulk wave scattering, IEEE Trans. Microwave Theory and Tech. MTT-17:873-882.

Bertoni, H.L. and Tamir, T. (1971) High Efficiency Wedge Transducers, Paper P-5, IEEE Ultrasonics Symposium, Miami, Florida.

Bush, H.J. (1971) Synchronization and Generation of Coded Sequences With Acoustic Surface Wave Techniques, RADC-TR-71-168 Technical Report, Rome Air Development Command (AFSC).

Bush, H.J., Entzminger, J.N., and Richard, W. (1970) A Synthesis of Coherent Frequency-Hopped, Phase Modulated Waveforms by Acoustic Surface Waves, Invention Disclosure RADC No. 7022.

Carr, P.H., DeVito, P.A., and Szabo, T.L. (1971) The effect of temperature and doppler shift on the performance of elastic surface wave encoders and decoders, IEEE Trans. Sonics and Ultrasonics (to be published).

Campbell, J.J. and Jones, W.R. (1968) A method for estimating optimal crystal cuts and propagation directions for excitation of piezoelectric surface waves, IEEE Trans. Sonics Ultrasonics SU-15:209-217.

Campbell, J.J. and Jones, W.R. (1970a) Propagation of surface waves at the boundary between a piezoelectric crystal and a fluid medium, IEEE Trans. Sonics Ultrasonics SU-17:71-76.

Campbell, J.J. and Jones, W.R. (1970b) Propagation of piezoelectric surface waves on cubic and hexagonal crystals, J.A.P. 41:2796-2801.

Golustein, H. (1970) Classical Mechanics, New York, Addison-Wesley.

Holland, M.G. and Schulz, M.B. (1970) Temperature effects in surface acoustic wave devices, Nerem Record: 18-19.

Lewis, M.F., Bell, G., and Patterson, E. (1971) Temperature dependence of surface elastic wave delay lines, J.A.P. 42:476-477.

Li, R.C.M. and Yen, K.H. (1971) A Simple Method for Efficient Excitation of Surface Acoustic Waveguides, Paper D-4, IEEE Ultrasonics Symposium, Miami, Florida.

Ohmachi, Y. and Uchida, N. (1970) Temperature dependence of elastic dielectric, and piezoelectric constants in TeO_2 single crystals, J.A.P. 41:2307-2311.

Reeder, T.M., Kino, G.S., and Adams, P.L. (1971) Enhancement of piezoelectric surface-wave coupling by thin-film perturbations, Appl. Phys. Letts. 19:279-280.

Schulz, M.B. and Holland, M.G. (1971) Temperature dependence of surface acoustic wave velocity in lithium tantalate, IEEE Trans. Sonics and Ultrasonics SU-19 (to be published).

Schulz, M.B., Matsinger, B.J., and Holland, M.G. (1970) Temperature dependence of surface acoustic wave velocity on α quartz, J.A.P. 41:2755-2765.

Slobodnik, A.J., Jr. (1972) Microwave Acoustics Handbook, Vol. 1A Surface Wave Velocities (to be published).

Slobodnik, A.J., Jr., Carr, P.H., and Budreau, A.J. (1970) Microwave frequency acoustic surface-wave loss mechanisms on $LiNbO_3$, J.A.P. 41:4380-4387.

Slobodnik, A.J., Jr. and Conway, E.D. (1970a) Microwave Acoustics Handbook, Vol. 1. Surface Wave Velocities, AFCRL-PSRP 414.

Slobodnik, A.J., Jr. and Conway, E.D. (1970b) New high-frequency high-coupling low-beam-steering cut for acoustic surface waves on $LiNbO_3$, Elect. Letts. 6:171-172.

Slobodnik, A.J., Jr. and Conway, E.D. (1970c) The Effect of Beam Steering on the Design of Microwave Acoustic Surface Wave Devices, G-MTT International Microwave Symposium Digest, 314-318.

Smith, R.T. and Welsh, F.S. (1971) Temperature dependence of the elastic, piezoelectric, and dielectric constants of lithium tantalate and lithium niobate, J.A.P. 42:2219-2230.

Smith, W.R. (1971) Coupling efficiency estimates for acoustic surface wave excitation with piezoelectric film overlays, J.A.P. 42:3016-3018.

Solie, L.P. (1971) Piezoelectric acoustic surface waves for a film on substrate, Appl. Phys. Lett. 18:111-112.

Warner, A.W., Onoe, M., and Coquin, G.A. (1967) Determination of elastic and piezoelectric constants for crystals in class (3m), J.A.S.A. 42:1223-1231.

Welsh, F.S. (1971) Surface wave temperature coefficients on lithium tantalate, IEEE Trans. Sonics Ultrasonics SU-18:108-109.

Zelenka, J. and Lee, C.V. (1971) On the temperature coefficients of the elastic stiffnesses and compliances of alpha-quartz, IEEE Trans. Sonics and Ultrasonics SU-18:79-80.

Appendix A

Material Constants and Their Temperature Coefficients

This appendix presents the material constants, the normalized temperature coefficients of the material constants, and the temperature coefficients of thermal expansion for $LiNbO_3$, $LiTaO_3$, quartz and TeO_2. All of the values for $LiNbO_3$ and $LiTaO_3$ were taken directly from Smith and Welsh (1971) except the temperature coefficient of density which was calculated from the coefficients of thermal expansion using the technique outlined in Appendix B. The values for quartz were taken directly from either Beckmann et al (1962) or from Zelenka and Lee (1971). The values for TeO_2 were taken from Ohmachi and Uchida (1970).

It should be noted that the velocity, $\Delta v/v$, and power flow angle calculations of Section 3 for $LiNbO_3$ and $LiTaO_3$ were taken from the Microwave Acoustics Handbook (Slobodnik, 1972) and therefore were made using the material constants given by Warner et al (1967).

Table A1. Temperature Coefficients of Material Constants. Material: $LiNbO_3$; Crystal Group: 3m; References: Smith and Welsh (1971).

		Room Temperature (25°C) Value of Constant, X	Normalized Temperature Coefficients	
			First Order, $\frac{1}{X}\frac{\partial X}{\partial T} = a_1$	Second Order $\frac{1}{2X}\frac{\partial^2 X}{\partial T^2} = a_2$
Elastic Constants	c_{11}^E	2.030×10^{11} N/m^2	-1.74×10^{-4}/°C	-
	c_{12}^E	0.573	-2.52	-
	c_{13}^E	0.752	-1.59	-
	c_{14}^E	0.085	-2.14	-
	c_{33}^E	2.424	-1.53	-
	c_{44}^E	0.595	-2.04	-
	c_{66}^E	0.7285	-1.43	-
Piezoelectric Constants	e_{15}	3.76 C/m^2	1.47	-
	e_{22}	2.43	0.79	-
	e_{31}	0.23	2.21	-
	e_{33}	1.33	8.87	-
Dielectric Constants	ϵ_{11}^S	39.2×10^{-11} F/m	3.23	-
	ϵ_{33}^S	24.7	6.27	-
Density	ρ	4.64×10^3 kg/m^3	-0.383	-

Table A2. Temperature Coefficients of Thermal Expansion. Material: $LiNbO_3$; Crystal Group: 3m; References: Smith and Welsh (1971)

		Temperature Coefficients (25°C)	
		First Order	Second Order
Thermal Expansion	α_{11}	0.154×10^{-4}/°C	0.053×10^{-7}/(°C)^2
	α_{33}	0.075	-0.077

Table A3. Temperature Coefficients of Material Constants. Material: $LiTaO_3$; Crystal Group: 3m; References: Smith and Welsh (1971)

		Room Temperature (25°C) Value of Constant, X	Normalized Temperature Coefficients	
			First Order, $\frac{1}{X}\frac{\partial X}{2T} = a_1$	Second Order $\frac{1}{2X}\frac{\partial^2 X}{\partial T^2} = a_2$
Elastic Constants	c^E_{11}	2.298×10^{11} N/m^2	-1.03×10^{-4}/°C	0.77×10^{-7}/(°C)^2
	c^E_{12}	0.440	-3.41	-1.18
	c^E_{13}	0.812	-0.50	6.00
	c^E_{14}	-0.104	6.67	16.7
	c^E_{33}	2.798	-0.96	-3.21
	c^E_{44}	0.968	-0.43	1.67
	c^E_{66}	0.929	-0.47	1.24
Piezo-electric Constants	e_{15}	2.72 C/m^2	-1.32	-7.17
	e_{22}	1.67	-0.60	-6.28
	e_{31}	-0.38	0.87	51.8
	e_{33}	1.09	1.54	1.41
Dielectric Constants	ϵ^S_{11}	37.7×10^{-11} F/m	3.29	4.28
	ϵ^S_{33}	37.9	11.6	78.0
Density	ρ	7.454×10^3 kg/m^3	-0.363	-

Table A4. Temperature Coefficients of Thermal Expansion. Material: $LiTaO_3$; Crystal Group: 3m; References: Smith and Welsh (1971).

		Temperature Coefficients (25°C)	
		First Order	Second Order
Thermal Expansion	α_{11}	0.161×10^{-4}/°C	0.070×10^{-7}/(°C)^2
	α_{33}	0.041	-0.100

Table A5. Temperature Coefficients of Material Constants. Material: Quartz; Crystal Group: 32; References: Bechmann et al (1962) and Zelenka and Lee (1971).

		Room Temperature (25°C) Value of Constants, X	Normalized Temperature Coefficients	
			First Order, $\frac{1}{X}\frac{\partial X}{\partial T} = a_1$	Second Order $\frac{1}{2X}\frac{\partial^2 X}{\partial T^2} = a_2$
Elastic Constants	c_{11}^E	8.674×10^{10} N/m^2	-0.443×10^{-4}/°C	-
	c_{12}^E	0.699	-26.90	-
	c_{13}^E	1.191	-5.50	-
	c_{14}^E	-1.791	1.17	-
	c_{33}^E	10.72	-1.60	-
	c_{44}^E	5.794	-1.754	-
	c_{66}^E	3.9875	1.876	-
Density	ρ	2.65×10^3 kg/m^3	-34.92×10^{-6}/°C	-15.9×10^{-9}/(°C)^2

Table A6. Temperature Coefficients of Thermal Expansion. Material: Quartz; Crystal Group: 32; References: Bechmann et al (1962).

		Temperature Coefficients (25°C)	
		First Order	Second Order
Thermal Expansion	α_{11}	13.71×10^{-6}/°C	6.5×10^{-9}/(°C)^2
	α_{33}	7.48	2.9

Table A7. Temperature Coefficients of Material Constants. Material: TeO_2; Crystal Group: 422; References: Ohmachi and Uchida (1970).

		Room Temperature (20°C) Value of Constant, X	Normalized Temperature Coefficients	
			First Order, $\frac{1}{X}\frac{\partial X}{\partial T} = a_1$	Second Order $\frac{1}{2X}\frac{\partial^2 X}{\partial T^2} = a_2$
Elastic Constants	c_{11}^E	5.57×10^{10} N/m^2	-2.70×10^{-4}/°C	-
	c_{12}^E	5.12	-3.28	-
	c_{13}^E	2.18	-0.54	-
	c_{14}^E	0	-	-
	c_{33}^E	10.58	-2.81	-
	c_{44}^E	2.65	-0.73	1
	c_{66}^E	6.59	-4.38	-
Density	ρ	5.99×10^3 kg/m^3	-46.6×10^{-6}/°C	-

Table A8. Temperature Coefficients of Thermal Expansion: Material: TeO_2; Crystal Group: 422; References: Ohmachi and Uchida (1970).

		Temperature Coefficients (20°C)	
		First Order	Second Order
Thermal Expansion	α_{11}	20.0×10^{-6}/°C	-
	α_{33}	6.6	-

Appendix B

The Temperature Coefficient of Density

The temperature coefficient of density can be obtained from the coefficients of thermal expansion as shown below.

By definition the density is the mass per unit volume

$$\rho(T) \equiv \frac{M}{\ell_1 \ell_2 \ell_3} = M\ell_1^{-1}\ell_2^{-1}\ell_3^{-1} \tag{B1}$$

where ℓ_1, ℓ_2, and ℓ_3 are unit lengths along the X, Y and Z crystalline axes, respectively. M is, of course, the mass. Taking the derivative of Eq. (B1) yields

$$\frac{\partial \rho}{\partial T} = M\ell_1^{-1}\frac{\partial \ell_2^{-1}\ell_3^{-1}}{\partial T} + M\ell_2^{-1}\ell_3^{-1}\frac{\partial \ell_1^{-1}}{\partial T} \tag{B2}$$

or

$$\frac{\partial \rho}{\partial T} = M\ell_1^{-1}\ell_2^{-1}\frac{\partial \ell_3^{-1}}{\partial T} + M\ell_1^{-1}\ell_3^{-1}\frac{\partial \ell_2^{-1}}{\partial T} + M\ell_2^{-1}\ell_3^{-1}\frac{\partial \ell_1^{-1}}{\partial T}. \tag{B3}$$

This is also equivalent to

$$\frac{\partial \rho}{\partial T} = -M\ell_1^{-1}\ell_2^{-1}\ell_3^{-2}\frac{\partial \ell_3}{\partial T} - M\ell_1^{-1}\ell_3^{-1}\ell_2^{-2}\frac{\partial \ell_2}{\partial T} - M\ell_2^{-1}\ell_3^{-1}\ell_1^{-2}\frac{\partial \ell_1}{\partial T}. \tag{B4}$$

Grouping terms yields

$$\frac{\partial \rho}{\partial T} = -M\ell_1^{-1}\ell_2^{-1}\ell_3^{-1}\left[\frac{1}{\ell_3}\frac{\partial \ell_3}{\partial T} + \frac{1}{\ell_2}\frac{\partial \ell_2}{\partial T} + \frac{1}{\ell_1}\frac{\partial \ell_1}{\partial T}\right]. \tag{B5}$$

Thus

$$\frac{1}{\rho}\frac{\partial \rho}{\partial T} = -\left[\frac{1}{\ell_1}\frac{\partial \ell_1}{\partial T} + \frac{1}{\ell_2}\frac{\partial \ell_2}{\partial T} + \frac{1}{\ell_3}\frac{\partial \ell_3}{\partial T}\right]. \tag{B6}$$

Or by definition of the thermal expansion coefficients

$$\frac{1}{\rho}\frac{\partial \rho}{\partial T} = -\left[\alpha_{11} + \alpha_{22} + \alpha_{33}\right]. \tag{B7}$$

Q. E. D.

Appendix C

Material Constants at 15°C, 25°C and 35°C

This appendix presents, in tabular form, the independent material constants of $LiNbO_3$, $LiTaO_3$, quartz and TeO_2 at 15°C, 25°C and 30°C (10°C, 20°C and 30°C for TeO_2). These quantities were computed using Eq. (3) along with the temperature coefficients listed in Appendix A.

Table C1. Independent Elastic (in 10^{11} N/m^2), Dielectric (in 10^{-11} F/m), and Piezoelectric (in C/m^2) Constants of $LiNbO_3$ at Various Temperatures. Density (in 10^3 kg/m^3) is also included. Complete matrices can be obtained using the symmetry of crystal group 3m (see for example Berlincourt et al, 1964).

	Constant	Temperature		
		15°C	25°C	35°C
$LiNbO_3$	c_{11}^E	2.03353	2.030	2.02647
	c_{12}^E	0.574444	0.573	0.571556
	c_{13}^E	0.753196	0.752	0.750804
	c_{14}^E	0.085182	0.085	0.084818
	c_{33}^E	2.42771	2.424	2.42029
	c_{44}^E	0.596214	0.595	0.593786
	c_{66}^E	0.729542	0.7285	0.727458
	e_{15}	3.75447	3.76	3.76553
	e_{22}	2.42808	2.43	2.43192
	e_{31}	0.229492	0.23	0.230503
	e_{33}	1.31820	1.33	1.34180
	ϵ_{11}^S	37.0734	39.2	39.3266
	ϵ_{33}^S	24.5451	24.7	24.8549
	ρ	4.64178	4.64	4.63822

Table C2. Independent Elastic (in 10^{11} N/m^2), Dielectric (in 10^{-11} F/m), and Piezoelectric (in C/m^2) Constants of $LiTaO_3$ at Various Temperatures. Density (in 10^3 kg/m^3) is also included. Complete matrices can be obtained using the symmetry of crystal group 3m (see for example Berlincourt et al, 1964).

	Constant	Temperature		
		15°C	25°C	35°C
$LiTaO_3$	c_{11}^E	2.30038	2.298	2.29565
	c_{12}^E	0.441495	0.440	0.438494
	c_{13}^E	0.812455	0.812	0.811643
	c_{14}^E	-0.103324	-0.104	-0.1047110
	c_{33}^E	2.80060	2.798	2.79522
	c_{44}^E	0.968432	0.968	0.967600
	c_{66}^E	0.929448	0.929	0.928575
	e_{15}	2.72340	2.72	2.71621
	e_{22}	1.67090	1.67	1.66889
	e_{31}	-0.379866	-0.38	-0.380527
	e_{33}	1.08834	1.09	1.09169
	ϵ_{11}^S	37.5776	37.7	37.8256
	ϵ_{33}^S	37.4899	37.9	38.3692
	ρ	7.45671	7.454	7.45129

Table C3. Independent Elastic (in 10^{11} N/m^2), Dielectric (in 10^{-11} F/m), and Piezoelectric (in C/m^2) Constants of Quartz at Various Temperatures. Density (in 10^3 kg/m^3) is also included. Complete matrices can be obtained using the symmetry of crystal groups 32 (see for example Berlincourt et al, 1964).

	Constant	Temperature		
		15°C	25°C	35°C
Quartz	c_{11}^E	0.867784	0.8674	0.867016
	c_{12}^E	0.071780	0.0699	0.06802
	c_{13}^E	0.119755	0.1191	0.118445
	c_{14}^E	-0.178890	-0.1791	-0.179310
	c_{33}^E	1.073715	1.072	1.070285
	c_{44}^E	0.580416	0.5794	0.578384
	c_{66}^E	0.398002	0.39875	0.399498
	e_{11}	-	0.171	-
	e_{14}	-	-0.0406	-
	ϵ_{11}^S	-	3.92	-
	ϵ_{33}^S	-	4.1	-
	ρ	2.65092	2.65	2.64907

Table C4. Independent Elastic (in 10^{11} N/m^2), Dielectric (in 10^{-11} F/m), and Piezoelectric (in C/m^2) Constants of TeO_2 at Various Temperatures. Density (in 10^3 kg/m^3) is also included. Complete matrices can be obtained using the symmetry of crystal group 422 (see for example Berlincourt et al, 1964).

	Constant	Temperature		
		10°C	20°C	30°C
TeO_2	c^E_{11}	0.5585	0.557	0.5555
	c^E_{12}	0.51368	0.512	0.51032
	c^E_{13}	0.218118	0.218	0.21788
	c^E_{33}	1.0610	1.058	1.0550
	c^E_{44}	0.26519	0.265	0.26481
	c^E_{66}	0.66189	0.659	0.65611
	e_{14}	-	0.216	-
	ϵ^S_{11}	-	20.1	-
	ϵ^S_{33}	-	21.9	-
	ρ	5.9928	5.99	5.9872

Appendix D

"Rotated Constants" and Euler Angle Notation

The meaning of the "rotated constant" Euler angle notation can best be explained with reference to several examples.

Figure D1 illustrates the standard starting coordinate system in which the propagation axes line up with the crystalline axes X, Y and Z. Thus, one can follow how the standard Euler angle notation 0, 90, *0* refers to rotation in the XZ plane, starting with a propagation direction along the X axis and a plate normal along the -Y axis. This is the Y-cut plate illustrated in Figure D2.

If, however, we first rotate through the Euler angles 45, 90, 35.264 then the 1 axis, or propagation direction, is initially aligned with the [111] crystalline axis and the 3 axis or plate normal would lie along the $[1\bar{1}0]$ crystalline axis. This is illustrated in Figure D3 which also indicates how further rotations can then be accomplished from this starting point. The notation used in the text to describe this situation is illustrated in Figure D4.

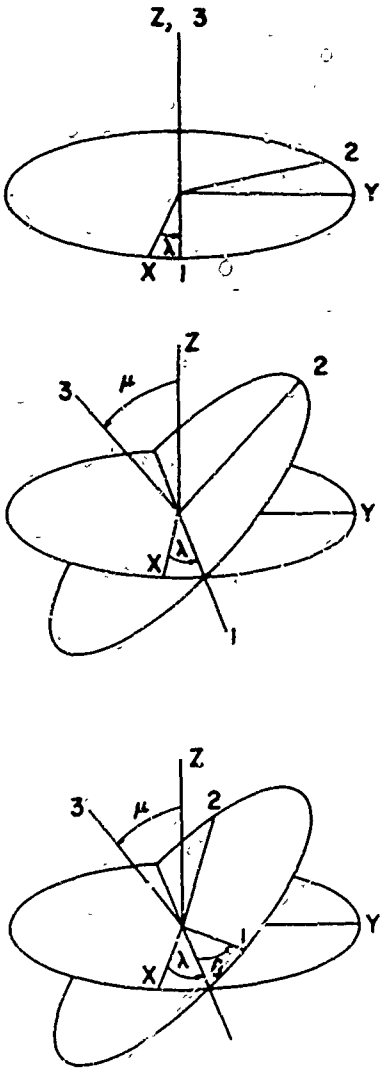

Figure D1. Coordinate System Used to Define Acoustic Surface Wave Propagation. The phase velocity vector lies along the 1 axis while the plate normal lies along the negative 3 axis. The crystalline axes are given by X, Y, and Z while the Euler angles are λ, μ, and θ (after H. Goldstein in Classical Mechanics).

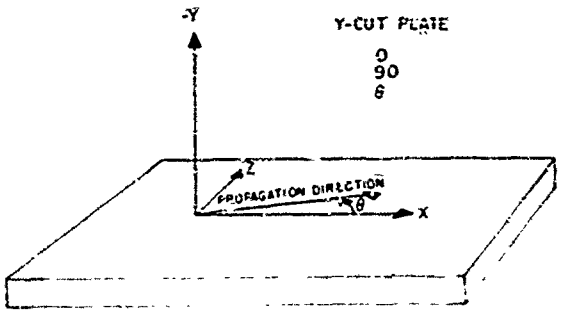

Figure D2. Standard Notation for a Y-cut Plate. Rotation of μ through the angle of 90° aligns the plate normal with the (-Y) crystalline axis while the propagation direction remains along the X axis. Further rotations in the plane of the plate are then accomplished through the angle θ

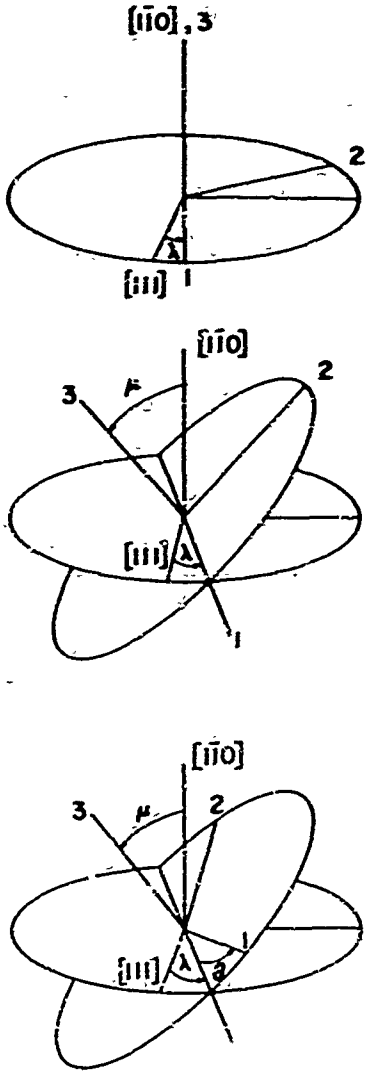

Figure D3. Coordinate System After Initial Rotation Through the Euler Angles 45, 90, 35.264. The phase velocity vector lies along the 1 axis while the plate line axis are given by [111] and [1$\bar{1}$0] while the Euler angles for further rotations from this starting point are λ, μ, and θ (after H. Goldstein in Classical Mechanics)

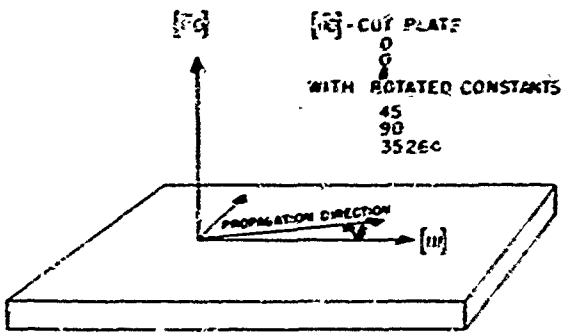

Figure D4. Standard Notation for a [1$\bar{1}$0]-cut Plate. Initial rotation through the Euler angles 45, 90, 35.264 aligns the propagation direction with the [111] crystalline axis and the plate normal with the [1$\bar{1}$0] crystalline axis. Further rotations in the plane of the plate are then accomplished through the angle θ